AD-A078 611 NATIONAL AERONAUTICS AND SPACE ADMINISTRATION HAMPTO--ETC F/G 16/4
SUPERSONIC STABILITY AND CONTROL CHARACTERISTICS OF A CRUCIFORM--ETC(U)
DEC 79 W A CORLETT

UNCLASSIFIED NASA-L-13149 NASA-TM-80171 NL

NASA Technical Memorandum 80171

LEVEL II

Supersonic Stability and Control Characteristics of a Cruciform Missile Model With Delta Wings and Aft Tail Fin Controls

William A. Corlett

DECEMBER 1979

NASA

NASA Technical Memorandum 80171

Supersonic Stability and Control Characteristics of a Cruciform Missile Model With Delta Wings and Aft Tail Fin Controls

William A. Corlett
Langley Research Center
Hampton, Virginia

NASA
National Aeronautics
and Space Administration

Scientific and Technical Information Branch

1979

SUMMARY

An investigation has been conducted to determine the static stability and control characteristics of a cruciform missile configuration with delta wings and aft tail fin controls. The tests were conducted in the Langley Unitary Plan wind tunnel at Mach numbers from 1.60 to 4.63 through an angle-of-attack range of -4° to 30°. Model roll orientation was varied from 0° to 135°.

The results indicated good longitudinal stability and control characteristics throughout the test Mach number range. Relatively high induced rolling and yawing moments were apparent at asymmetric model roll angles for the lower test Mach numbers; however, sufficient roll and yaw control was available to trim to relatively high angles of attack and lift coefficients.

INTRODUCTION

In support of the development of highly maneuverable air-to-air and surface-to-air missiles, the National Aeronautics and Space Administration has performed wind-tunnel tests to determine the stability and control characteristics of a cruciform missile configuration with delta wings and aft tail fin controls. Other missile configurations which add to the data base for maneuverable missiles are presented in references 1 to 29.

The investigation was performed in the Langley Unitary Plan wind tunnel at Mach numbers of 1.60, 2.10, 2.50, 2.86, 3.95, and 4.63. Static aerodynamic characteristics were determined at a nominal angle-of-attack range from -4° to 30° at model roll orientations of 0° to 135°. The test Reynolds number was 9.84×10^{6} per meter.

SYMBOLS

The aerodynamic-coefficient data are referred to the body-axis system except for lift and drag, which are referred to the stability-axis system. The moment reference was located at 56 percent of the body length aft of the nose. Model dimensions are given in SI Units with U.S. Customary Units in parentheses.

A maximum cross-sectional area of body, 45.60 cm^2 (7.07 in^2)

C_A axial-force coefficient, $\dfrac{\text{Axial force}}{qA}$

$C_{A,c}$ base-cavity axial-force coefficient

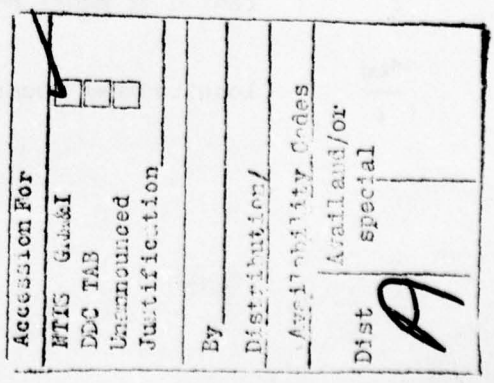

C_D drag coefficient, $\frac{\text{Drag}}{qA}$

$C_{D,c}$ base-cavity drag coefficient

$C_{D,o}$ drag coefficient at $\alpha = 0^o$

C_L lift coefficient, $\frac{\text{Lift}}{qA}$

$C_{L,trim}$ trimmed lift coefficient ($C_m = 0$)

C_l rolling-moment coefficient, $\frac{\text{Rolling moment}}{qAd}$

C_m pitching-moment coefficient, $\frac{\text{Pitching moment}}{qAl}$

C_{m_δ} pitching-moment coefficient per degree control deflection ($\alpha = 0^o$)

C_N normal-force coefficient, $\frac{\text{Normal force}}{qA}$

C_n yawing-moment coefficient, $\frac{\text{Yawing moment}}{qAd}$

C_Y side-force coefficient, $\frac{\text{Side force}}{qA}$

d reference body diameter, 7.62 cm (3.00 in.)

l body length, 91.44 cm (36.00 in.)

M free-stream Mach number

q free-stream dynamic pressure, Pa

r radius of model nose, 2.54 cm (1.00 in.)

$\frac{x_{ac}}{l}$ longitudinal location of aerodynamic center referenced to body length

$\frac{x_{cg}}{l}$ longitudinal location of center of gravity referenced to body length

α angle of attack, deg

δ wing tab deflection angle, deg

δ_{pitch} pitch-control deflection (negative, leading edge down), deg

δ_{roll} roll-control deflection (positive to provide a clockwise rotation as viewed from rear), deg

δ_{yaw} yaw-control deflection (negative, leading edge left as viewed from above), deg

ϕ model roll angle (positive clockwise when viewed from rear; symmetrical configuration "+" equals 0^{o} with wing tab on bottom), deg

Model components:

B body with protuberances

B_o body without protuberances

T tail

W wing

APPARATUS AND TESTS

Tunnel

The investigation was conducted in both the high and low Mach number test sections of the Langley Unitary Plan wind tunnel. This is a continuous-flow, variable-pressure facility with two test sections, each 1.22 m by 1.22 m in cross section and 2.13 m in length. The nozzles leading to the test sections are of the asymmetric sliding-block type, which permits continuous variation in Mach number from 1.47 to 2.86 in test section 1 and from 2.29 to 4.63 in test section 2.

Model

The test configuration was a cruciform missile with delta wings and aft tail fin controls. Dimensional details of the model are presented in figure 1, and a photograph of the model mounted in the test section is shown in figure 2. The model fuselage is a 7.62-cm-diameter cylinder with a hemispherical nose having a 2.54-cm radius. Attached to the fuselage are cruciform delta-planform wings and clipped-delta-planform tail fins mounted in line with the wings. The wings and tail fin controls have circular-arc cross sections with thickness-to-

chord ratios of 0.045 and 0.06, respectively. Wing 3 (fig. 1) is provided with an aileron-type trim tab. The model also had eight removable protuberances on the fuselage which simulated various equipment ducts.

Test Conditions

The tests were performed at Mach numbers of 1.60, 2.10, 2.50, 2.86, 3.95, and 4.63 at a Reynolds number of 9.84×10^6 per meter. A stagnation temperature of 339 K was maintained for Mach numbers from 1.60 to 2.86, and 353 K was maintained for Mach numbers of 3.95 and 4.63. The dew point was maintained at a level sufficiently low to assure negligible condensation effects. Angles of attack were varied from approximately -4° to 30° at model roll orientations from 0° to 135°. Transition strips were placed 1.02 cm aft of the leading edge on the wing and tail surfaces and 3.05 cm aft of the nose. The transition strips were composed of No. 50 sand (0.032 cm in diameter) for Mach numbers of 1.60 to 2.86 and No. 40 sand (0.046 cm in diameter) for the higher Mach numbers.

Measurements and Corrections

Aerodynamic forces and moments on the model were measured by means of a six-component, electrical strain-gage balance which was internally mounted near the moment reference center of the model. The balance was attached to a sting which, in turn, was rigidly fastened to the tunnel model-support system. Model base-cavity pressure was measured with two static-pressure tubes extending into the balance cavity.

The results have been adjusted to free-stream static pressure acting over the model base. Angles of attack have been corrected for deflections of the balance and sting due to aerodynamic loads and for tunnel airflow angularity.

PRESENTATION OF RESULTS

The results are presented in the following figures:

RESULTS AND DISCUSSION

Longitudinal Characteristics

Longitudinal stability and control characteristics are presented in figures 4 and 5 for $\phi = 0^{o}$ and $\phi = 45^{o}$, respectively, and are summarized in figures 6 and 7.

The vehicle has relatively linear pitching-moment curves (figs. 4 and 5). However, a slight pitch-up tendency is noted at $\phi = 45^{o}$ at the lower Mach numbers. This tendency results in an effective reduction in stability level of about 5 percent body length at angles of attack above 15^{o} (fig. 5) when compared with the $\phi = 0^{o}$ configuration (fig. 4). The lift-curve slope $C_{L_{\alpha}}$ generally shows an increase with increase in angle of attack.

The aft tail fins provide effective pitch control throughout the Mach number and angle-of-attack test ranges (figs. 4 and 5). At the higher Mach numbers, the pitch-control effectiveness $C_{m_{\delta}}$ increases with increase in angle of attack; the control effectiveness, therefore, remains nearly constant with increase in Mach number at high angles of attack. (Note the large reduction in $C_{m_{\delta}}$ with increase in Mach number at $\alpha = 0^{o}$ as presented in fig. 7.)

The characteristic reduction in lift and increase in drag with negative control deflection are apparent in figures 4 and 5. Pitch control is approximately 40 percent more effective at $\phi = 45^{o}$ than at $\phi = 0^{o}$, since four fins are deflected instead of two. Lift characteristics for the model at $\phi = 0^{o}$ and $\phi = 45^{o}$ are similar.

Variations of trimmed lift coefficient with center-of-gravity location are presented in figure 6. This figure shows the maximum lift coefficients obtainable with the indicated pitch-control deflections at various center-of-gravity locations. Thus, the aerodynamic potential for maneuverability (instantaneous normal acceleration) of this configuration can be compared with other configurations on the basis of lift available divided by lift required for the missile to maintain level flight.

The variation at $\alpha = 0^{\circ}$ of longitudinal aerodynamic parameters with Mach number is presented in figure 7. A reduction in pitch-control effectiveness with increase in Mach number is apparent for both $\phi = 0^{\circ}$ and $\phi = 45^{\circ}$. The aerodynamic center remains nearly constant at 60 to 61 percent body length for the test Mach number range of 1.60 to 4.63. The blunt hemispherical nose contributes to a relatively high $C_{D,o}$ throughout the Mach number test range.

The effects of component parts on the longitudinal aerodynamic characteristics at $\phi = 0^{\circ}$ and $\phi = 45^{\circ}$ are presented in figures 8 and 9, respectively. Addition of the protuberances in the form of equipment ducts and various fairings produces a zero-lift drag increase of about 5 percent and a noticeable reduction in stability for the wing-body-tail configuration.

Lateral Characteristics

Effects of model roll orientation ϕ at angles varying from 0° to 135° are presented in figure 10. The asymmetric roll angles of 14.0°, 26.5°, and 67.5° produce large induced rolling and yawing moments starting at angles of attack below 10° at $M = 1.60$. These effects are delayed to higher angles of attack and are less pronounced as Mach number is increased. Figure 11 shows the effect of pitch controls at various model roll orientations (for controls deflected to provide a moment in the same plane as the model pitch plane). It is apparent when comparing figures 10 and 11, that pitch deflections have little effect on the induced rolling and yawing moments.

Figures 12 and 13 show the roll and yaw control power available to nullify the induced rolling and yawing moments. The tail fins as controls are very effective in providing roll and yaw control. It appears that this missile configuration can trim to relatively high angles of attack and lift coefficients at all model roll orientations. However, no attempt was made to run a sufficient data matrix at combined controls to establish the control boundaries.

The effects of a trim tab located on wing 3 are shown in figure 14.

CONCLUDING REMARKS

An investigation has been conducted to determine the static stability and control characteristics of a cruciform missile configuration with delta wings and aft tail fin controls. The tests were conducted in the Langley Unitary Plan wind tunnel at Mach numbers from 1.60 to 4.63 through an angle-of-attack range of -4° to 30°. Model roll orientation was varied from 0° to 135°.

The results indicated that the vehicle had relatively linear pitching-moment curves and only a 1-percent aerodynamic-center variation throughout the Mach number test range. Pitch controls were effective at all test conditions and were capable of providing high trimmed-lift coefficients. Relatively high induced rolling and yawing moments were apparent at asymmetric model roll angles at low Mach numbers; however, sufficient roll and yaw control was available to nullify these moments at relatively high angles of attack.

Langley Research Center
National Aeronautics and Space Administration
Hampton, VA 23665
November 2, 1979

REFERENCES

1. Corlett, William A.; and Fuller, Dennis E.: Aerodynamic Characteristics at Mach 1.60, 2.00, and 2.50 of a Cruciform Missile Configuration With In-Line Tail Controls. NASA TM X-1112, 1965.

2. Fuller, Dennis E.; and Corlett, William A.: Supersonic Aerodynamic Characteristics of a Cruciform Missile Configuration With Low-Aspect-Ratio Wings and In-Line Tail Controls. NASA TM X-1025, 1964.

3. Foster, Gerald V.; and Corlett, William A.: Aerodynamic Characteristics at Mach Numbers From 0.40 to 2.86 of a Missile Model Having All-Movable Wings and Interdigitated Tails. NASA TM X-1184, 1965.

4. Hayes, Clyde; and Fournier, Roger H.: Effect of Fin-Flare Combinations on the Aerodynamic Characteristics of a Body at Mach Numbers 1.61 and 2.20. NASA TN D-2623, 1965.

5. Corlett, William A.; and Richardson, Celia S.: Effect of First-Stage Geometry on Aerodynamic Characteristics in Pitch of Two-Stage Rocket Vehicles From Mach 1.57 to 2.86. NASA TN D-2709, 1965.

6. Corlett, William A.: Aerodynamic Characteristics of a Maneuverable Missile With Cruciform Wings and In-Line Canard Surfaces at Mach Numbers From 0.50 to 4.63. NASA TM X-1309, 1966.

7. Spearman, M. Leroy; and Corlett, William A.: Aerodynamic Characteristics at Mach Numbers of 3.95 and 4.63 for a Missile Model Having All-Movable Wings and Interdigitated Tails. NASA TM X-1332, 1967.

8. Spearman, M. Leroy; and Corlett, William A.: Aerodynamic Characteristics at Mach Numbers From 1.50 to 4.63 of a Maneuverable Missile With In-Line Cruciform Wings and Canard Surfaces. NASA TM X-1352, 1967.

9. Spearman, M. Leroy; and Corlett, William A.: Aerodynamic Characteristics of a Winged Cruciform Missile Configuration With Aft Tail Controls at Mach Numbers From 1.60 to 4.63. NASA TM X-1416, 1967.

10. Hayes, Clyde: Supersonic Aerodynamic Characteristics of a Model of an Air-to-Ground Missile. NASA TM X-1491, 1968.

11. Fuller, Dennis E.; and Richardson, Celia S.: Aerodynamic Characteristics at Mach 2.50 of a Cruciform Missile Configuration With In-Line Inlets, Wings, and Tail Surfaces. NASA TM X-1492, 1968.

12. Corlett, William A.: Aerodynamic Characteristics of a Modified Missile Model With Trapezoidal Wings and Aft Tail Controls at Mach Numbers of 2.50 to 4.63. NASA TM X-1751, 1969.

13. Fuller, Dennis E.: Aerodynamic Characteristics of a Cruciform Winged Missile With Trailing-Edge Controls at Mach Numbers From 1.60 to 4.63. NASA TM X-1743, 1969.

14. Corlett, William A.: Aerodynamic Characteristics of a Modified Missile Model With Cruciform Wings and In-Line Tail Controls at Mach 1.60 to 4.63. NASA TM X-1805, 1969.

15. Corlett, William A.: Aerodynamic Characteristics of a Cruciform-Wing Missile Model With a Systematic Variation of Canard and Tail Locations at Mach 1.60 to 4.63. NASA TM X-1834, 1969.

16. Spearman, M. Leroy; and Trescot, Charles D., Jr.: Effects of Wing Planform on the Static Aerodynamics of a Cruciform Wing-Body Missile for Mach Numbers Up to 4.63. NASA TM X-1839, 1969.

17. Spearman, M. Leroy; and Fournier, Roger H.: Aerodynamic Characteristics of a Maneuverable Missile With Cruciform Delta Wings and Aft Tail Controls at Mach Numbers From 1.50 to 4.63. NASA TM X-1863, 1969.

18. Corlett, William A.: Aerodynamic Characteristics at Mach 2.50 to 4.63 of a Cruciform Missile Model With Delta Wings and Trapezoidal-Tail Controls Including Effects of Wing Location. NASA TM X-2364, 1971.

19. Corlett, William A.: Aerodynamic Characteristics at Mach Numbers From 1.60 to 2.86 of a Current Missile Configuration With Modified Wing and Tail Components. NASA TM X-2455, 1972.

20. Corlett, William A.: Aerodynamic Characteristics at Mach Numbers From 0.40 to 2.86 of a Maneuverable Missile With Cruciform Trapezoidal Wings and Aft Tail Controls. NASA TM X-2681, 1972.

21. Monta, William J.; and Foster, Gerald V.: Aerodynamic Characteristics of a Wing-Control Air-To-Air Missile Configuration at Mach Numbers From 2.00 to 4.62. NASA TM X-2487, 1972.

22. Corlett, William A.; and Howell, Dorothy T.: Aerodynamic Characteristics at Mach 0.60 to 4.63 of Two Cruciform Missile Models, One Having Trapezoidal Wings With Canard Controls and the Other Having Delta Wings With Tail Controls. NASA TM X-2780, 1973.

23. Jernell, Lloyd S.; Monta, William J.; and Flechner, Stuart G.: Stability and Control Characteristics of a Cruciform Missile Model With Large Delta Wings and Tail Controls at Mach 0.60 to 4.63. NASA TM X-3037, 1974.

24. Blair, A. B., Jr.: Aerodynamic Characteristics of a Tandem-Canard Missile at Mach Numbers From 1.83 to 4.63. NASA TM X-3040, 1974.

25. Fournier, Roger H.; Foster, Gerald V.; and Watson, Carolyn B.: Aerodynamic Characteristics at Mach 0.60 to 2.86 of a Canard-Controlled Span Constrained Missile for Missions at Low to Moderate Altitudes. NASA TM X-3436, 1976.

26. Graves, Ernald B.; and Fournier, Roger H.: Stability and Control Characteristics at Mach Numbers From 0.20 to 4.63 of a Cruciform Air-to-Air Missile With Triangular Canard Controls and a Trapezoidal Wing. NASA TM X-3070, 1974.

27. Sawyer, Wallace C.; and Sangiorgio, Giuliana: Stability and Control Characteristics of a Monoplanar Elliptic Missile Model at Mach Numbers From 1.60 to 2.86. NASA TP-1352, 1979.

28. Monta, William J.: Supersonic Aerodynamic Characteristics of a Sparrow III Type Missile Model With Wing Controls and Comparison With Existing Tail-Control Results. NASA TP-1078, 1977.

29. Howell, Dorothy T.: Wind-Tunnel Investigation of Supersonic Aerodynamic Characteristics of a Model Simulating the SA-N-3 (Goblet) Missile. NASA TM-80050, 1979.

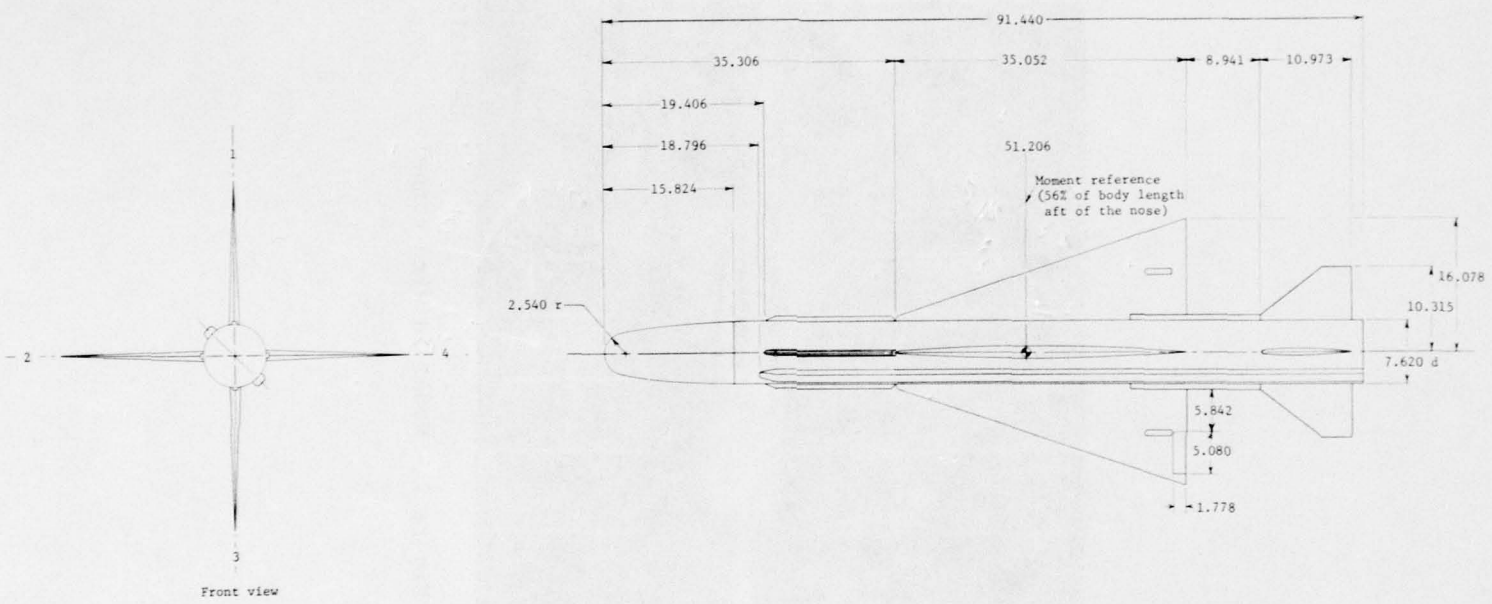

Figure 1.- Model details. (All dimensions are in centimeters.)

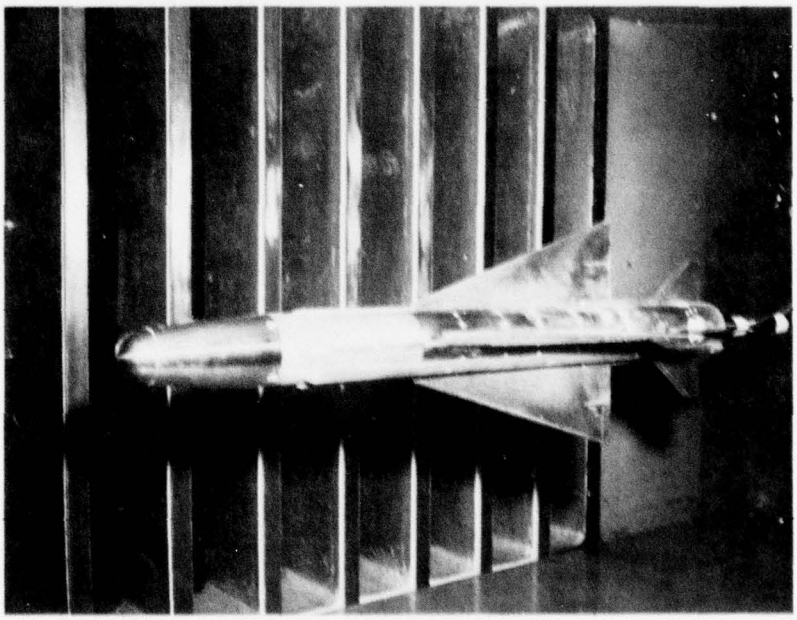

L-79-315

Figure 2.- Model in wind tunnel.

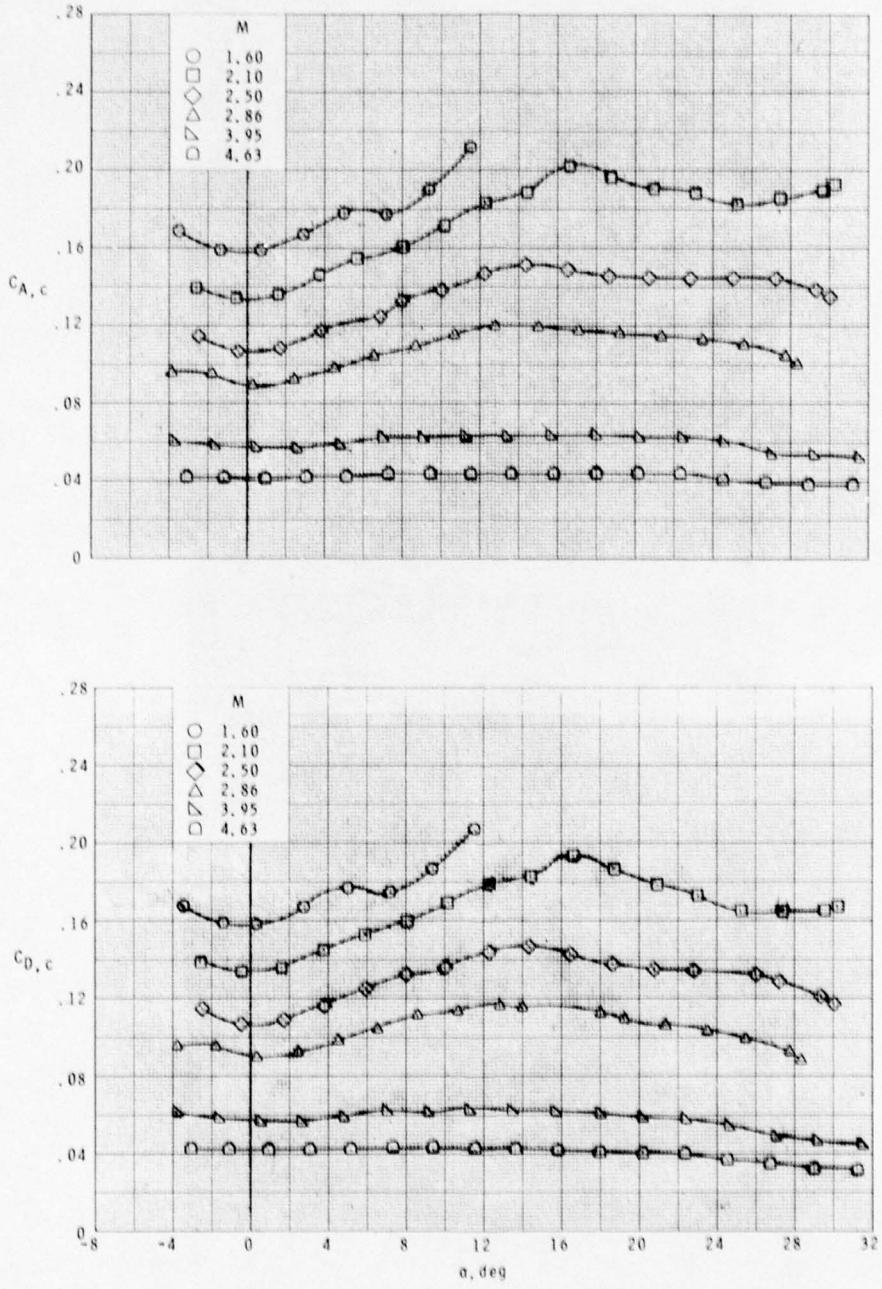

Figure 3.- Variation of base-cavity axial-force and drag coefficients with angle of attack; BTW configuration.

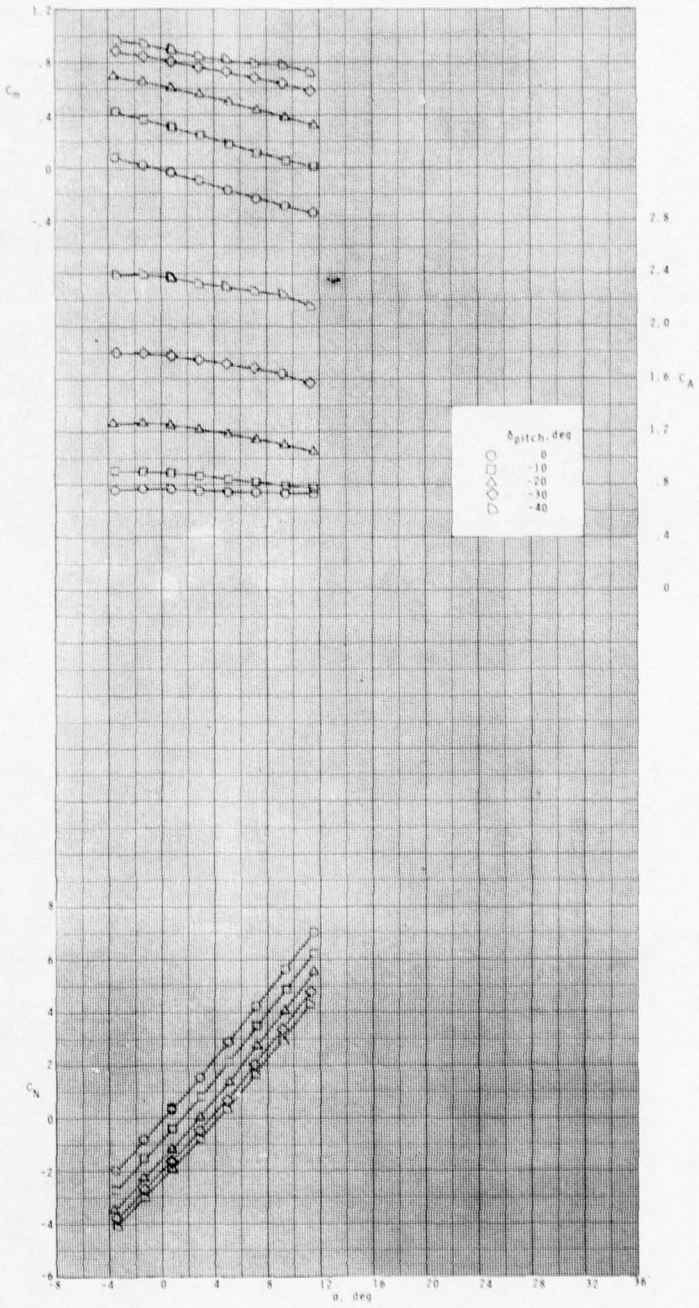

(a) M = 1.60.

Figure 4.- Effect of pitch-control deflections on longitudinal aerodynamic characteristics; $\phi = 0^{o}$, BTW configuration.

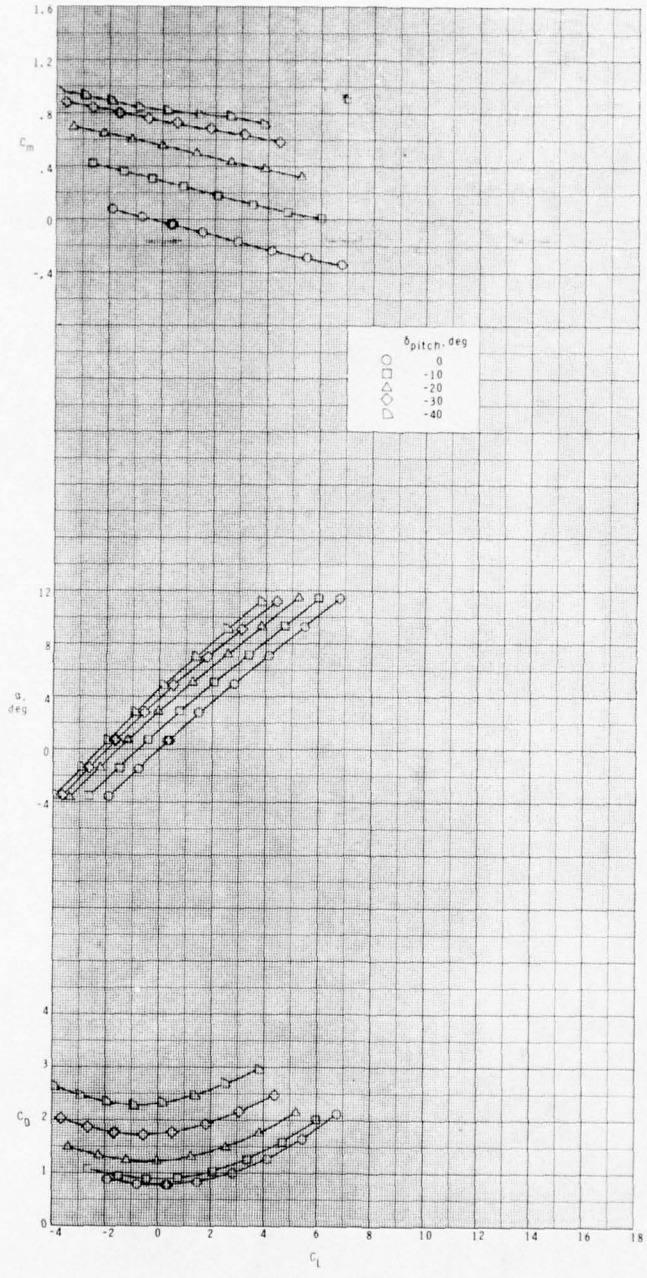

(a) Concluded.

Figure 4.- Continued.

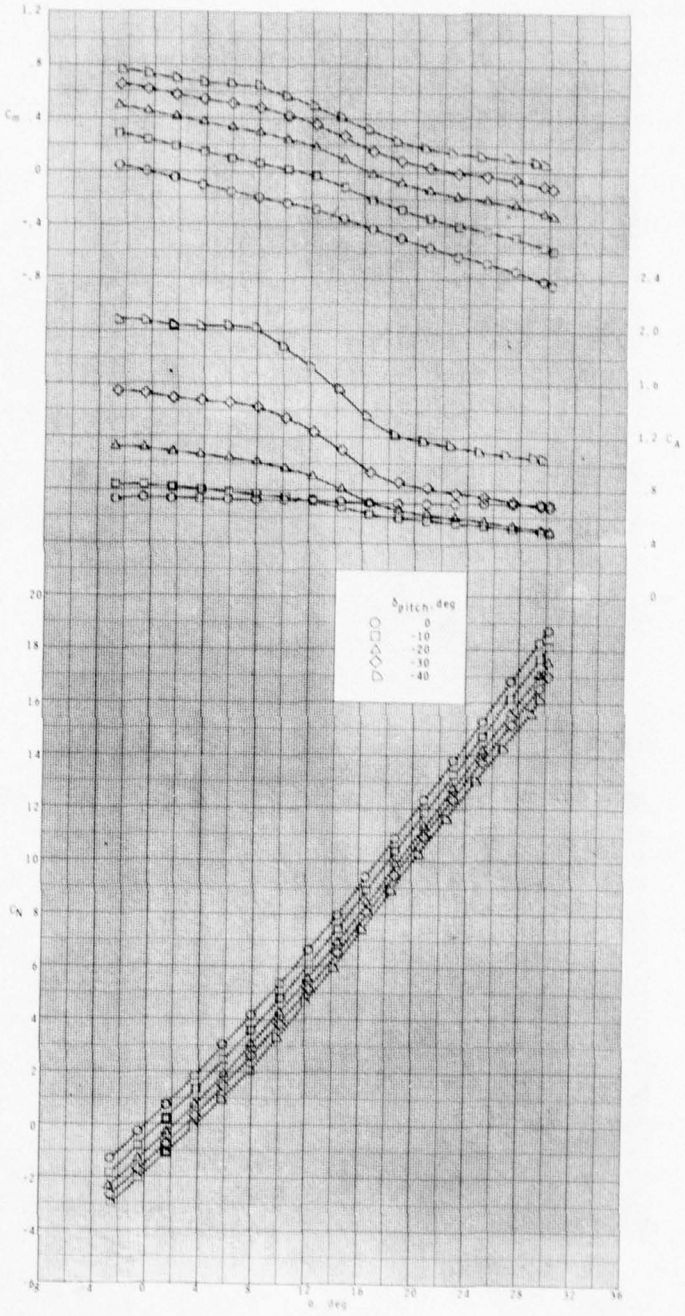

(b) M = 2.10.

Figure 4.- Continued.

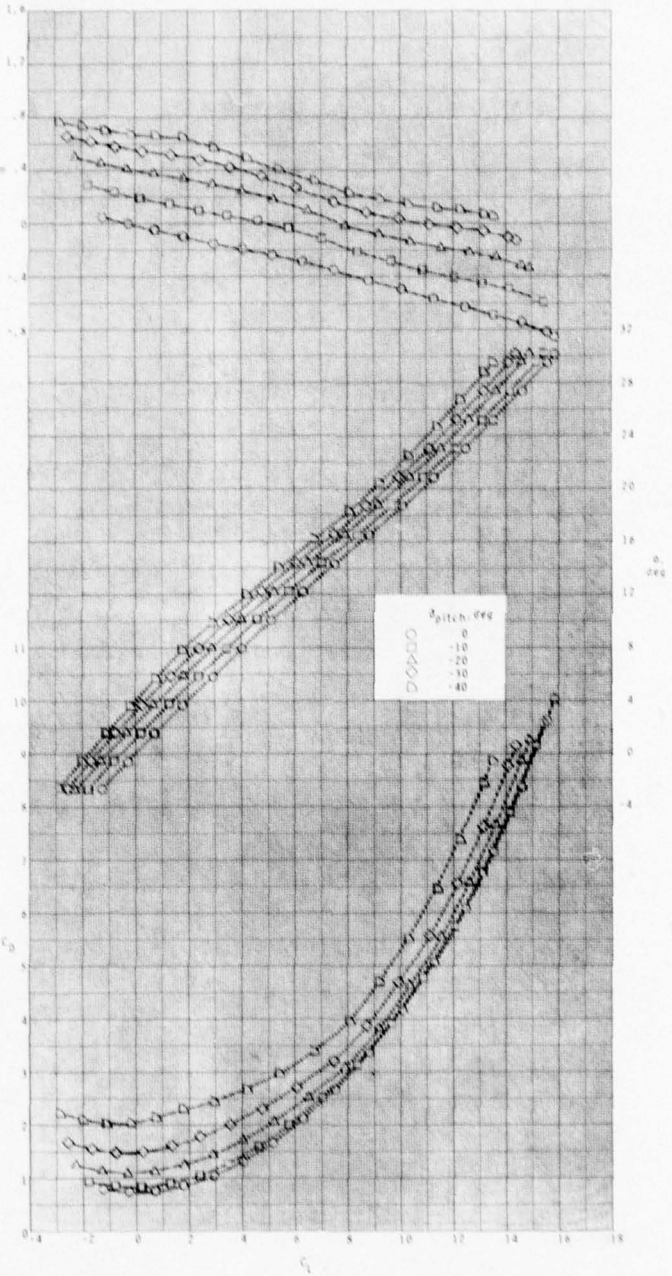

(b) Concluded.

Figure 4.- Continued.

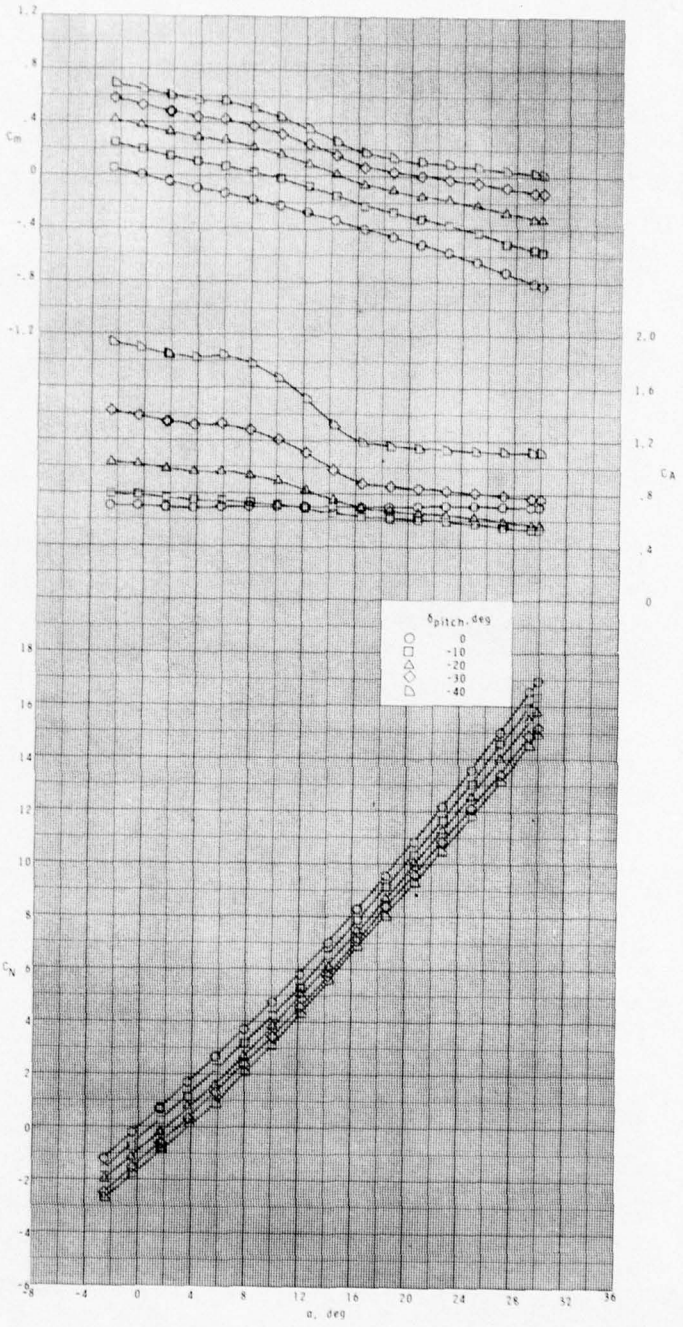

(c) M = 2.50.

Figure 4.- Continued.

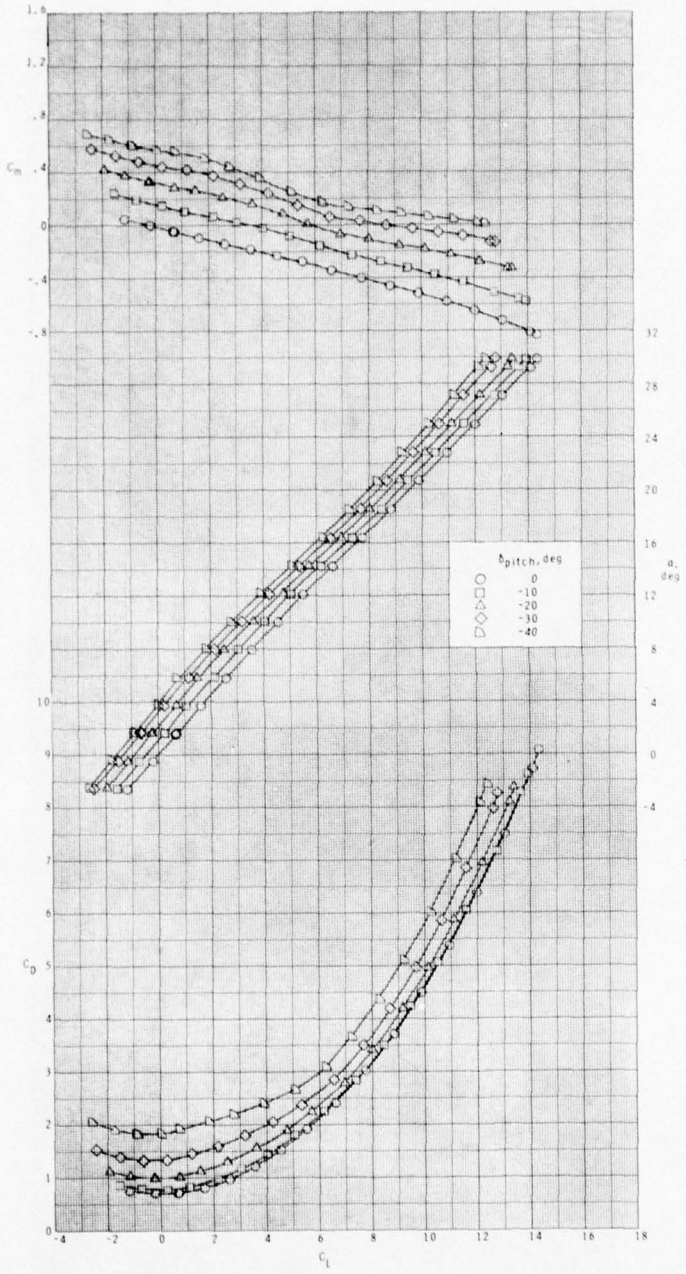

(c) Concluded.

Figure 4.- Continued.

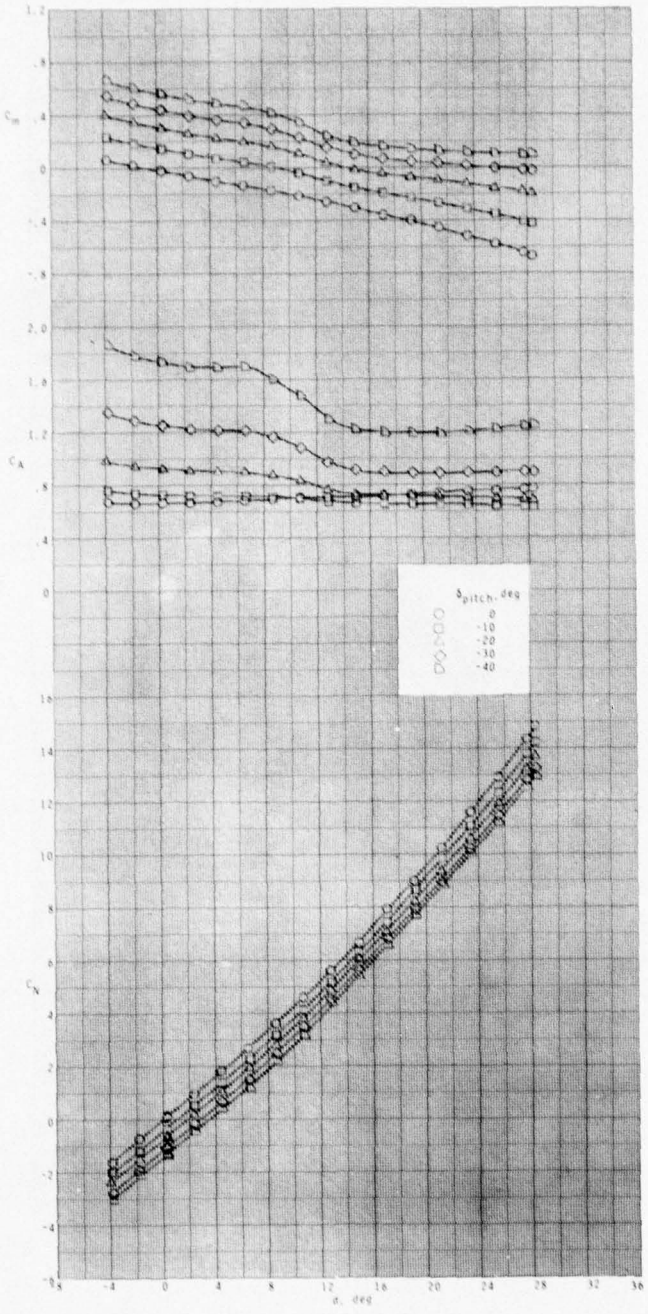

(d) M = 2.86.

Figure 4.- Continued.

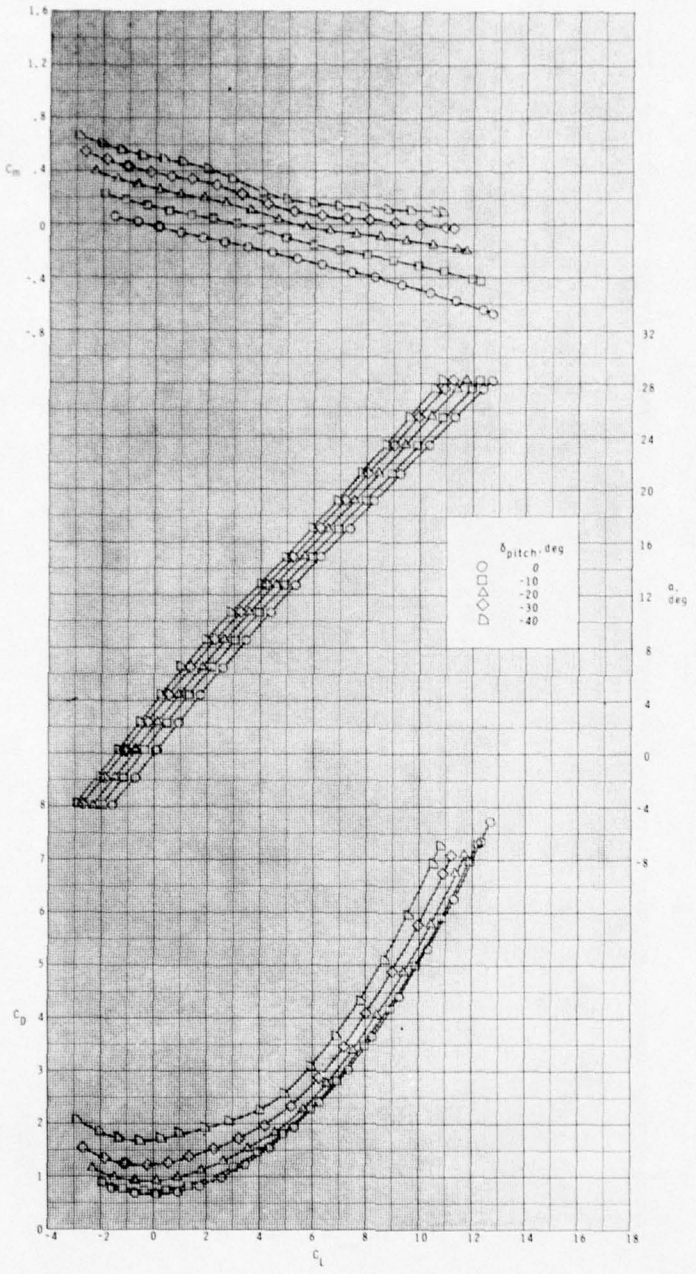

(d) Concluded.

Figure 4.- Continued.

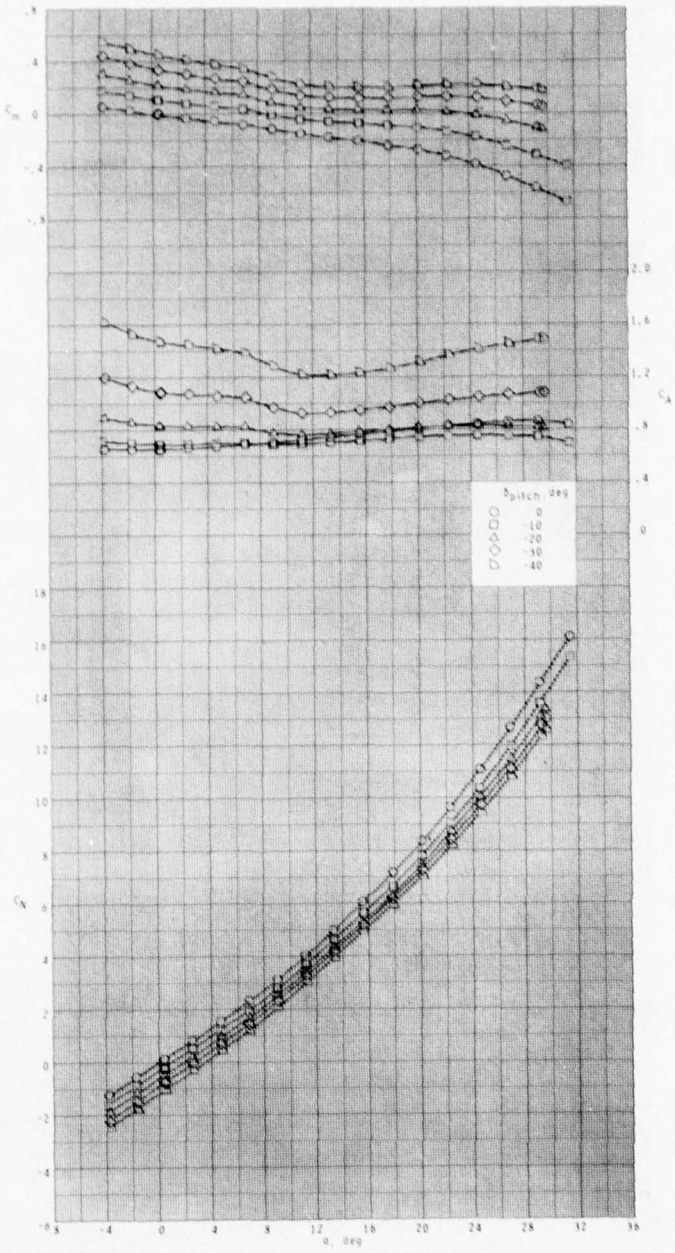

(e) M = 3.95.

Figure 4.- Continued.

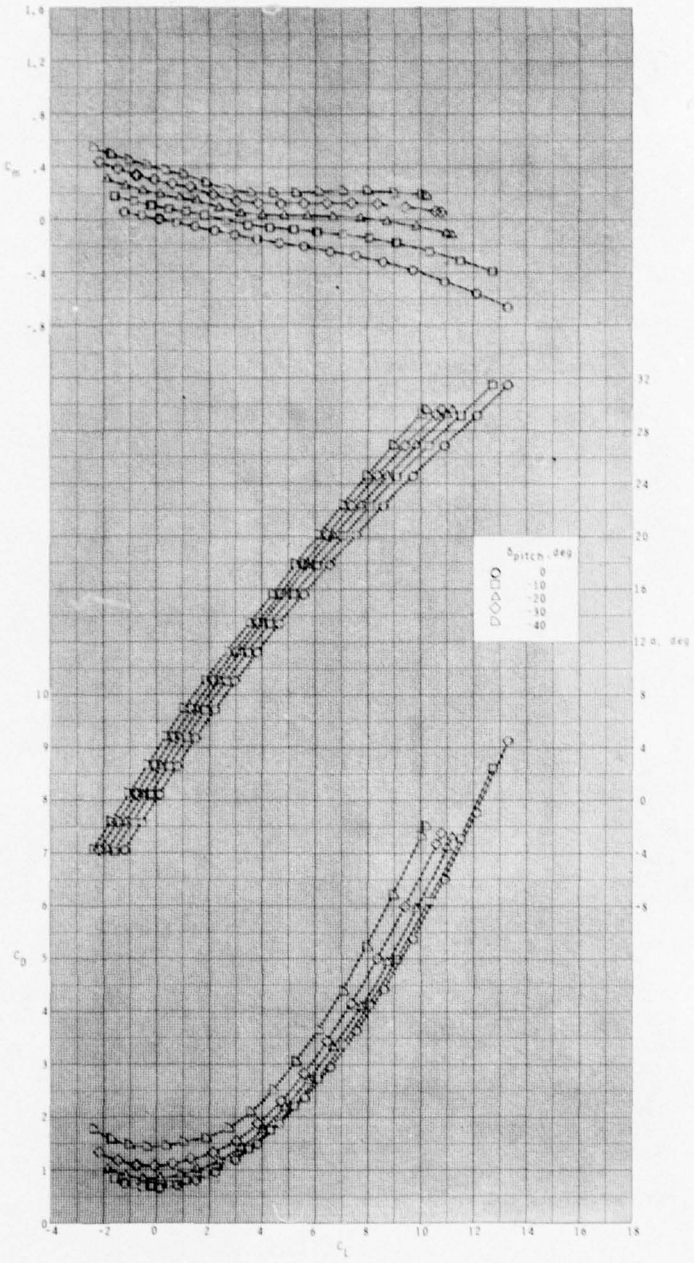

(e) Concluded.

Figure 4.- Continued.

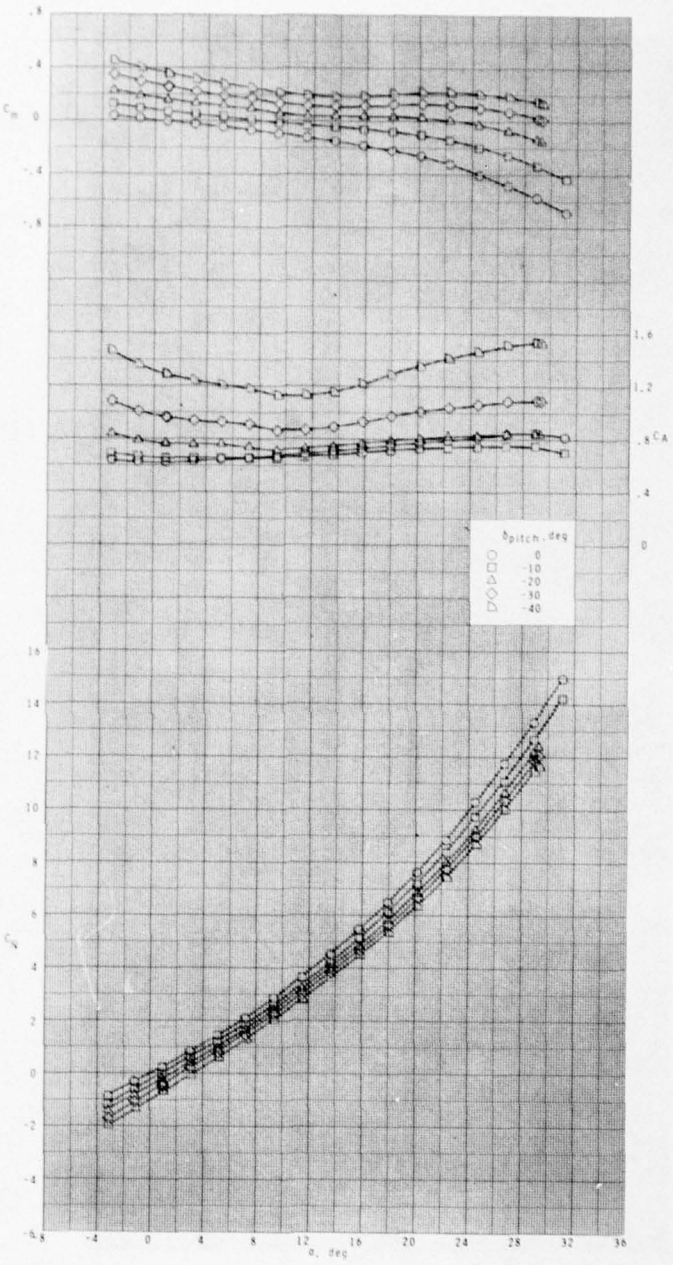

(f) M = 4.63.

Figure 4.- Continued.

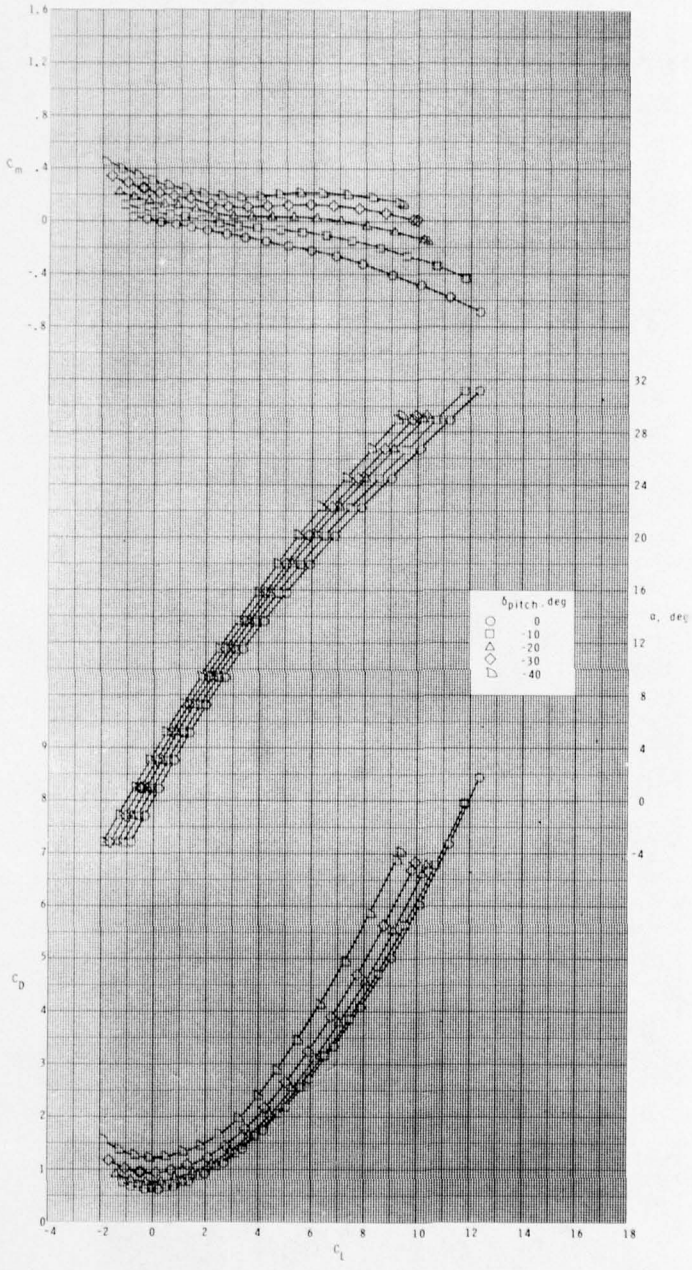

(f) Concluded.

Figure 4.- Concluded.

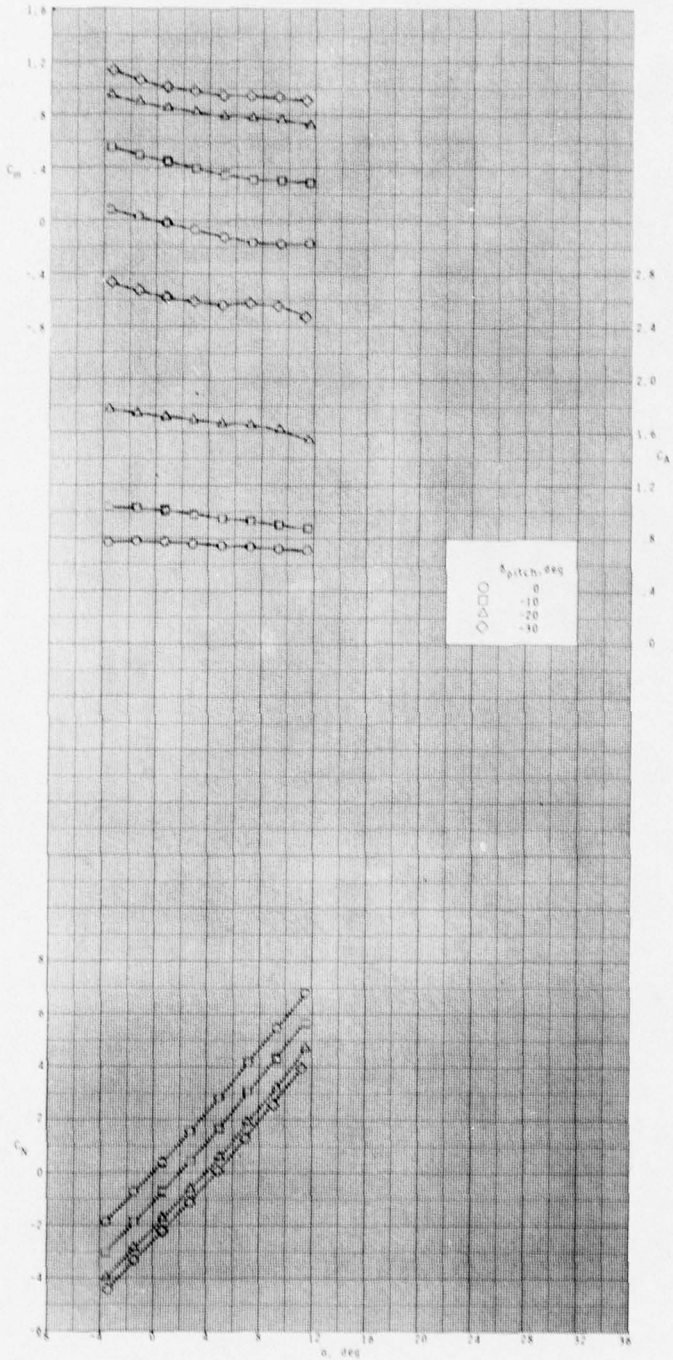

(a) M = 1.60.

Figure 5.- Effect of pitch-control deflections on longitudinal aerodynamic characteristics; $\phi = 45^{o}$, BTW configuration.

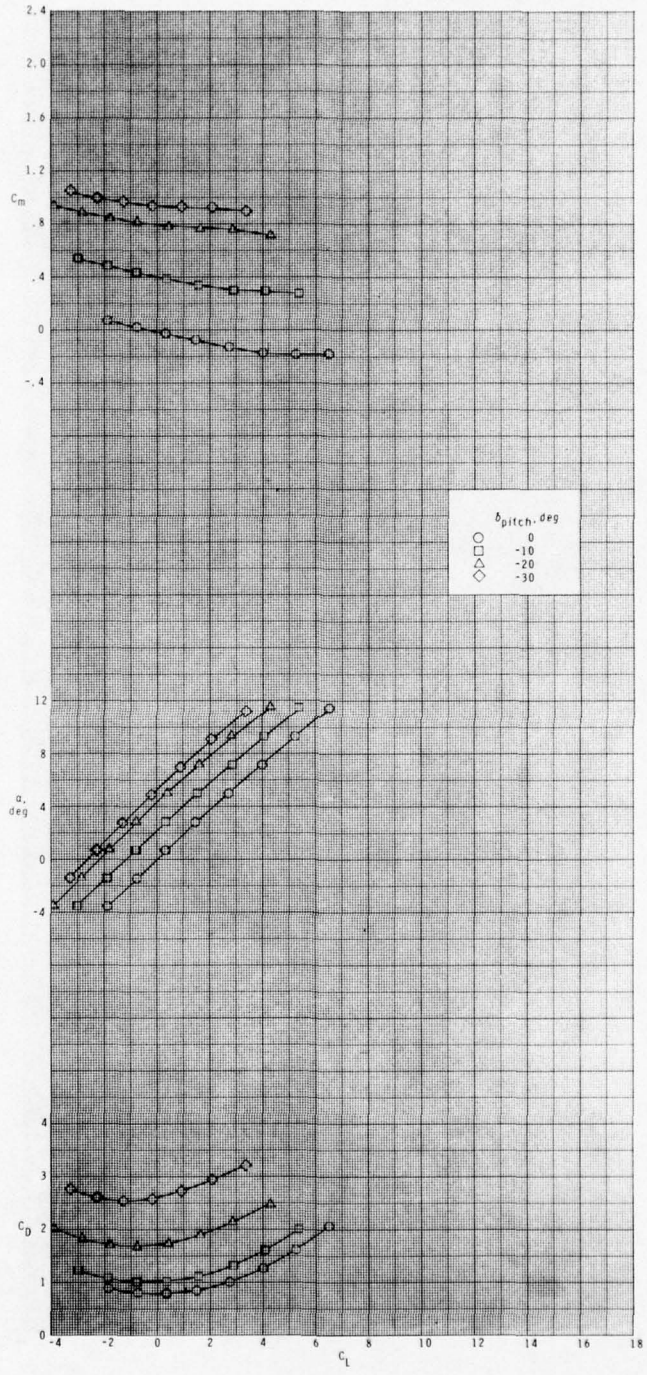

(a) Concluded.

Figure 5.- Continued.

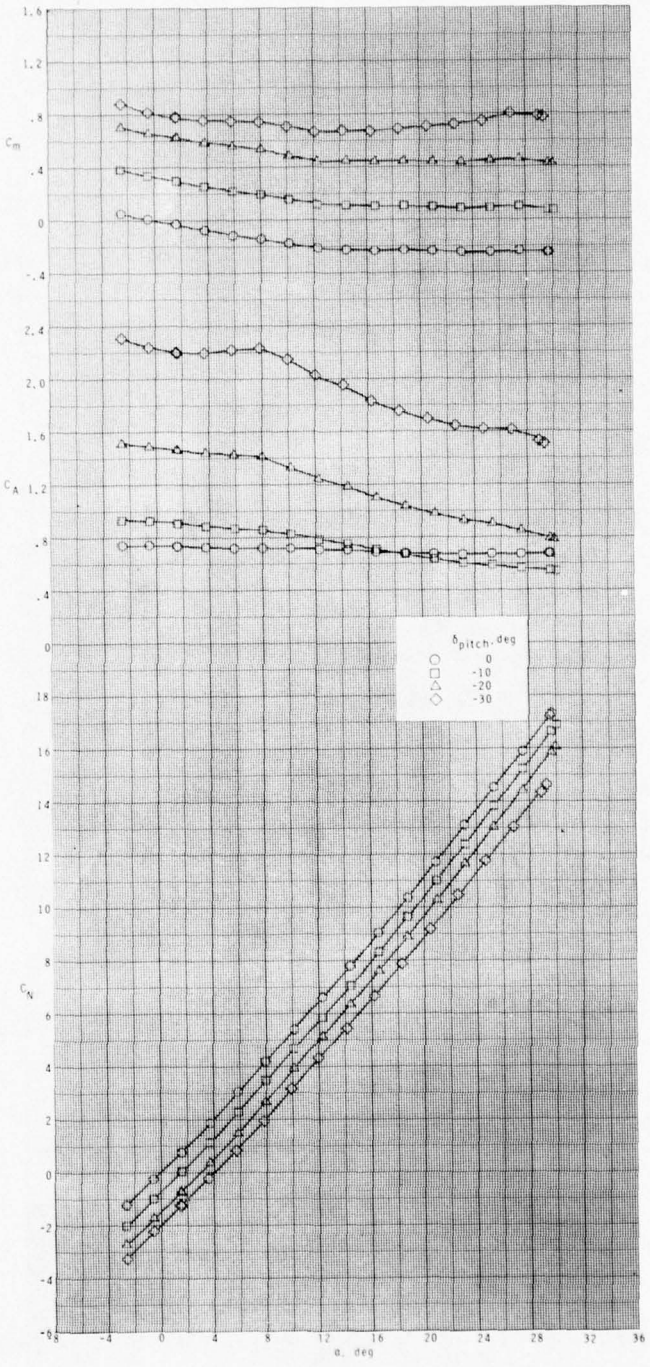

(b) M = 2.10.

Figure 5.- Continued.

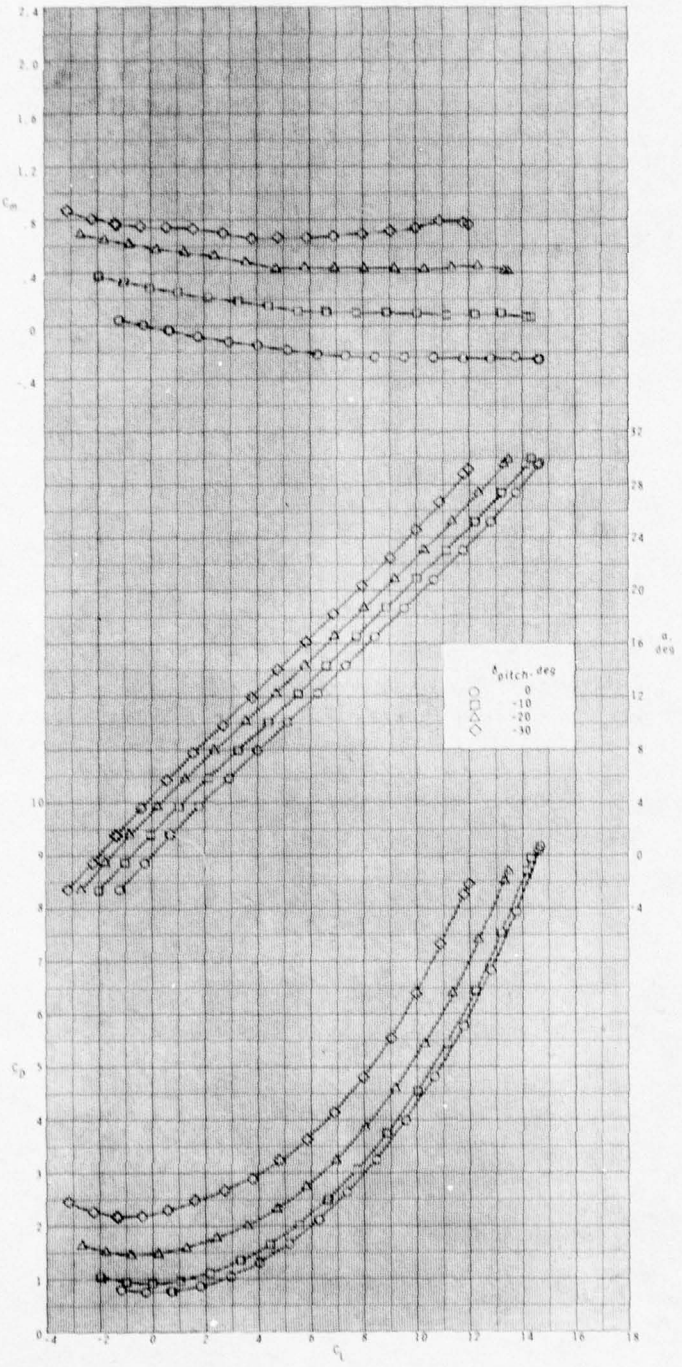

(b) Concluded.

Figure 5.- Continued.

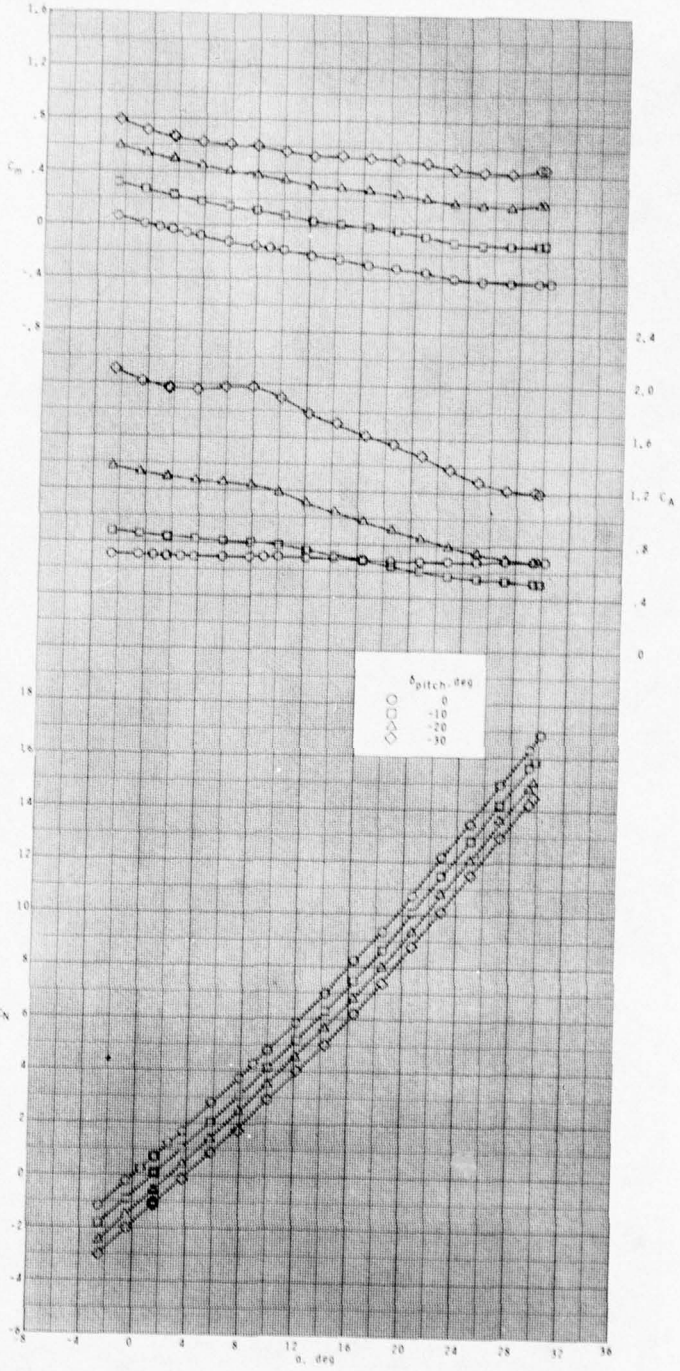

(c) M = 2.50.

Figure 5.- Continued.

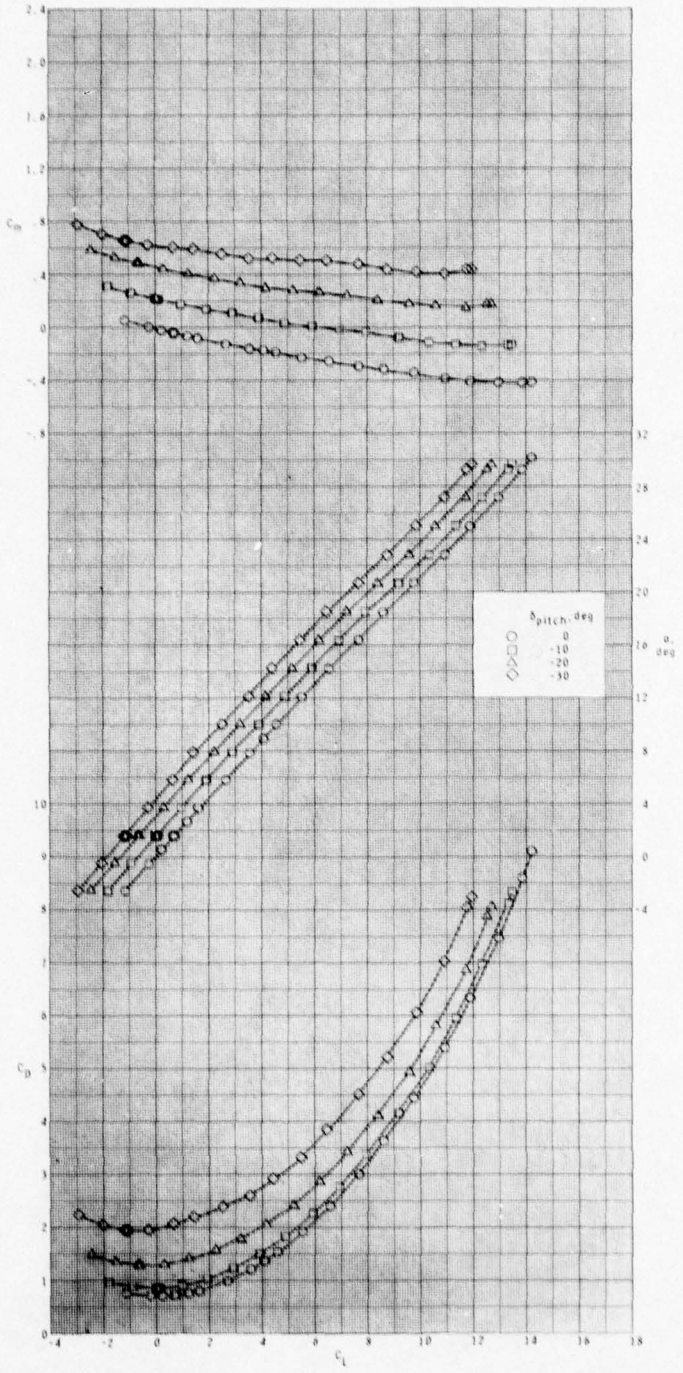

(c) Concluded.

Figure 5.- Continued.

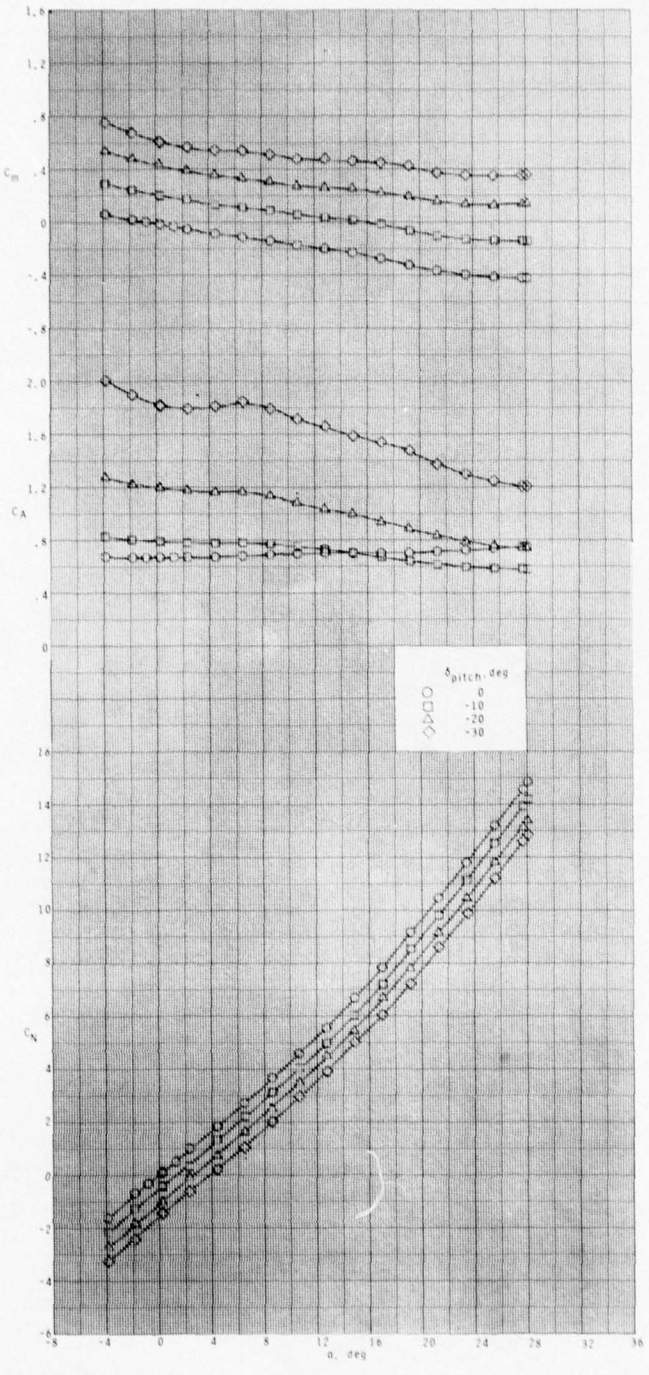

(d) M = 2.86.

Figure 5.- Continued.

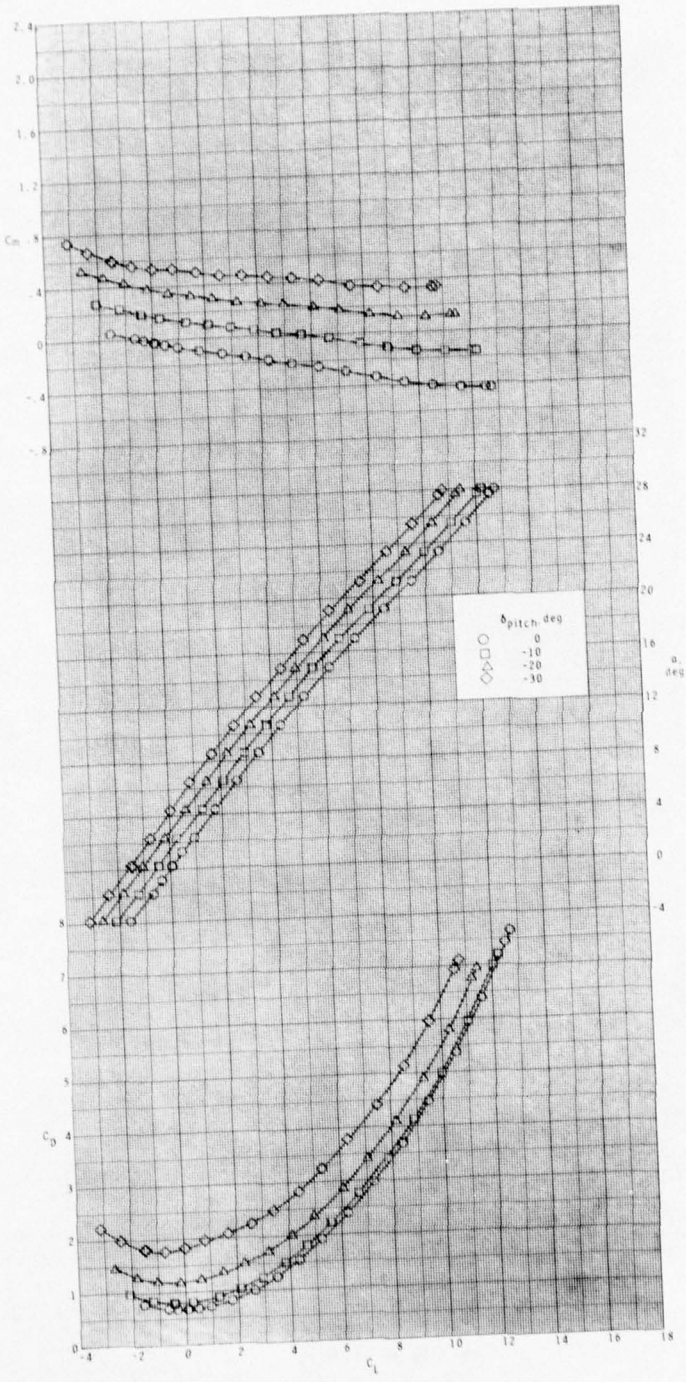

(d) Concluded.

Figure 5.- Continued.

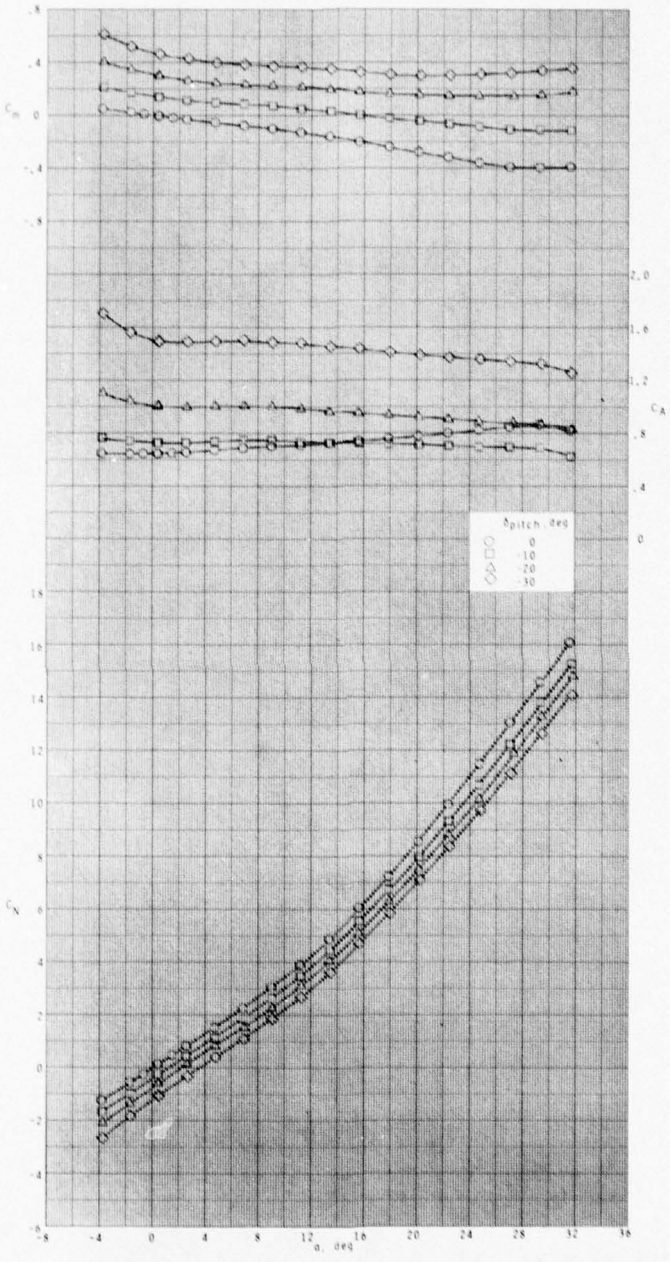

(e) M = 3.95.

Figure 5.- Continued.

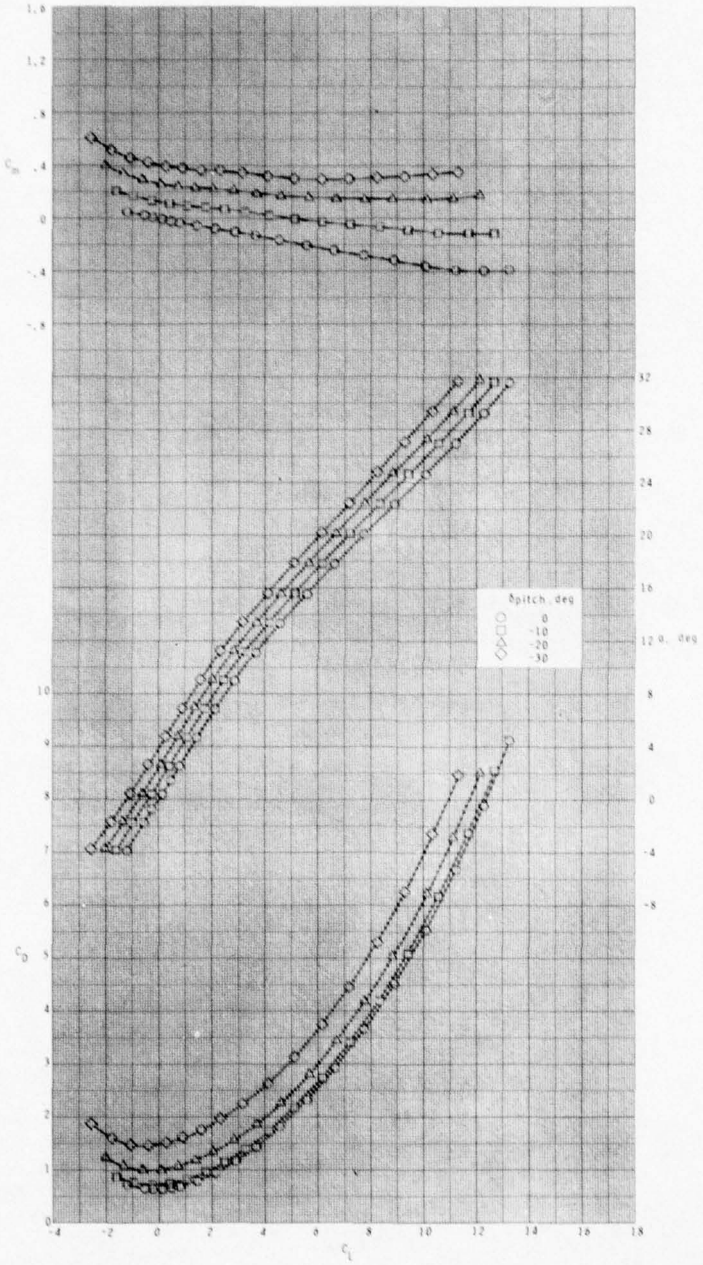

(e) Concluded.

Figure 5.- Continued.

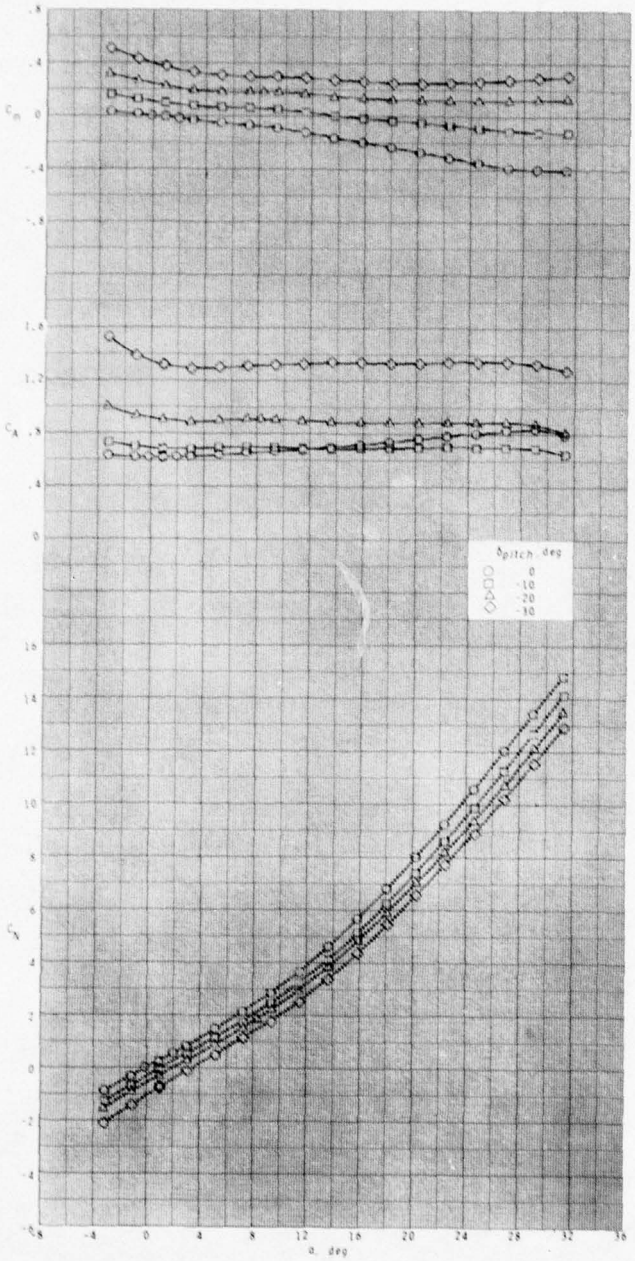

(f) M = 4.63.

Figure 5.- Continued.

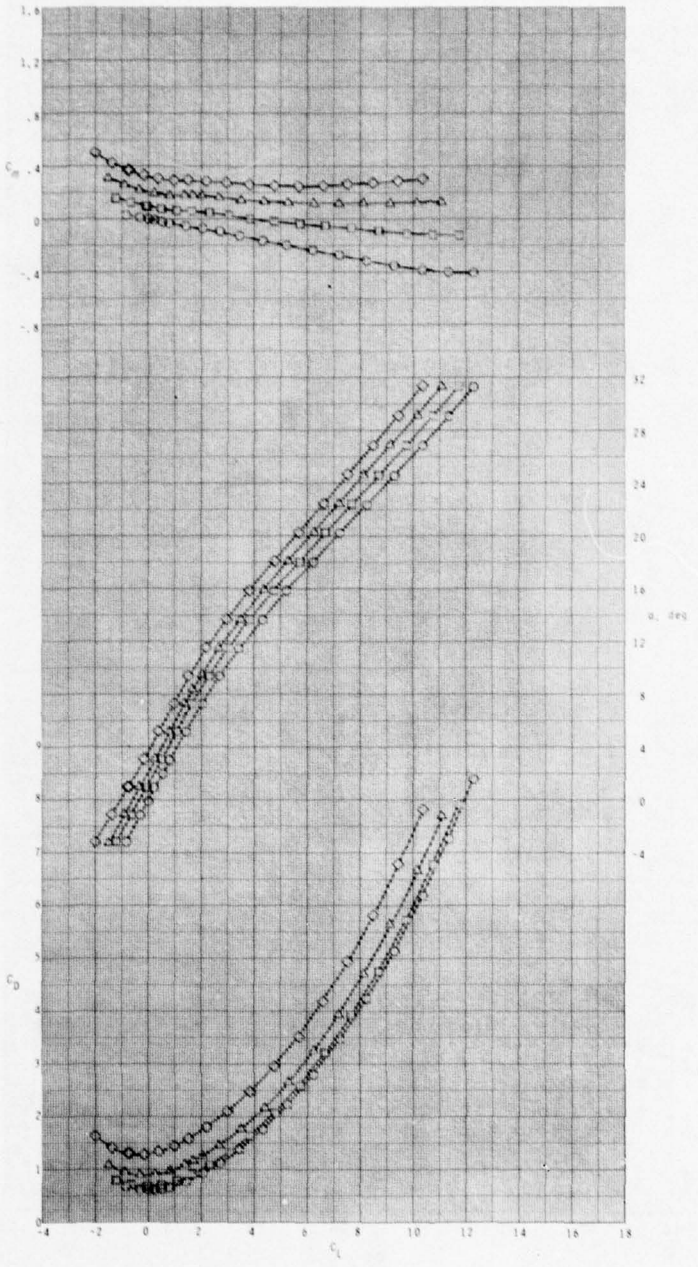

(f) Concluded.

Figure 5.- Concluded.

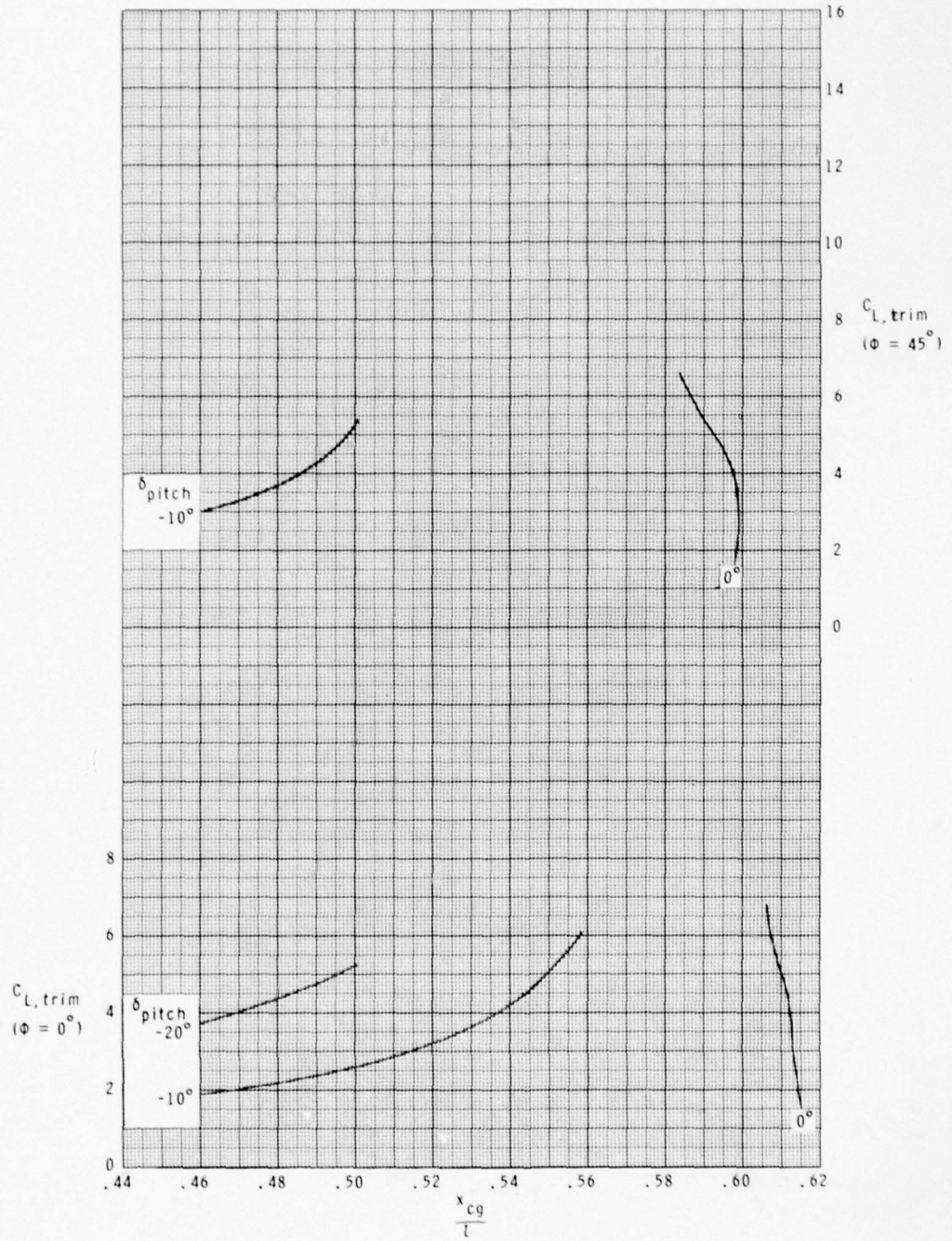

(a) M = 1.60.

Figure 6.- Variation of trimmed lift coefficient with center-of-gravity location; BTW configuration.

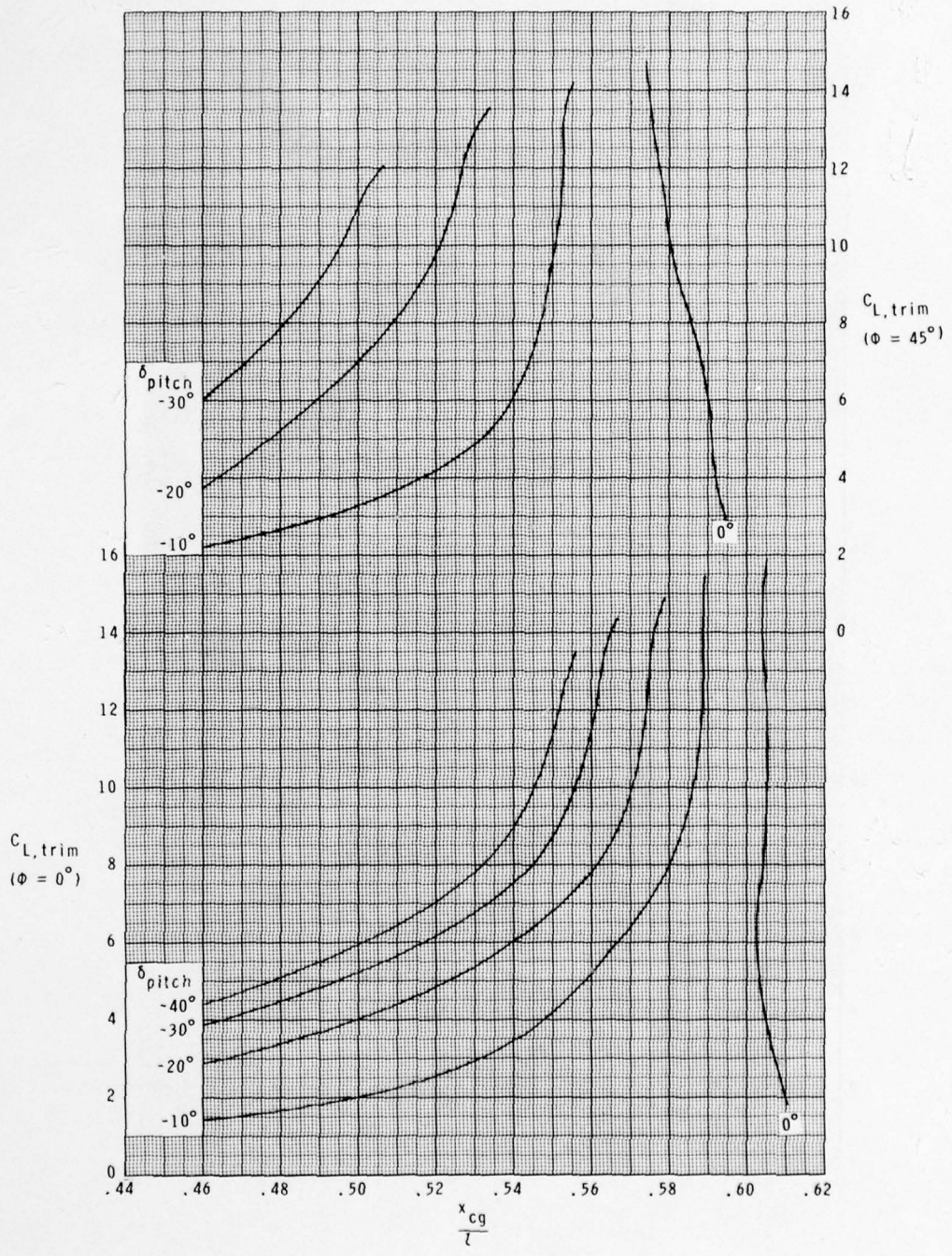

(b) M = 2.10.

Figure 6.- Continued.

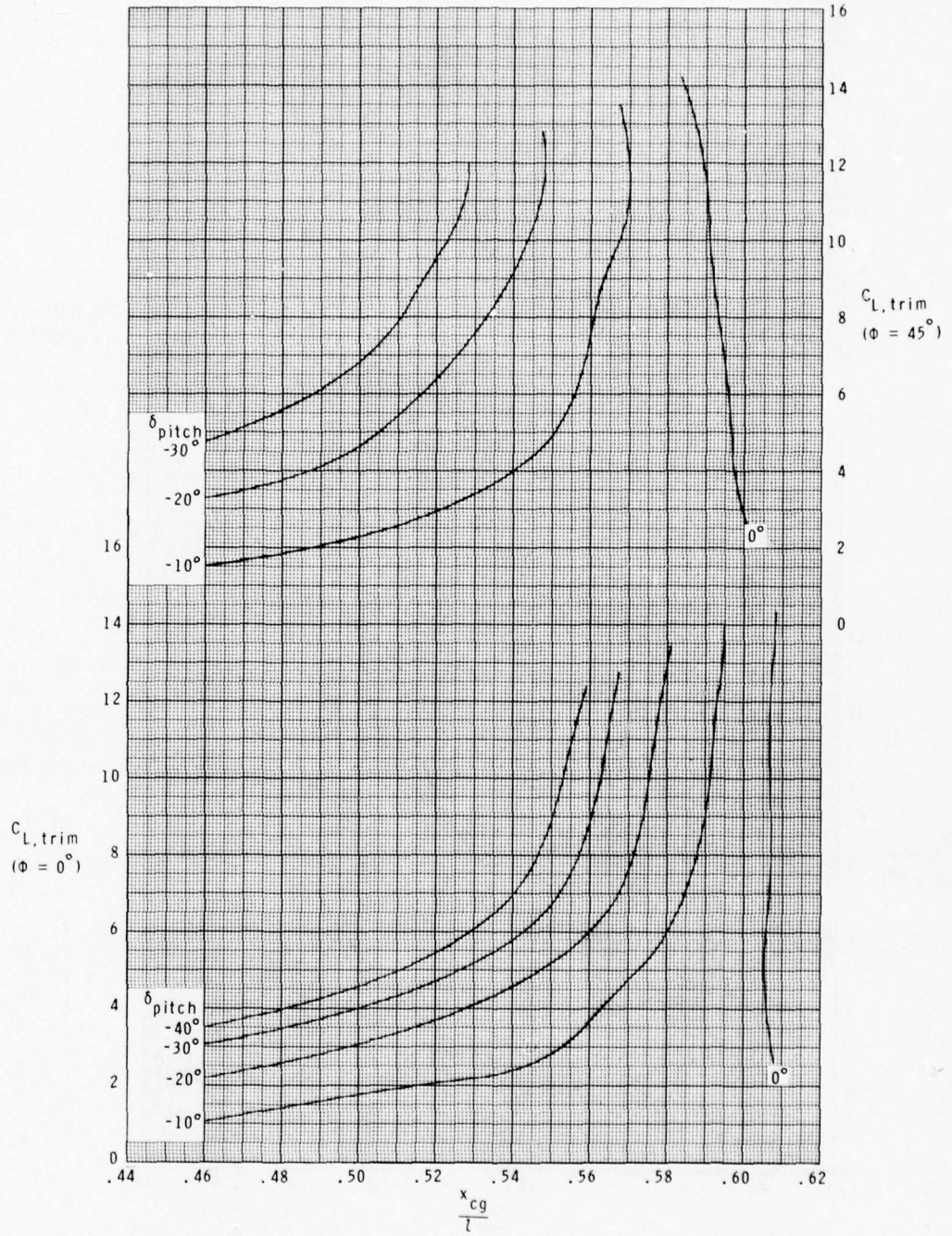

(c) M = 2.50.

Figure 6.- Continued.

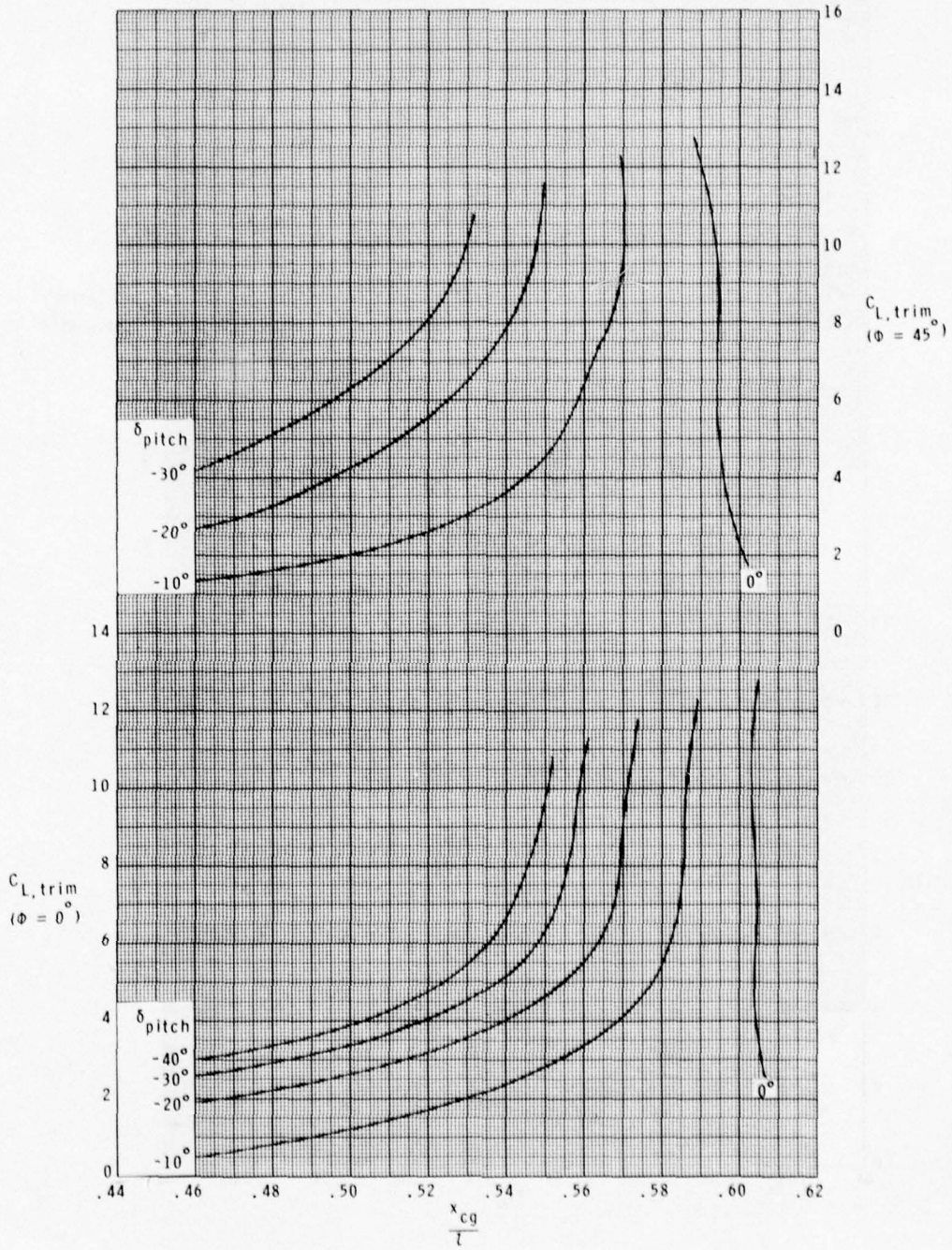

(d) M = 2.86.

Figure 6.- Continued.

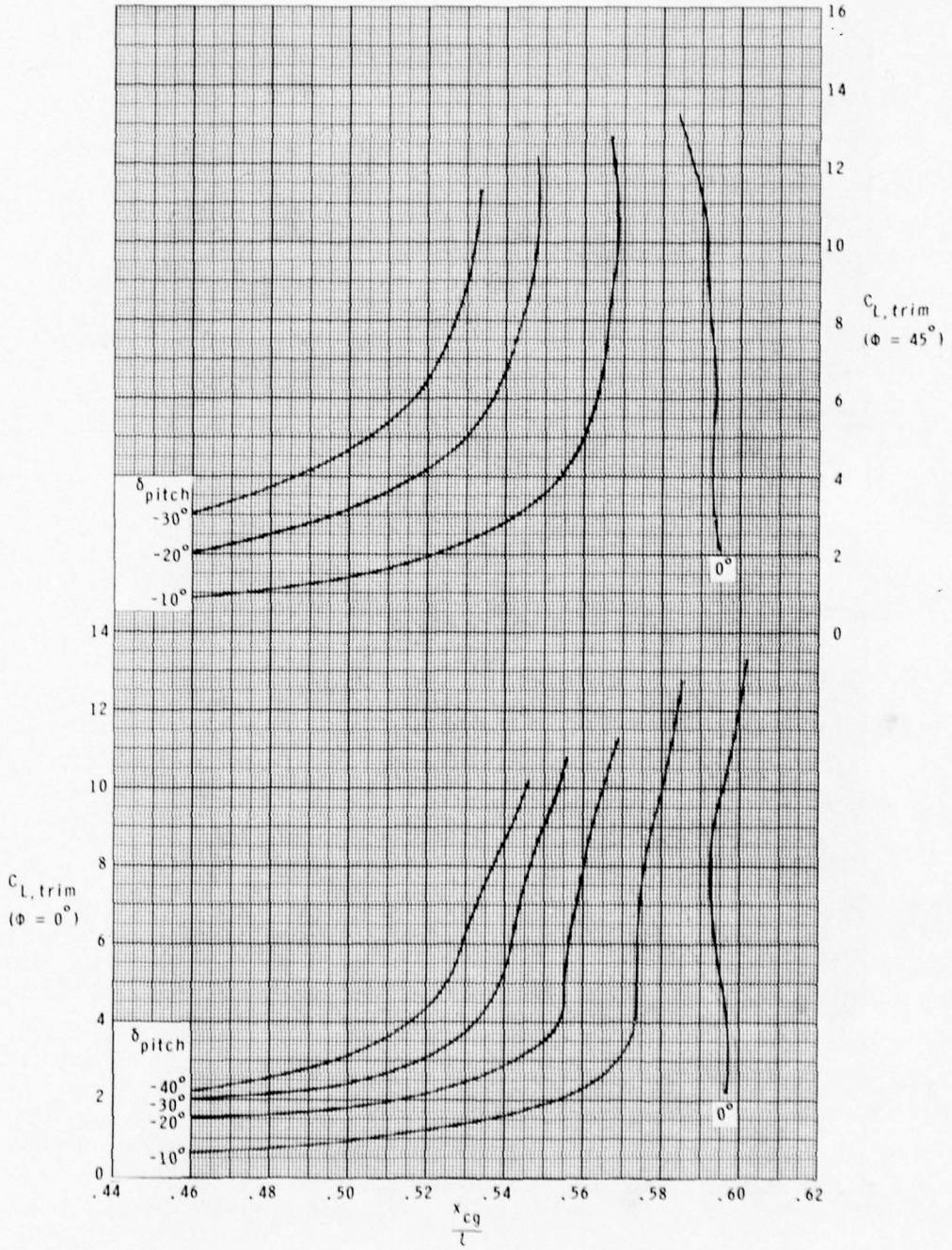

(e) M = 3.95.

Figure 6.- Continued.

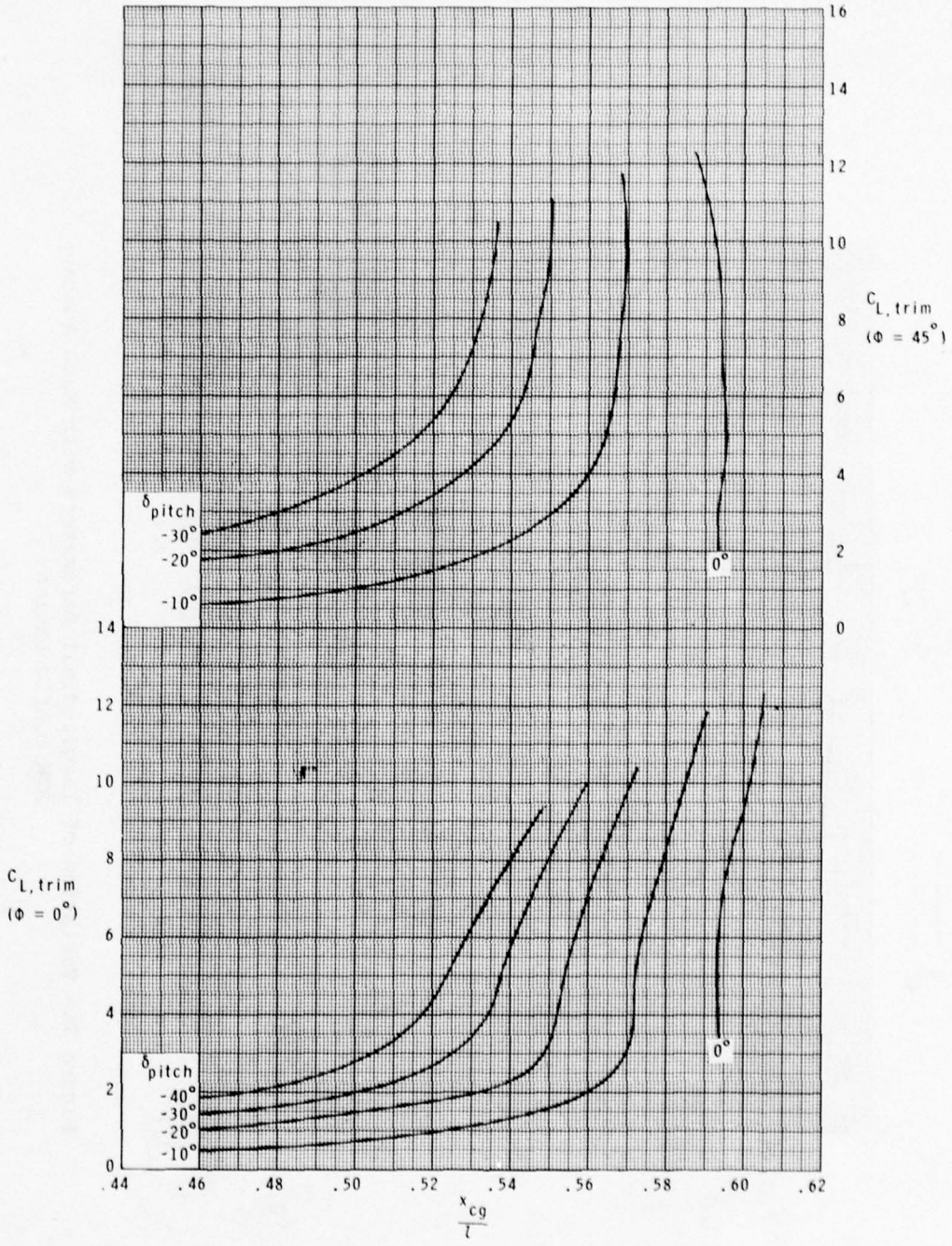

(f) M = 4.63.

Figure 6.- Concluded.

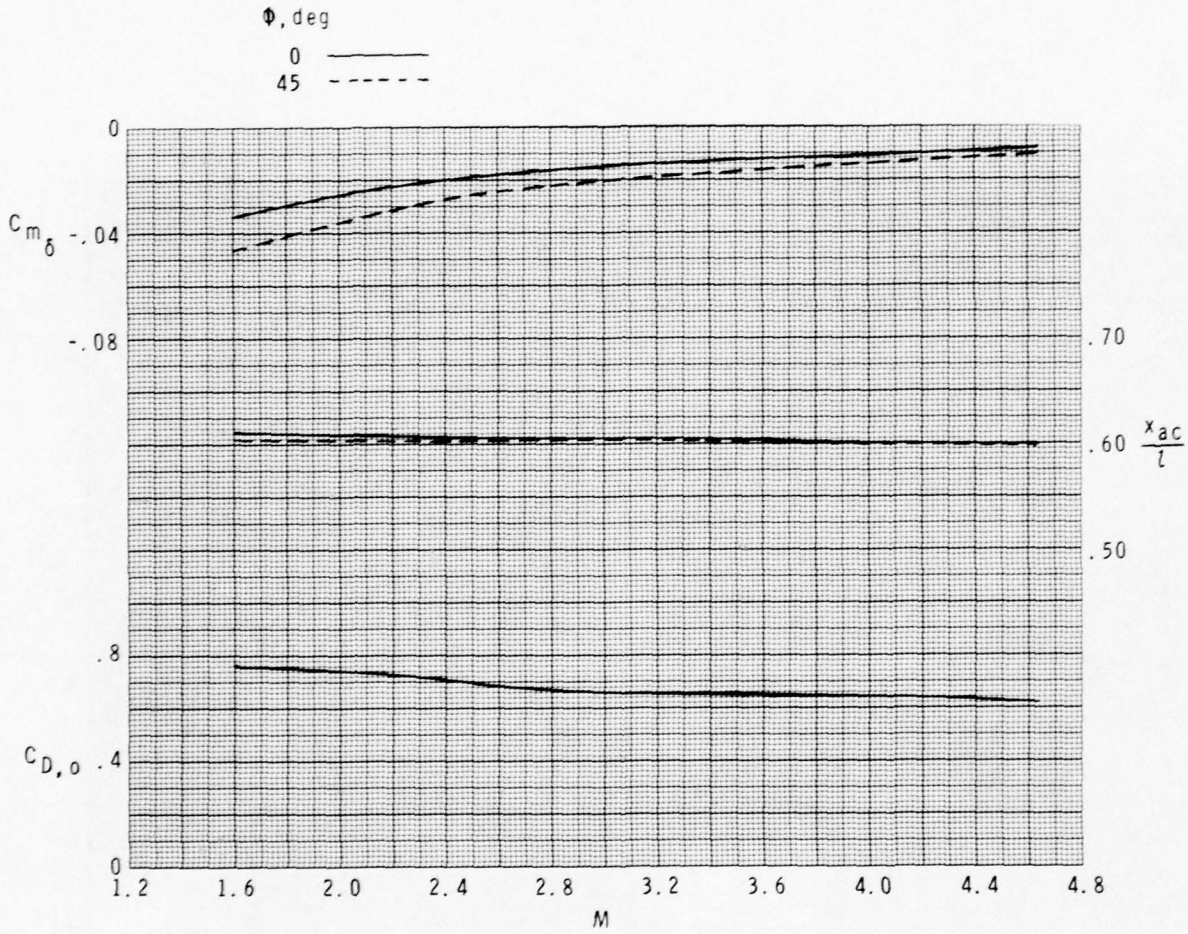

Figure 7.- Variation of longitudinal parameters with Mach number; BTW configuration.

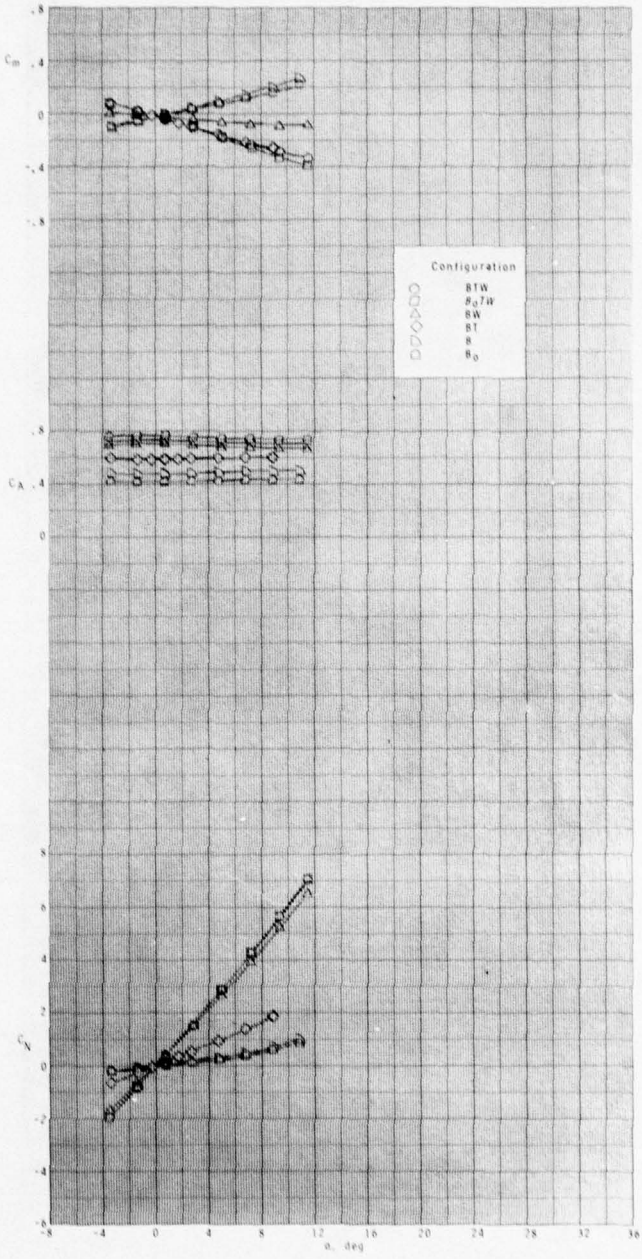

(a) M = 1.60.

Figure 8.- Effect of component parts on the longitudinal aerodynamic characteristics at $\phi = 0^o$.

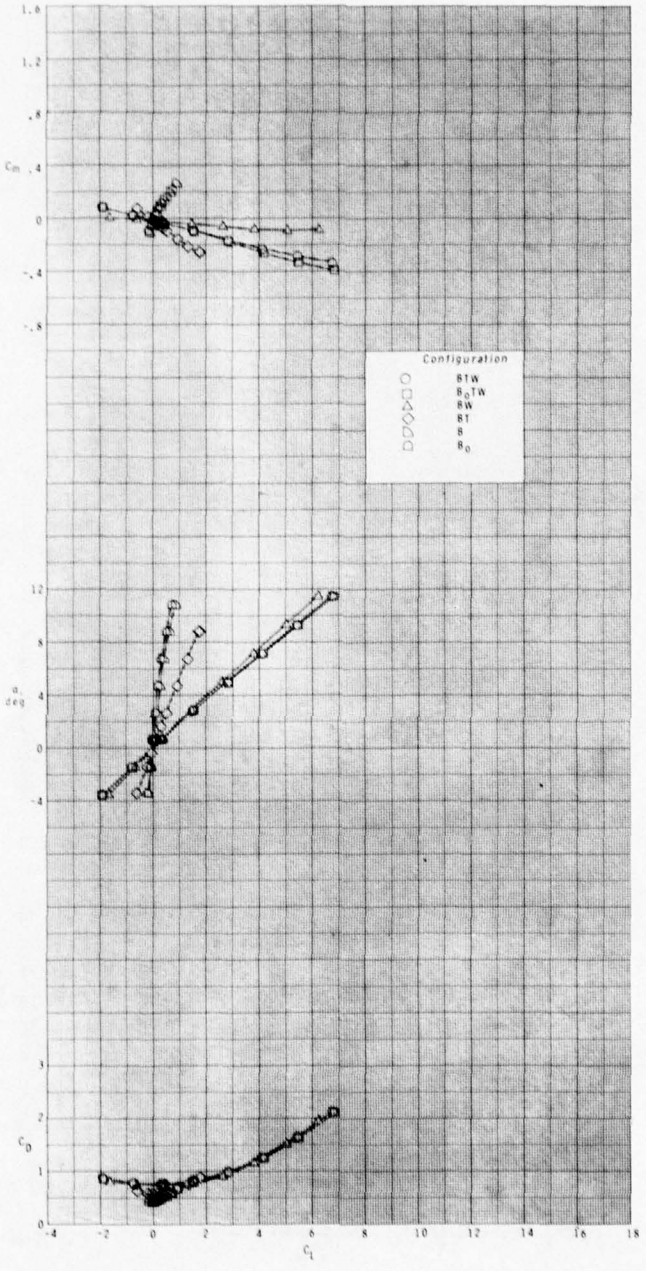

(a) Concluded.

Figure 8.- Continued.

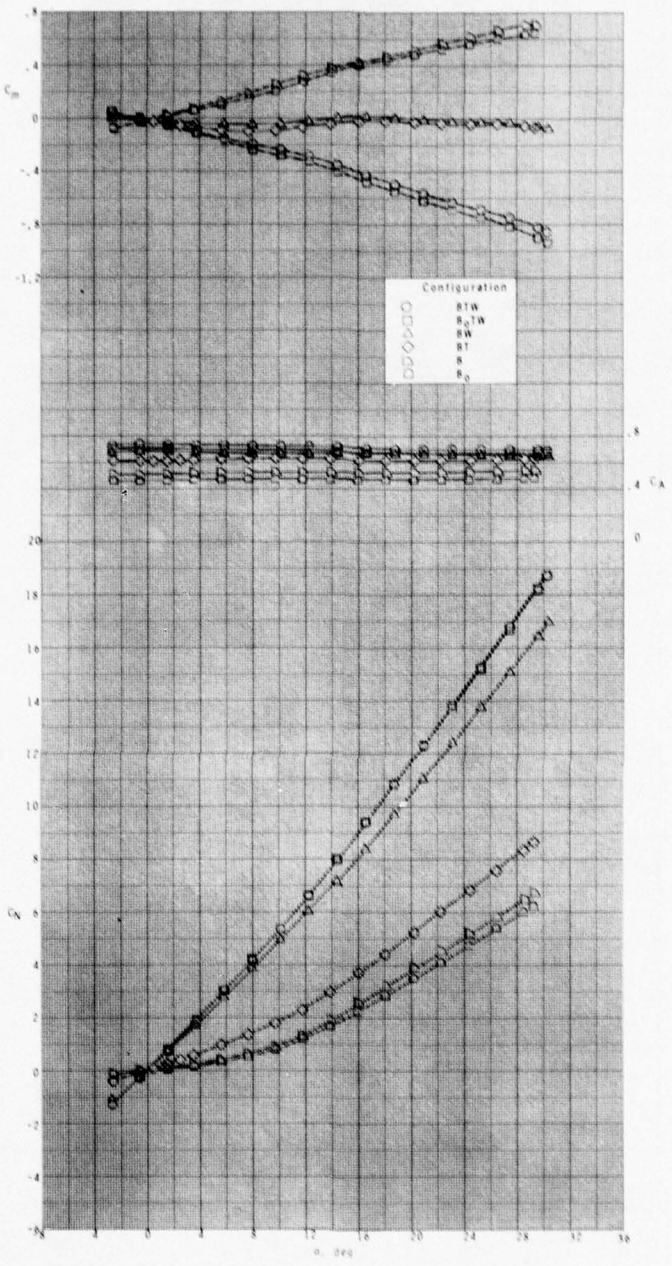

(b) M = 2.10.

Figure 8.- Continued.

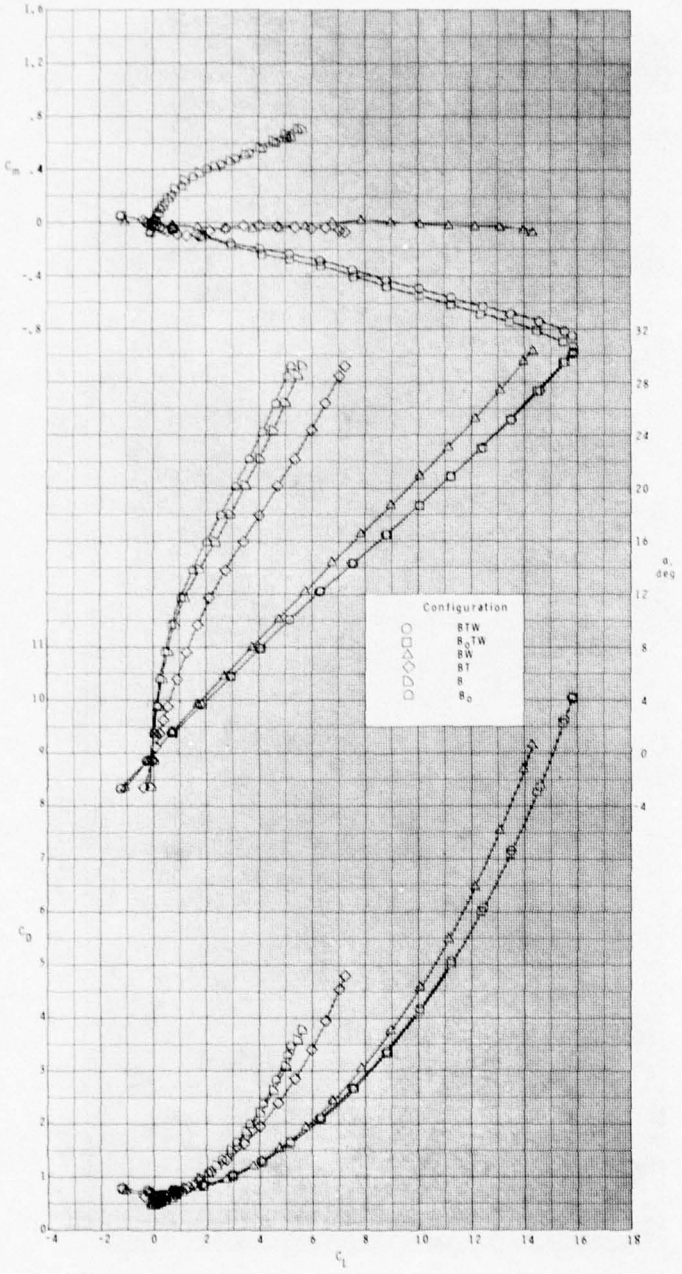

(b) Concluded.

Figure 8.- Continued.

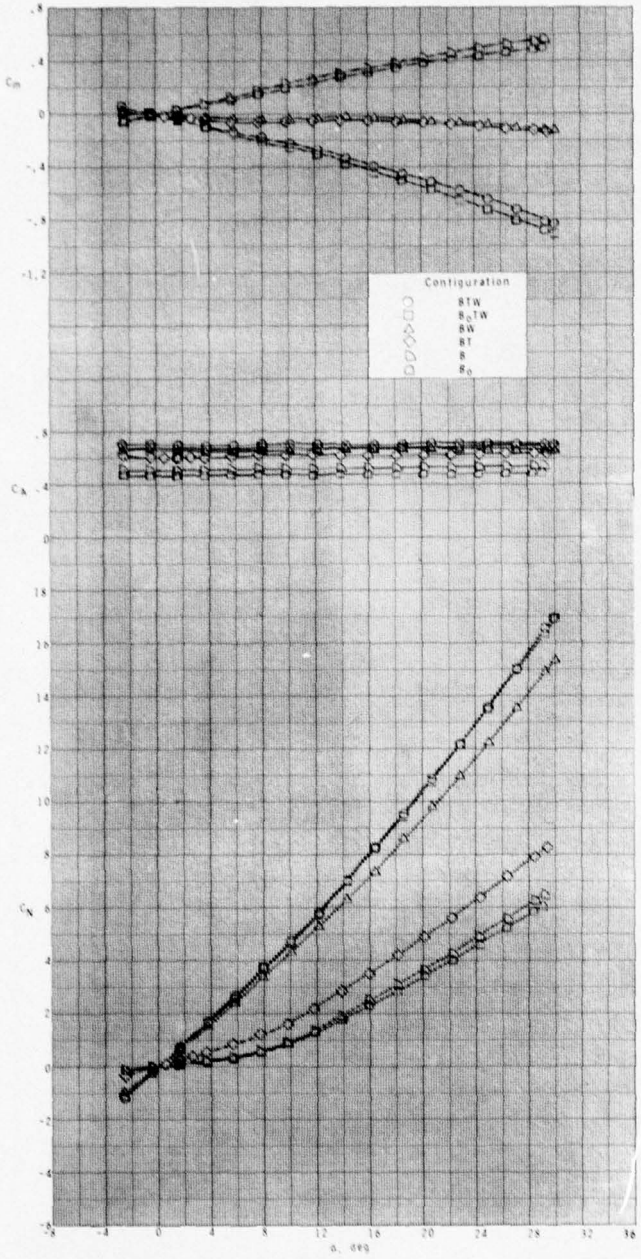

(c) M = 2.50.

Figure 8.- Continued.

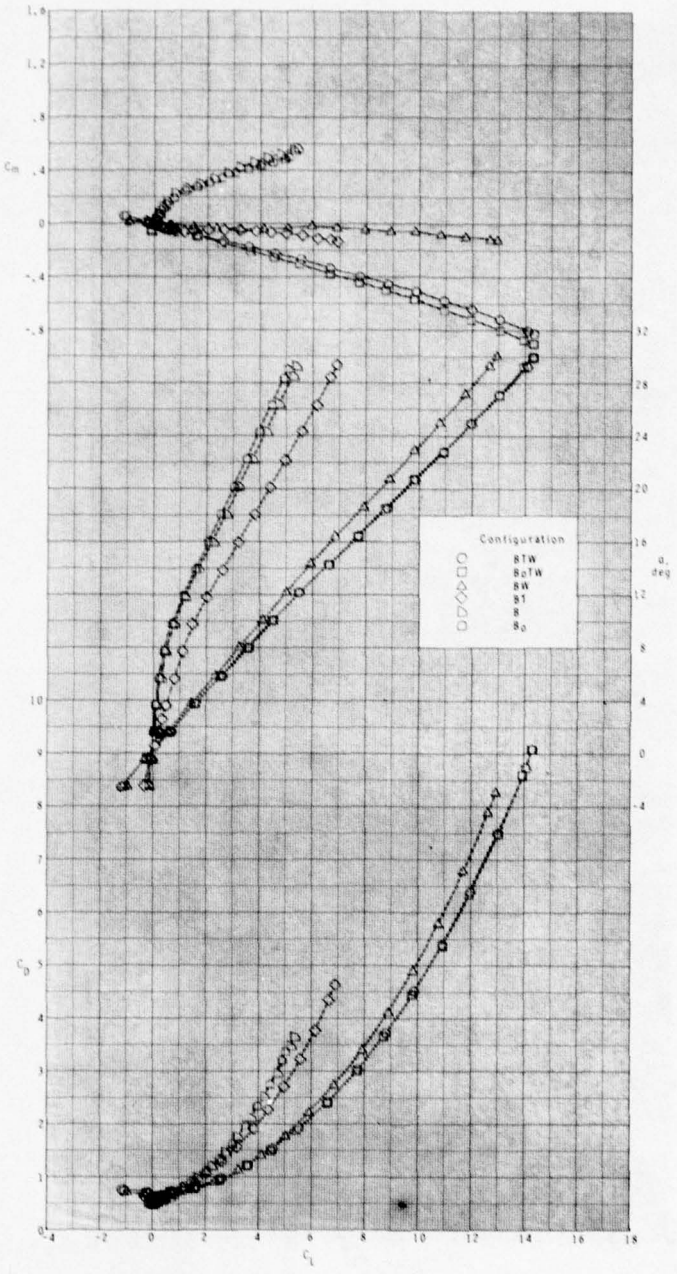

(c) Concluded.

Figure 8.- Continued.

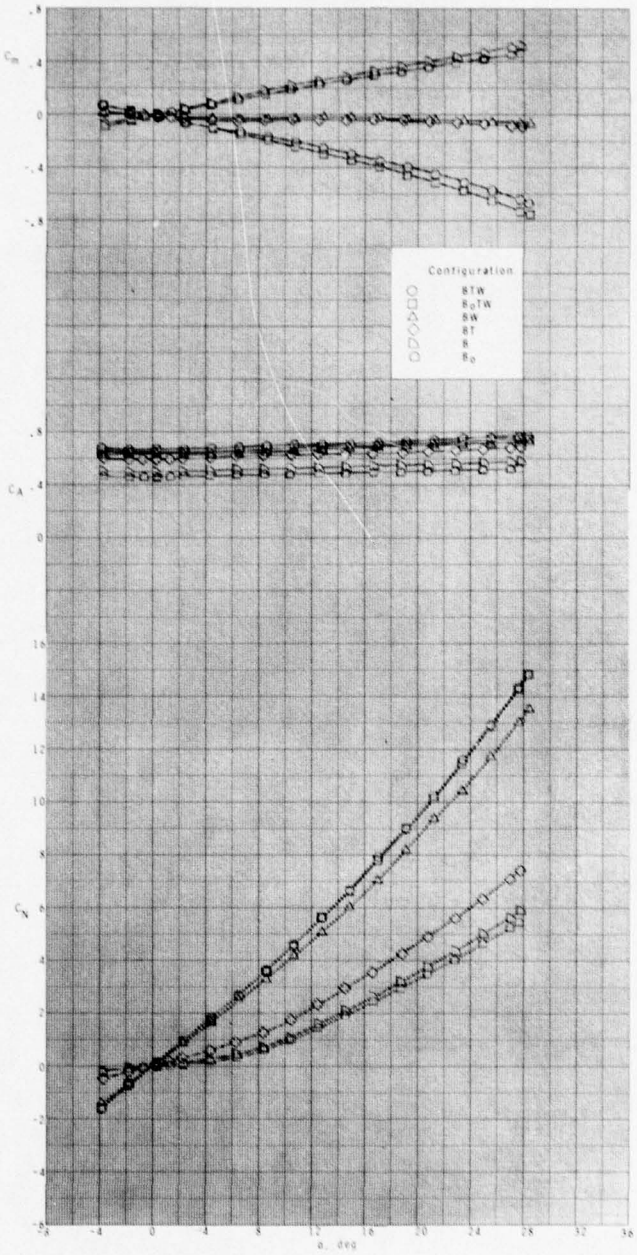

(d) M = 2.86.

Figure 8.- Continued.

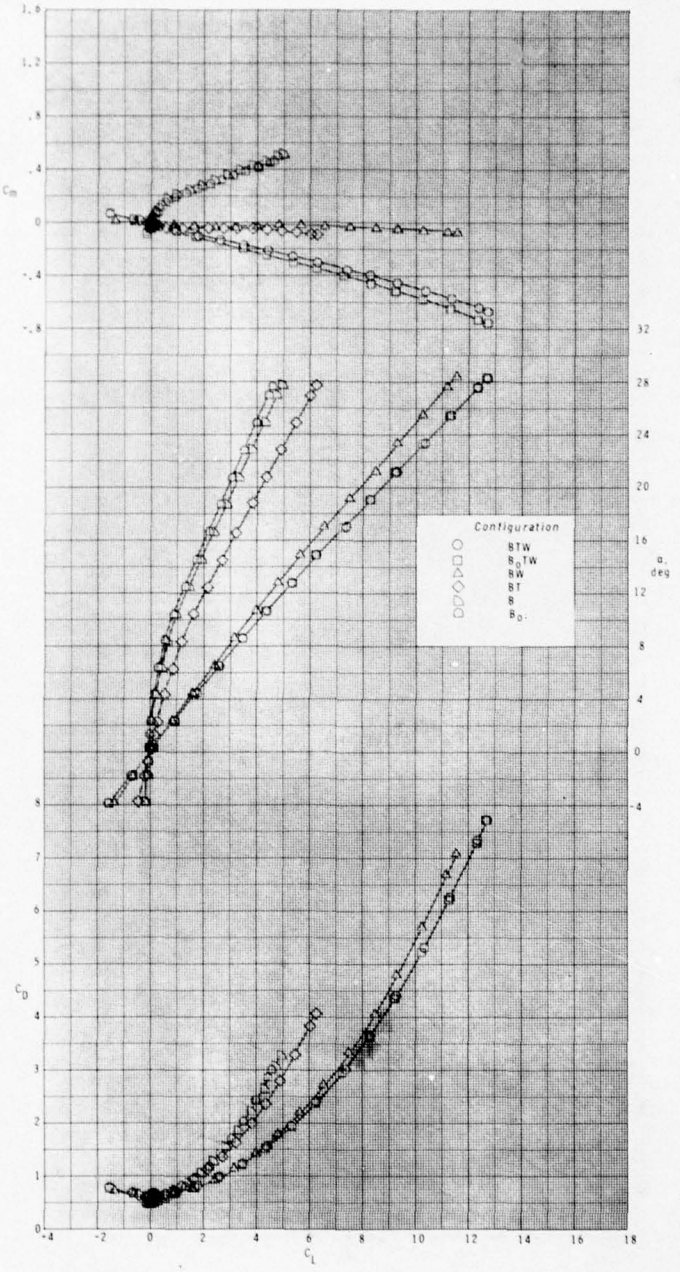

(d) Concluded.

Figure 8.- Concluded.

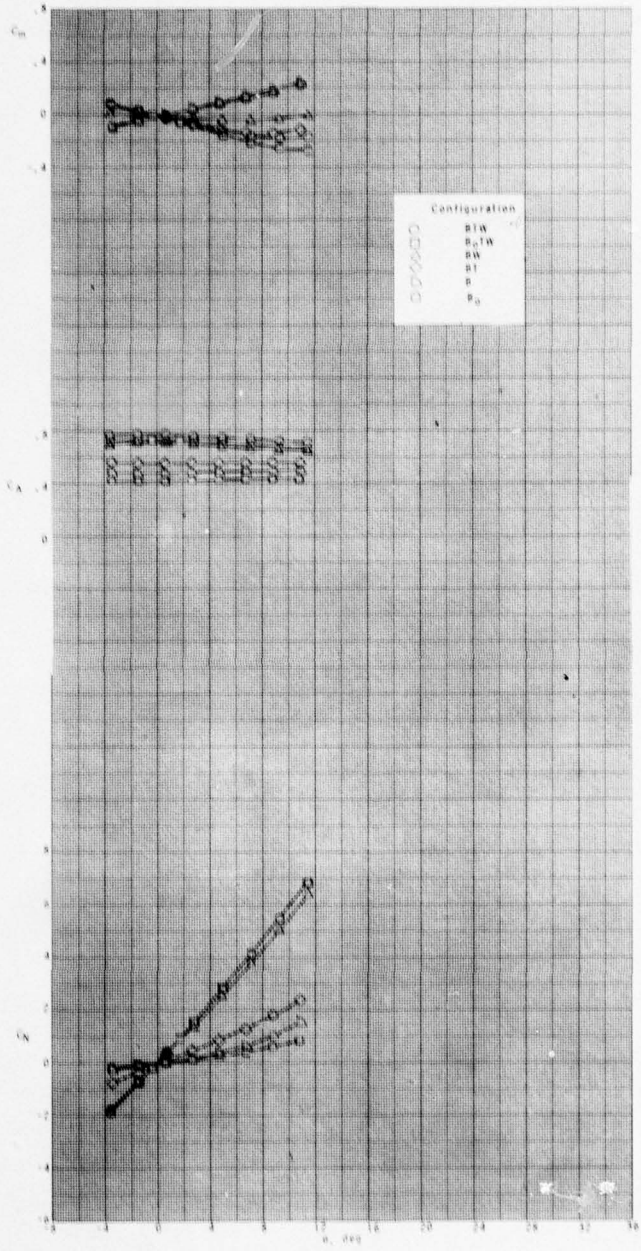

(a) M = 1.60.

Figure 9.- Effect of component parts on the longitudinal aerodynamic characteristics at $\phi = 45^{o}$.

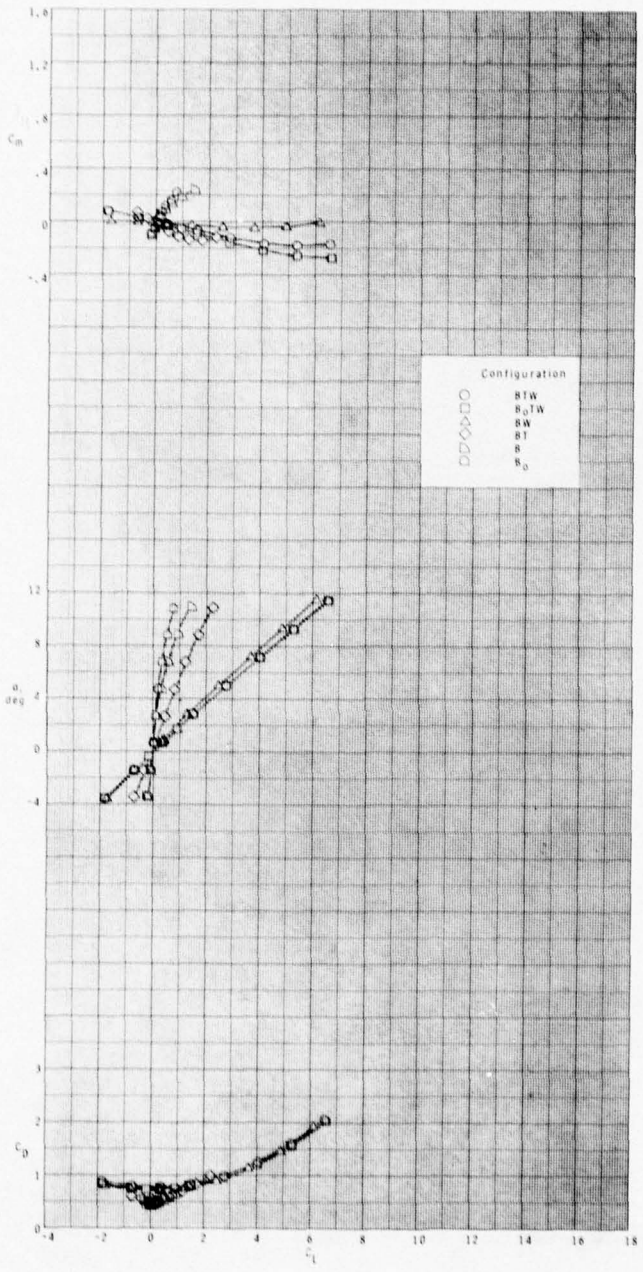

(a) Concluded.

Figure 9.- Continued.

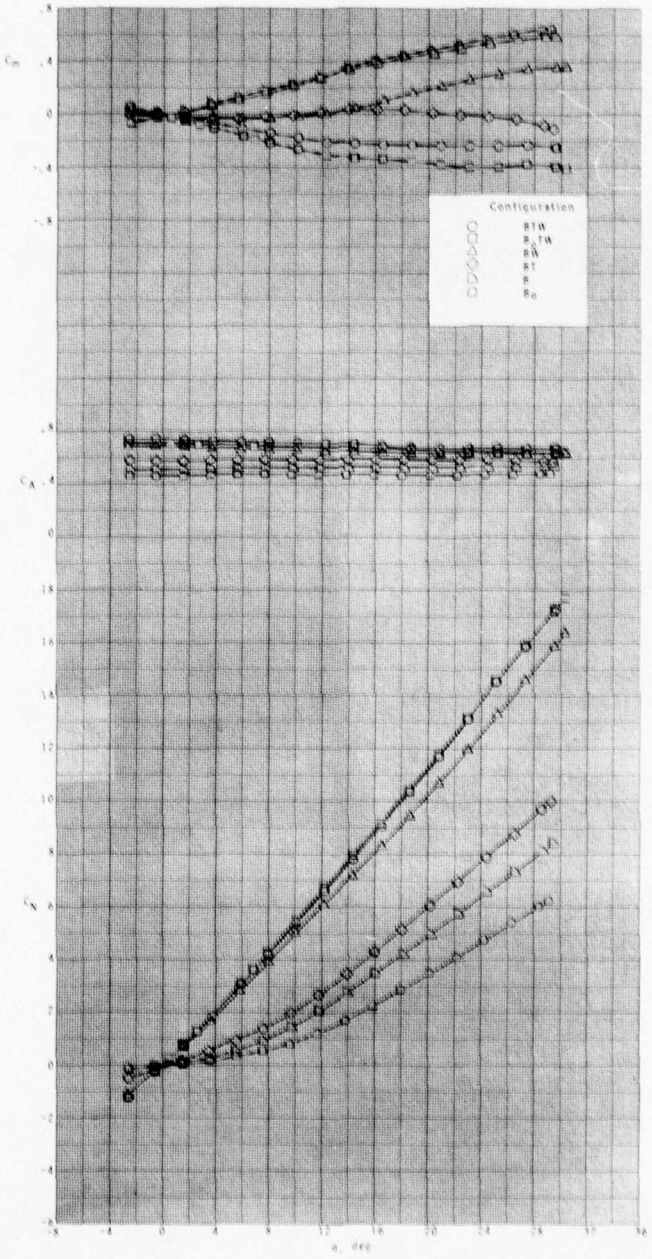

(b) M = 2.10.

Figure 9.- Continued.

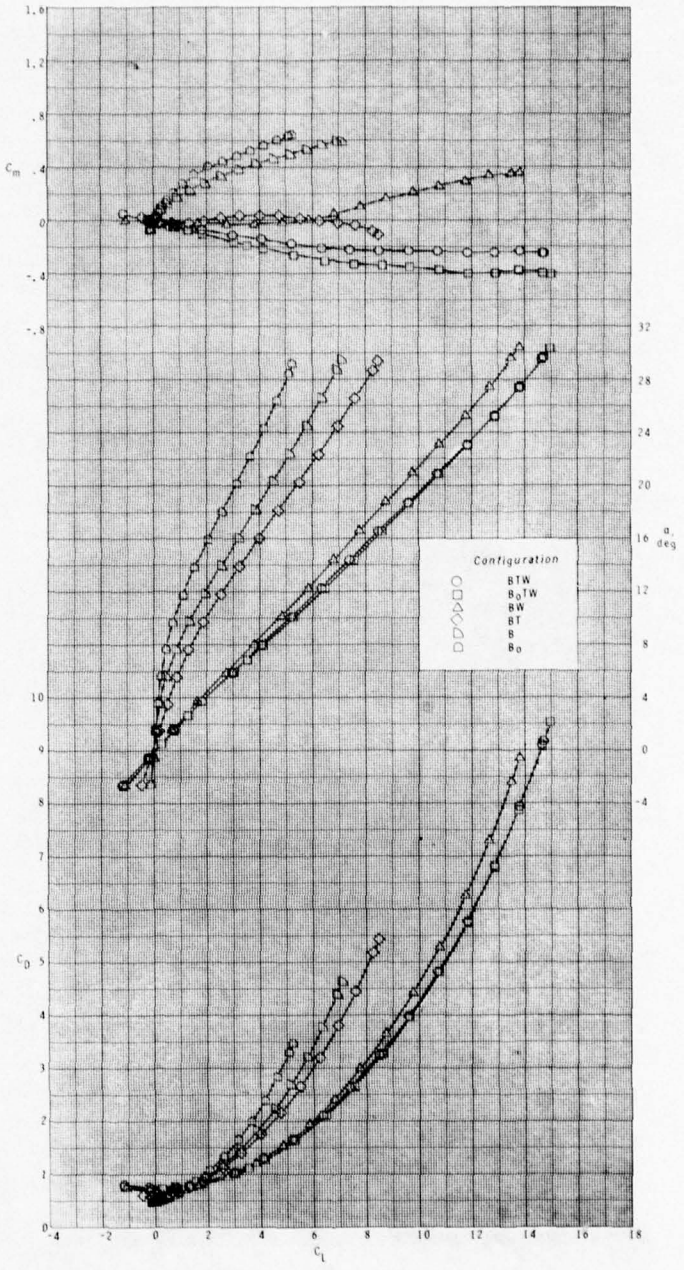

(b) Concluded.

Figure 9.- Continued.

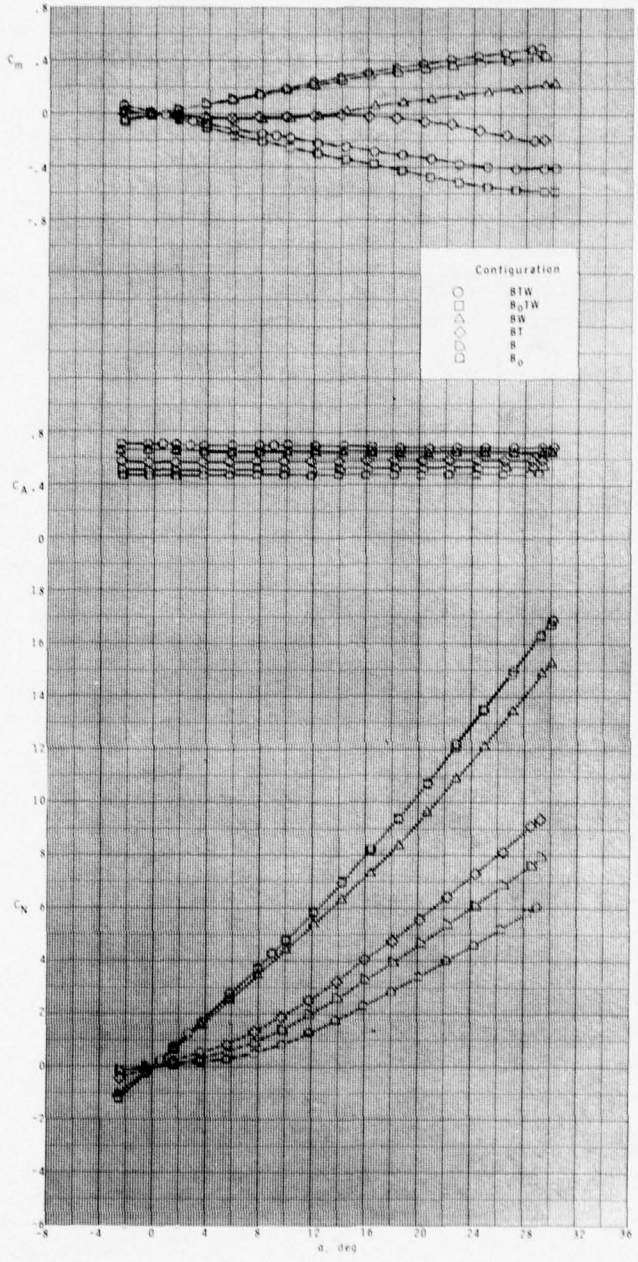

(c) M = 2.50.

Figure 9.- Continued.

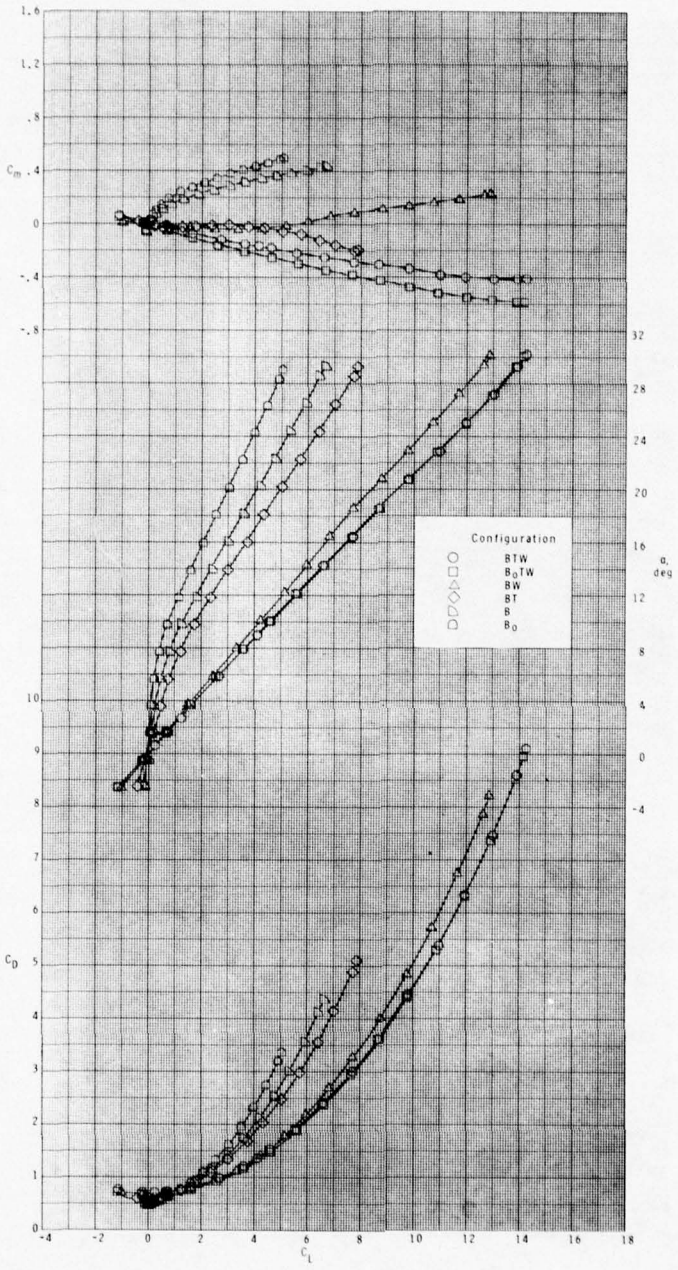

(c) Concluded.

Figure 9.- Continued.

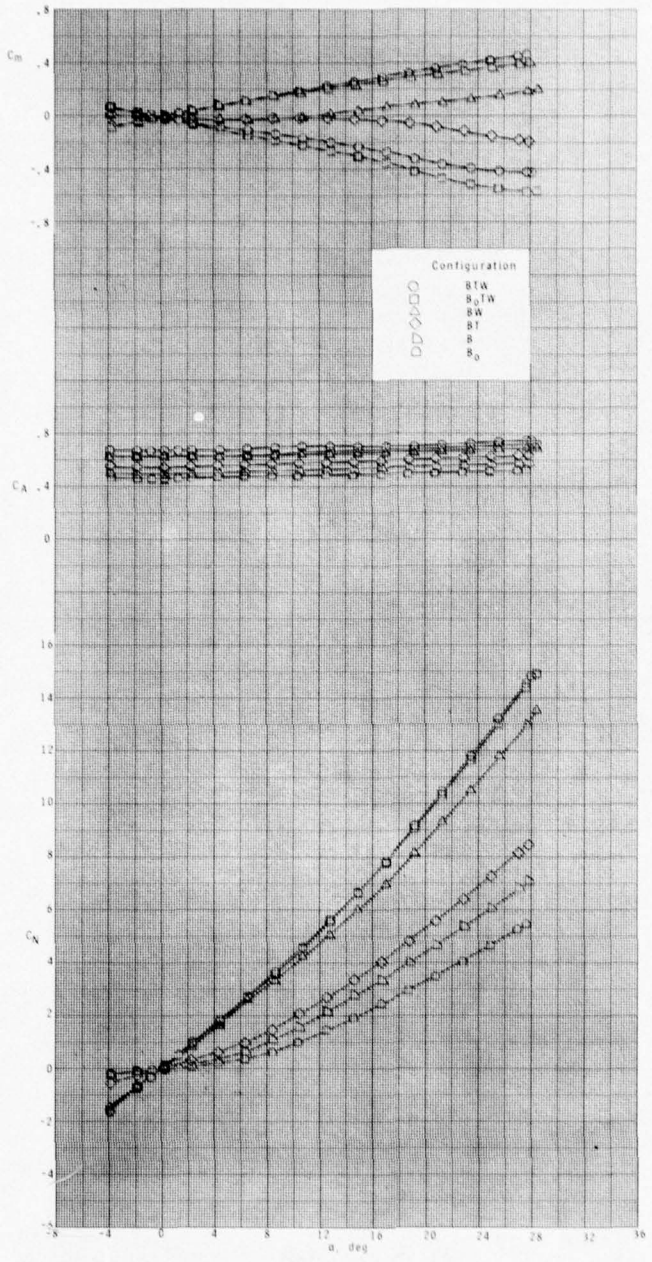

(d) M = 2.86.

Figure 9.- Continued.

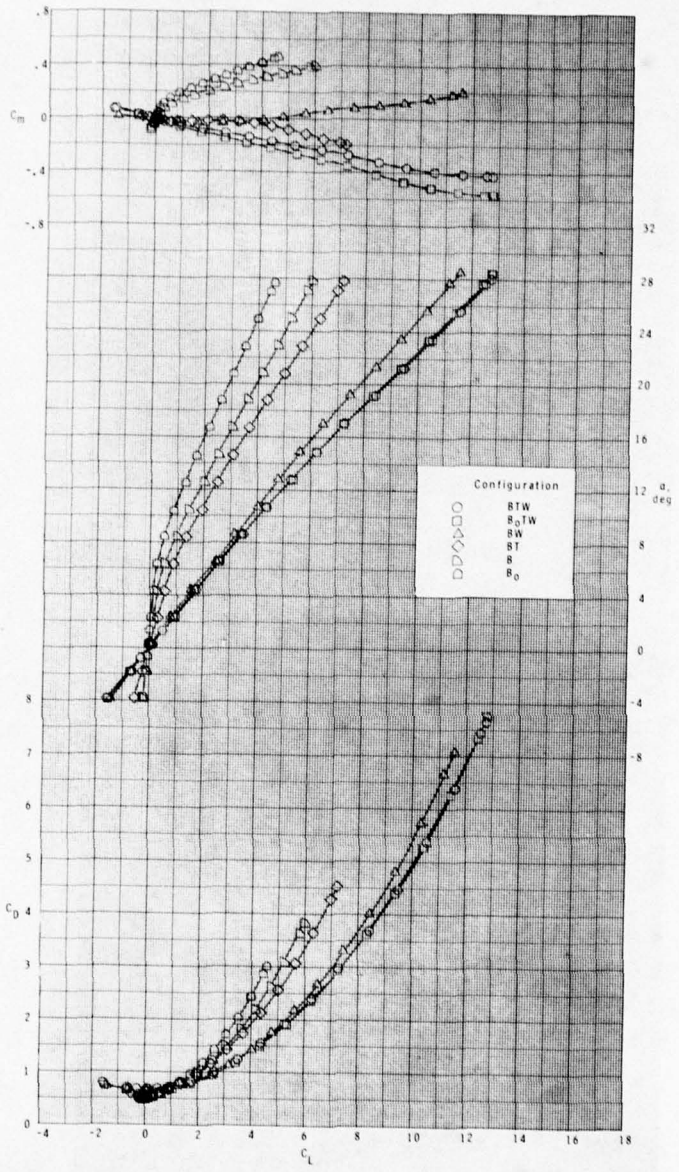

(d) Concluded.

Figure 9.- Concluded.

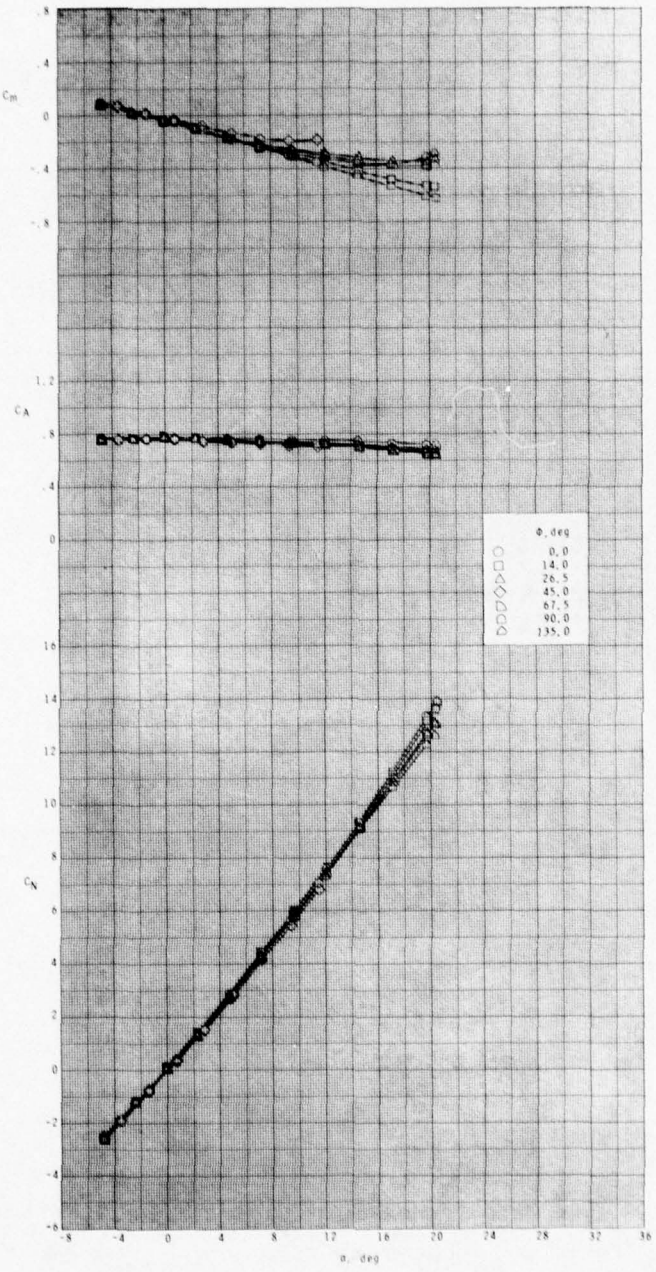

(a) M = 1.60.

Figure 10.- Effect of model roll orientation on longitudinal and lateral aerodynamic characteristics; BTW configuration.

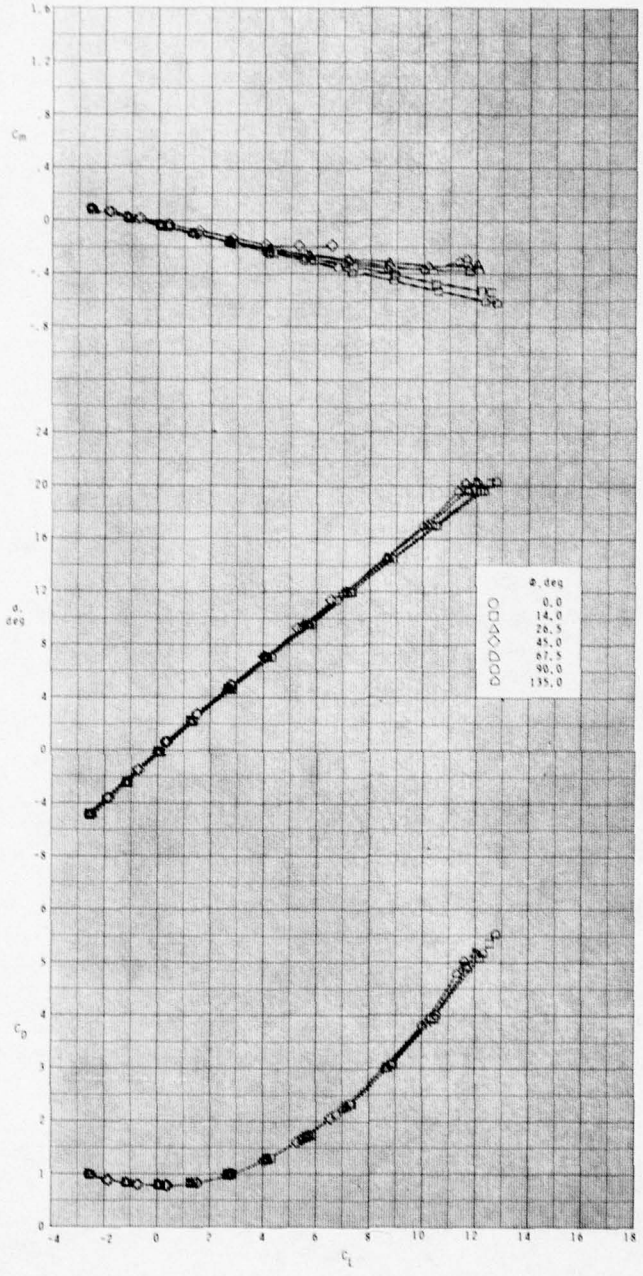

(a) Continued.

Figure 10.- Continued.

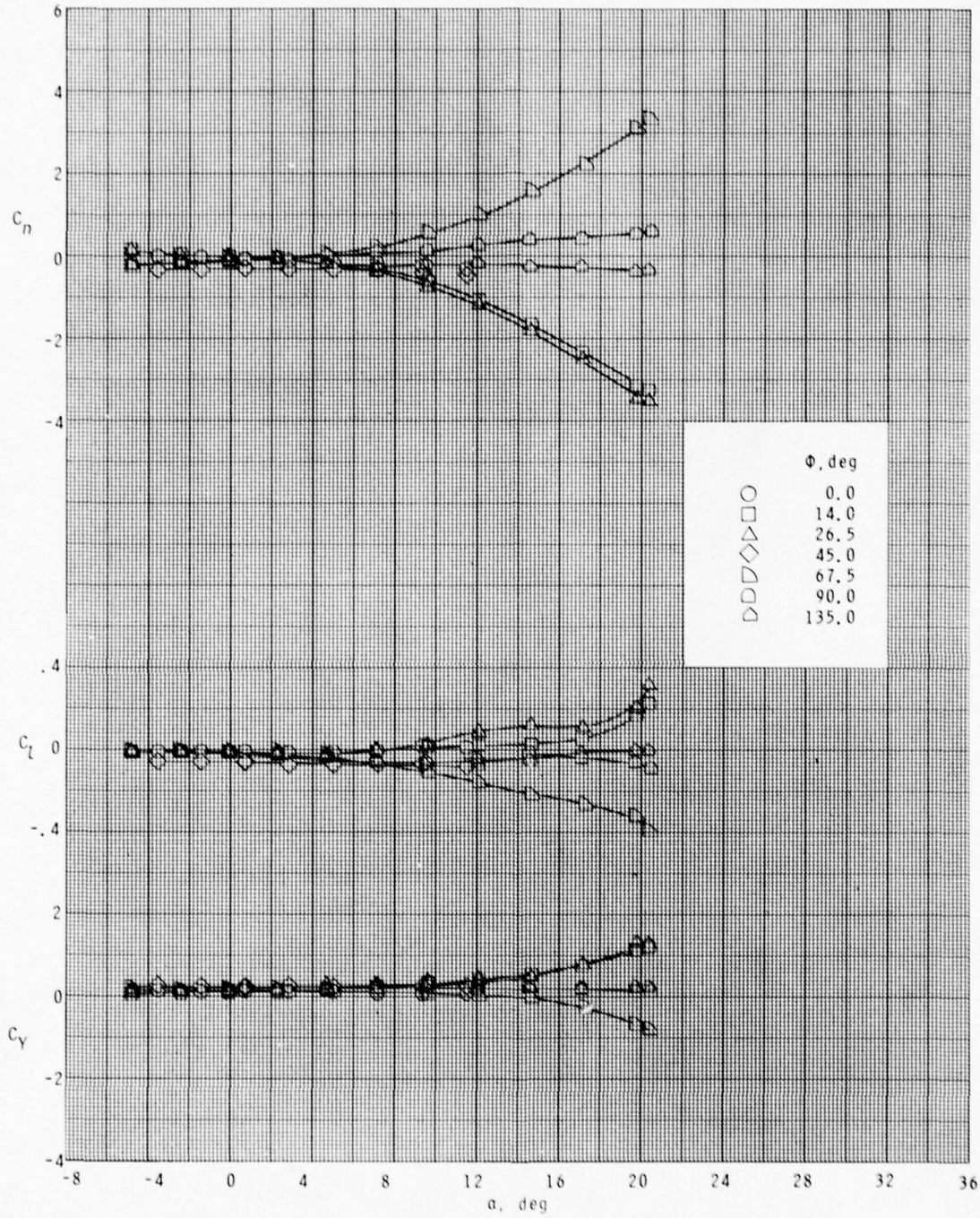

(a) Concluded.

Figure 10.- Continued.

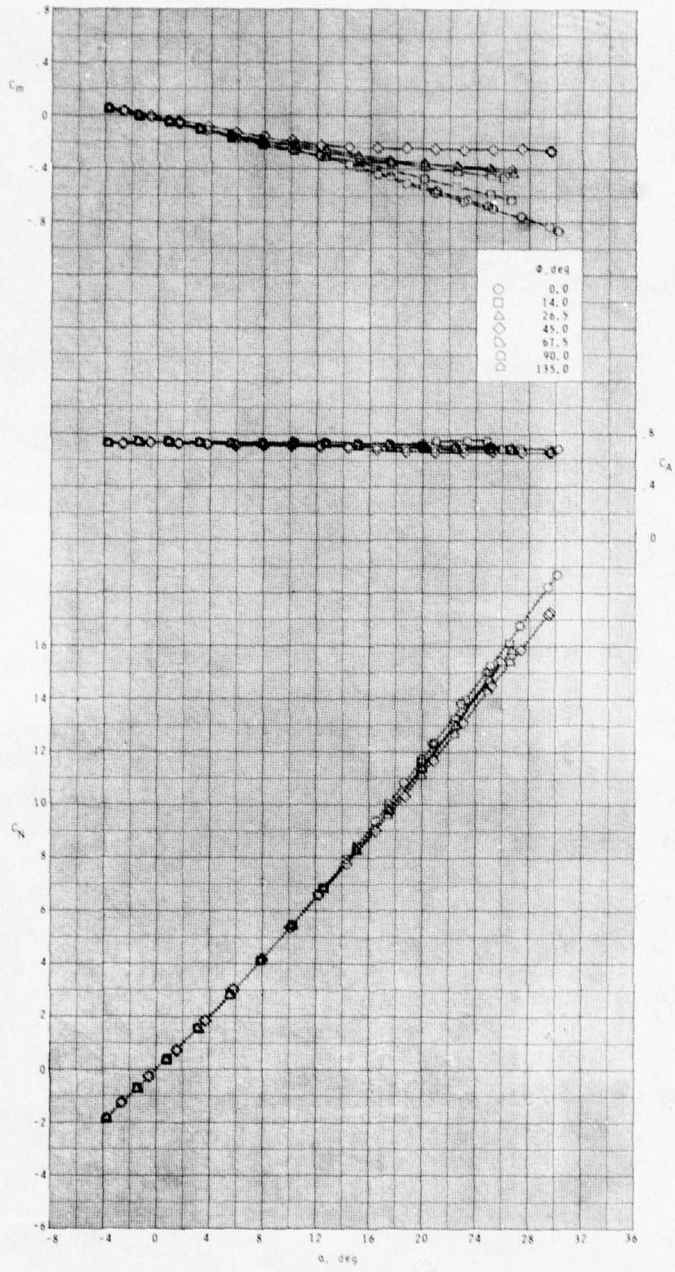

(b) M = 2.10.

Figure 10.- Continued.

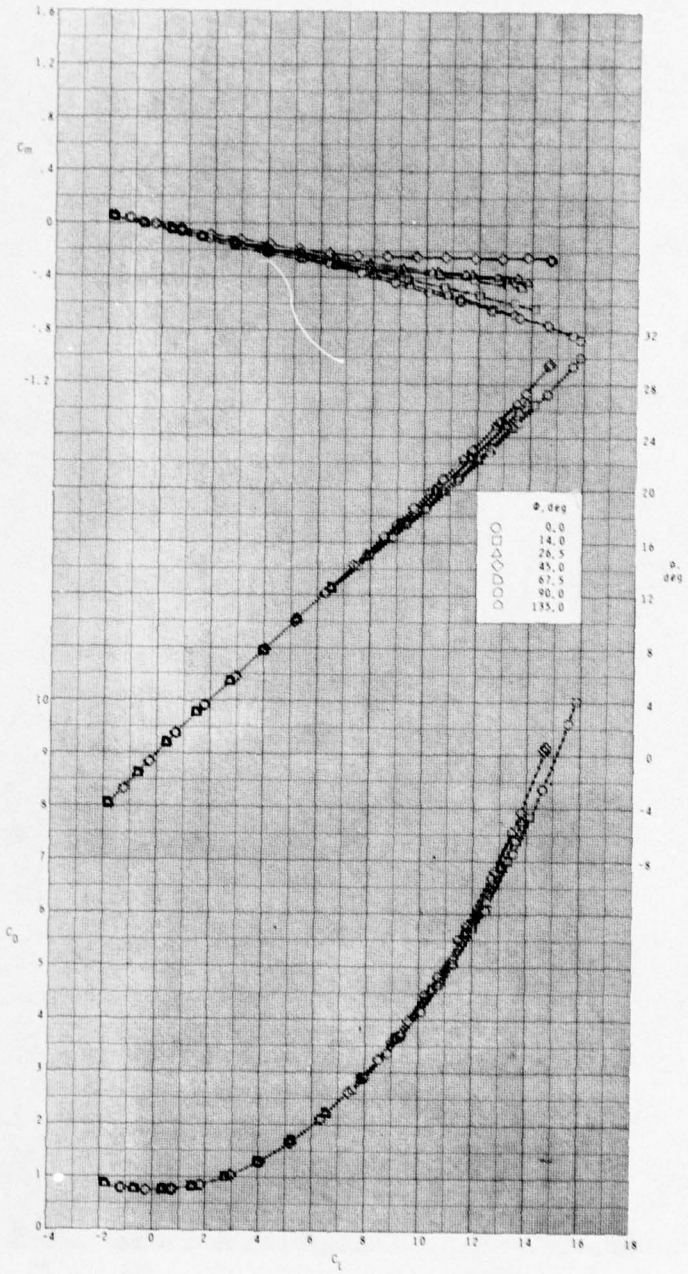

(b) Continued.

Figure 10.- Continued.

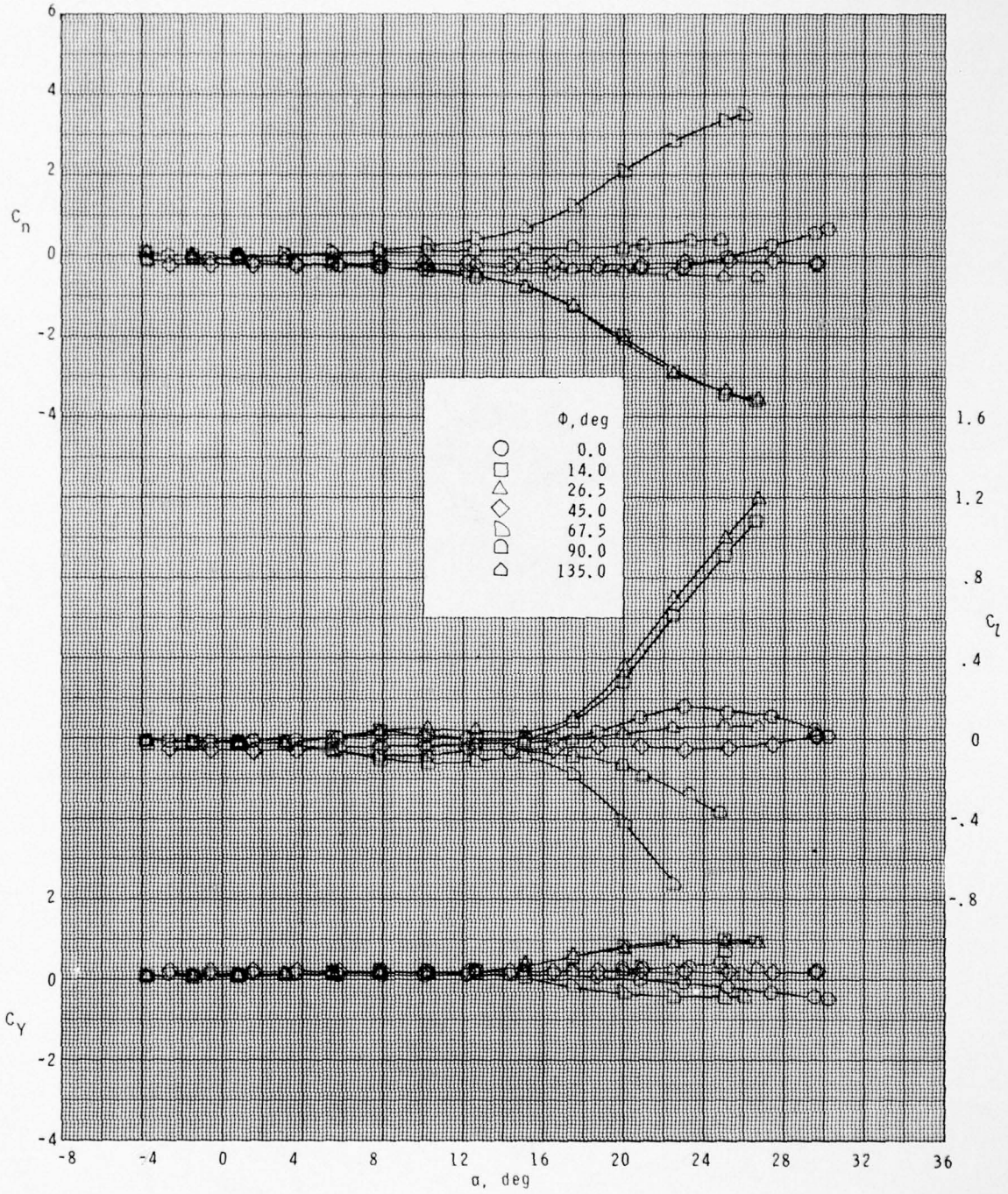

(b) Concluded.

Figure 10.- Continued.

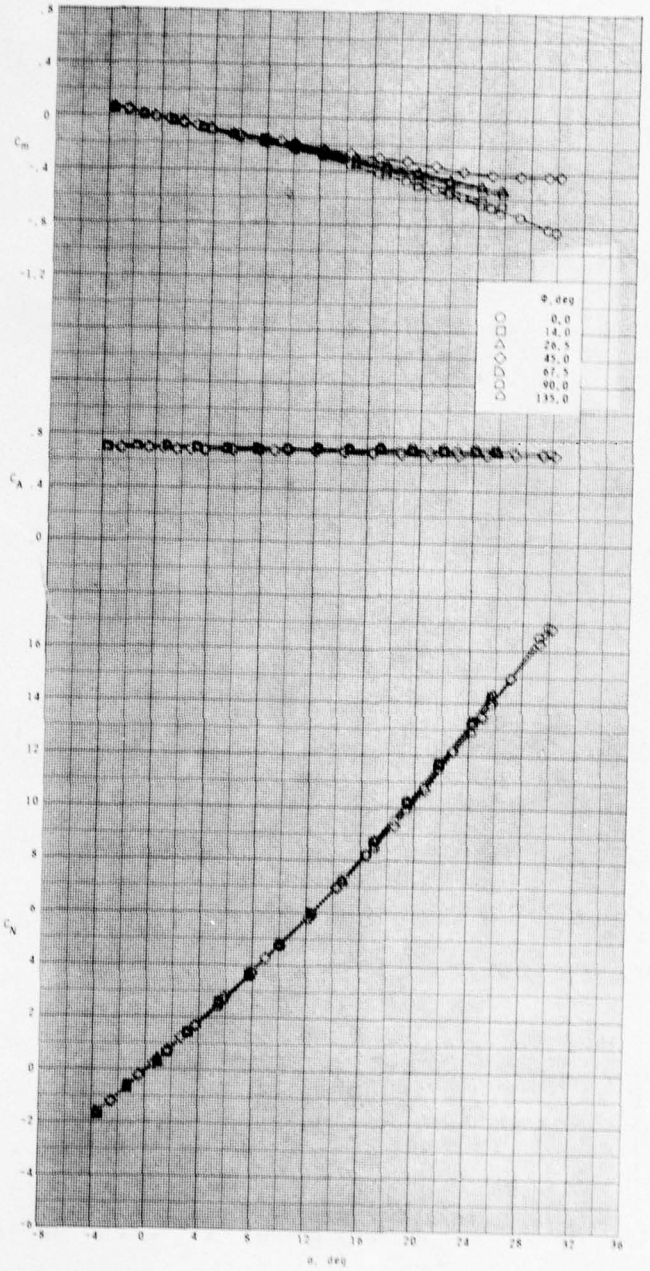

(c) M = 2.50.

Figure 10.- Continued.

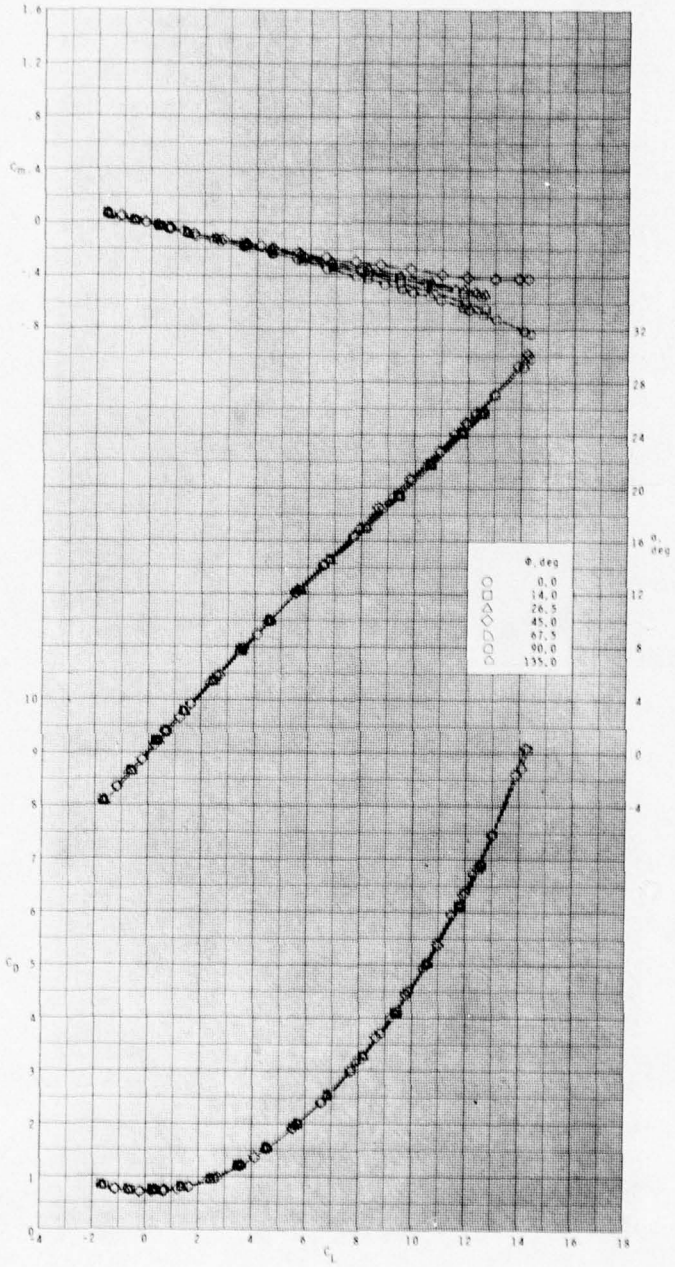

(c) Continued.

Figure 10.- Continued.

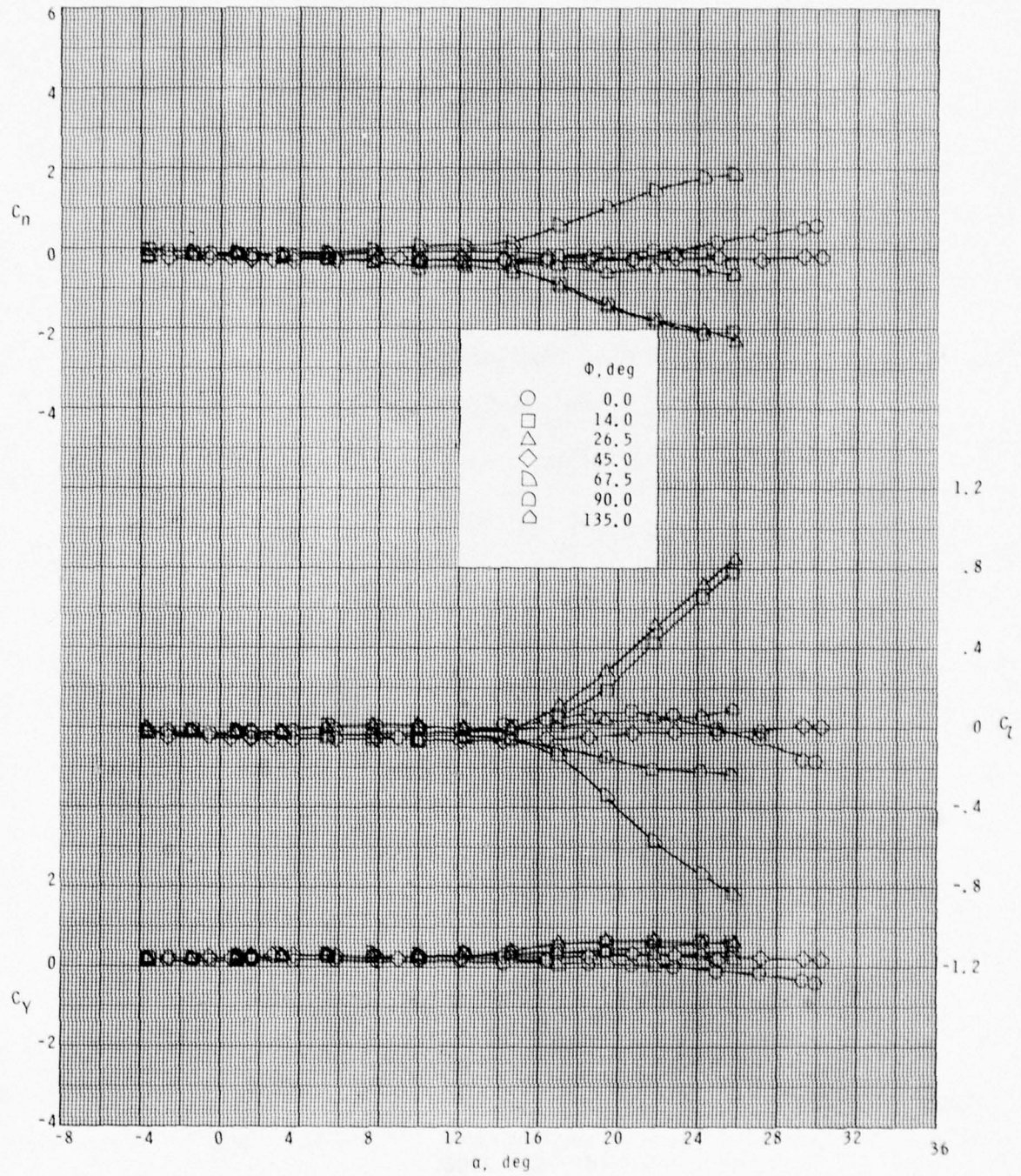

(c) Concluded.

Figure 10.- Continued.

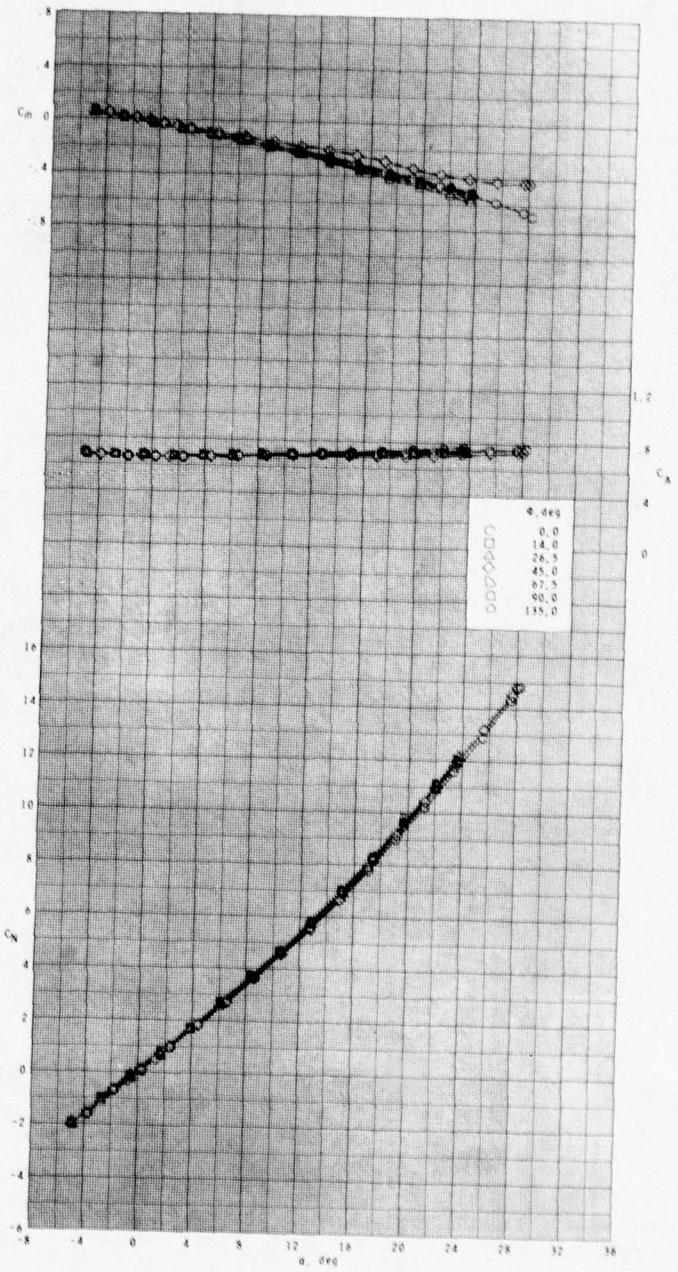

(d) M = 2.86.

Figure 10.- Continued.

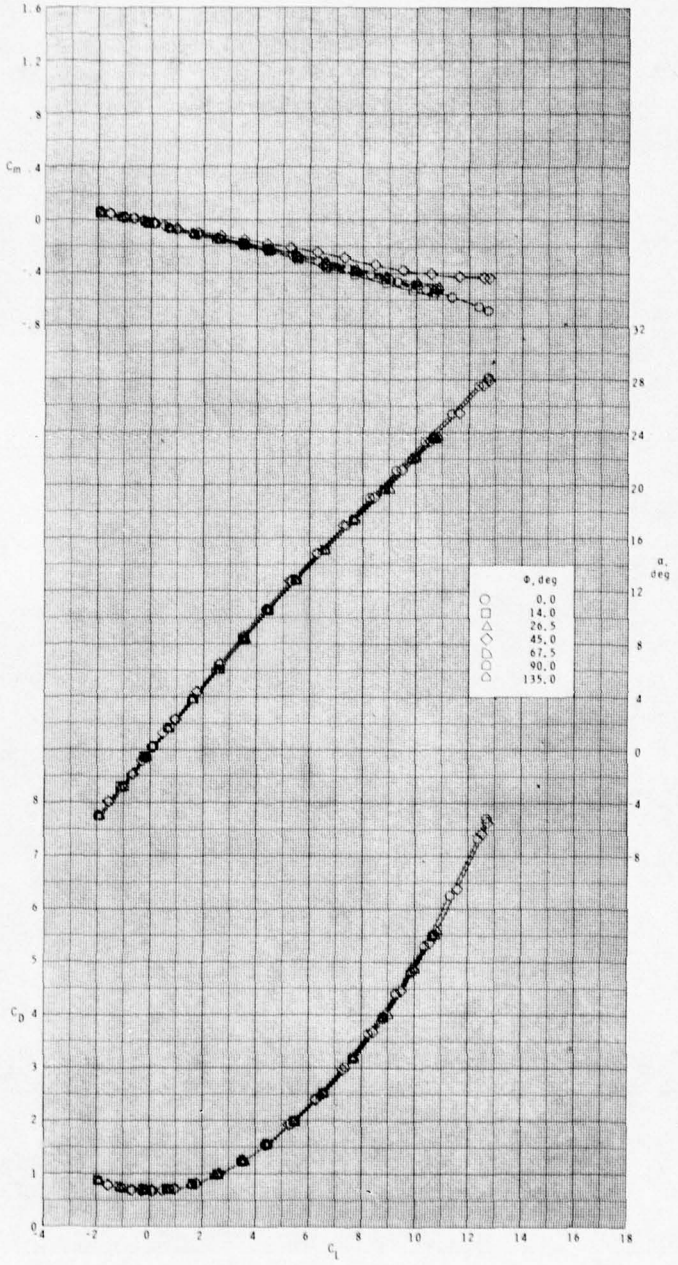

(d) Continued.

Figure 10.- Continued.

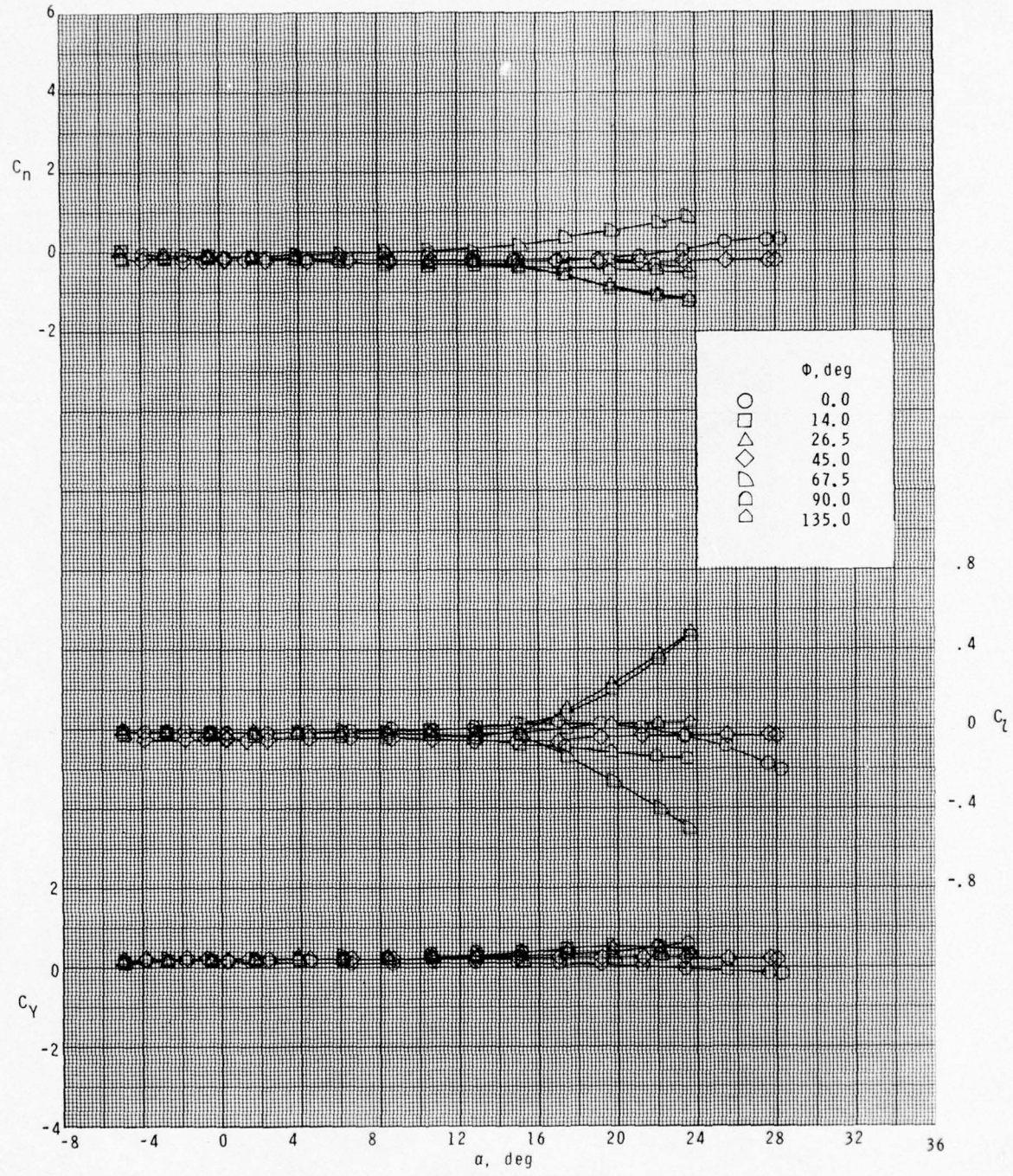

(d) Concluded.

Figure 10.- Continued.

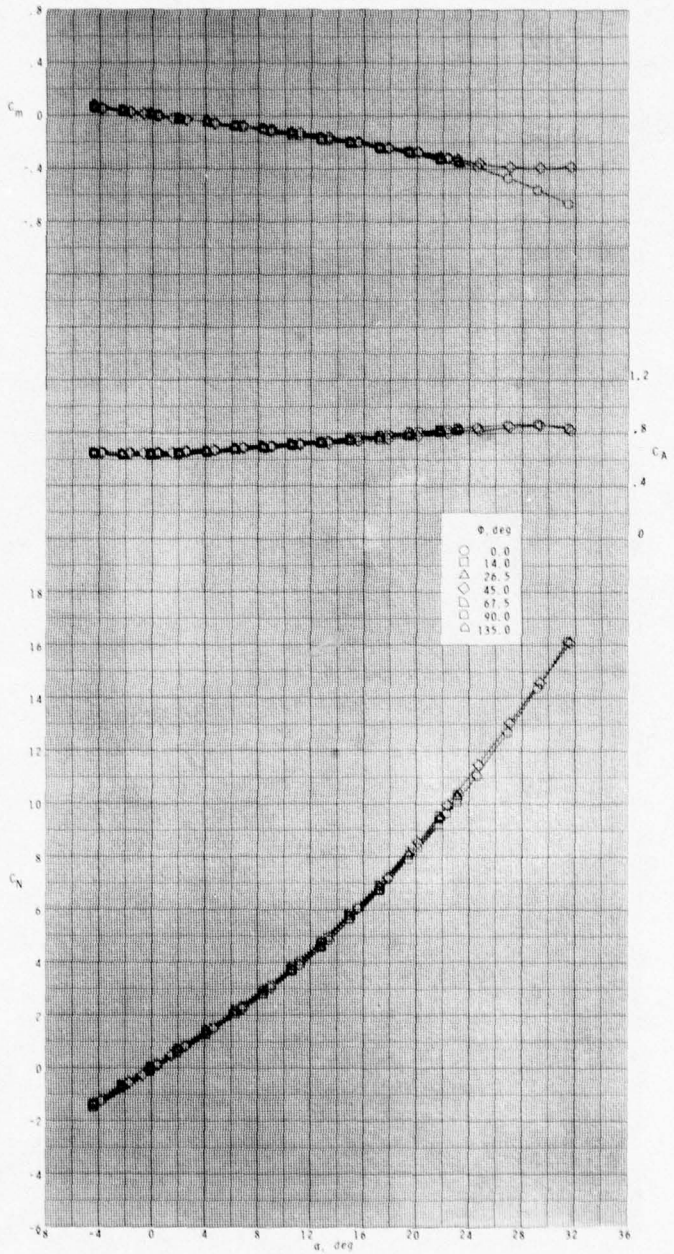

(e) M = 3.95.

Figure 10.- Continued.

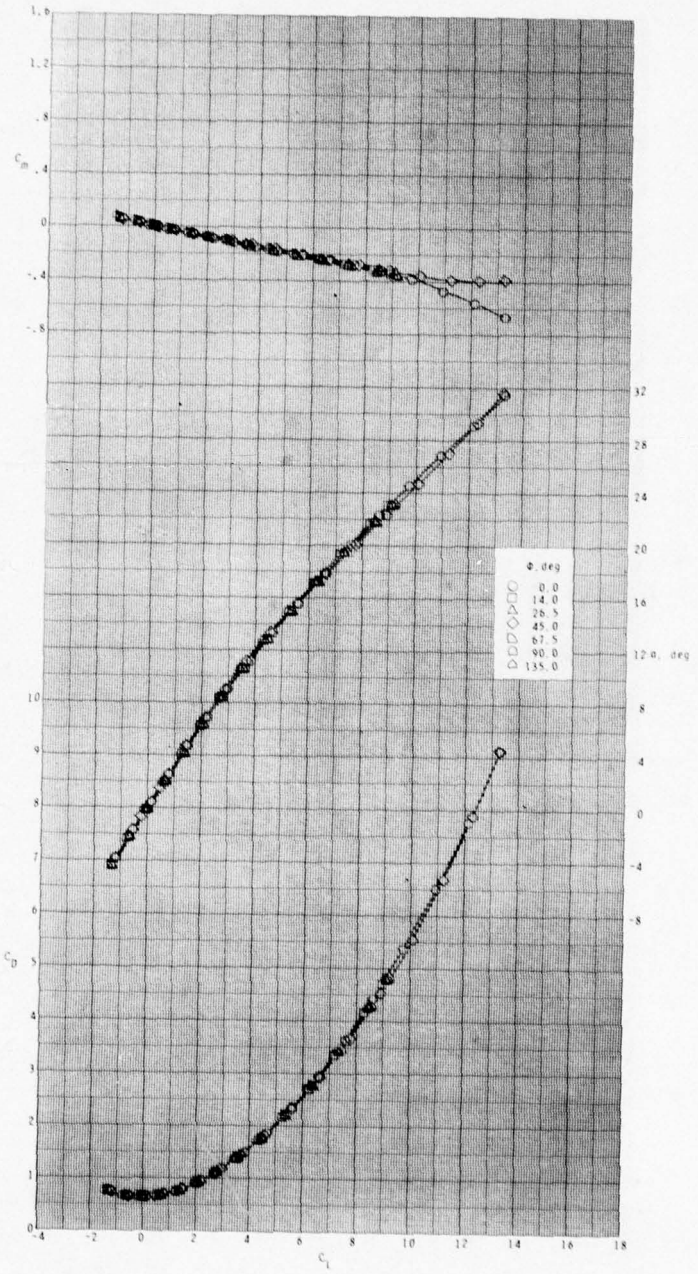

(e) Continued.

Figure 10.- Continued.

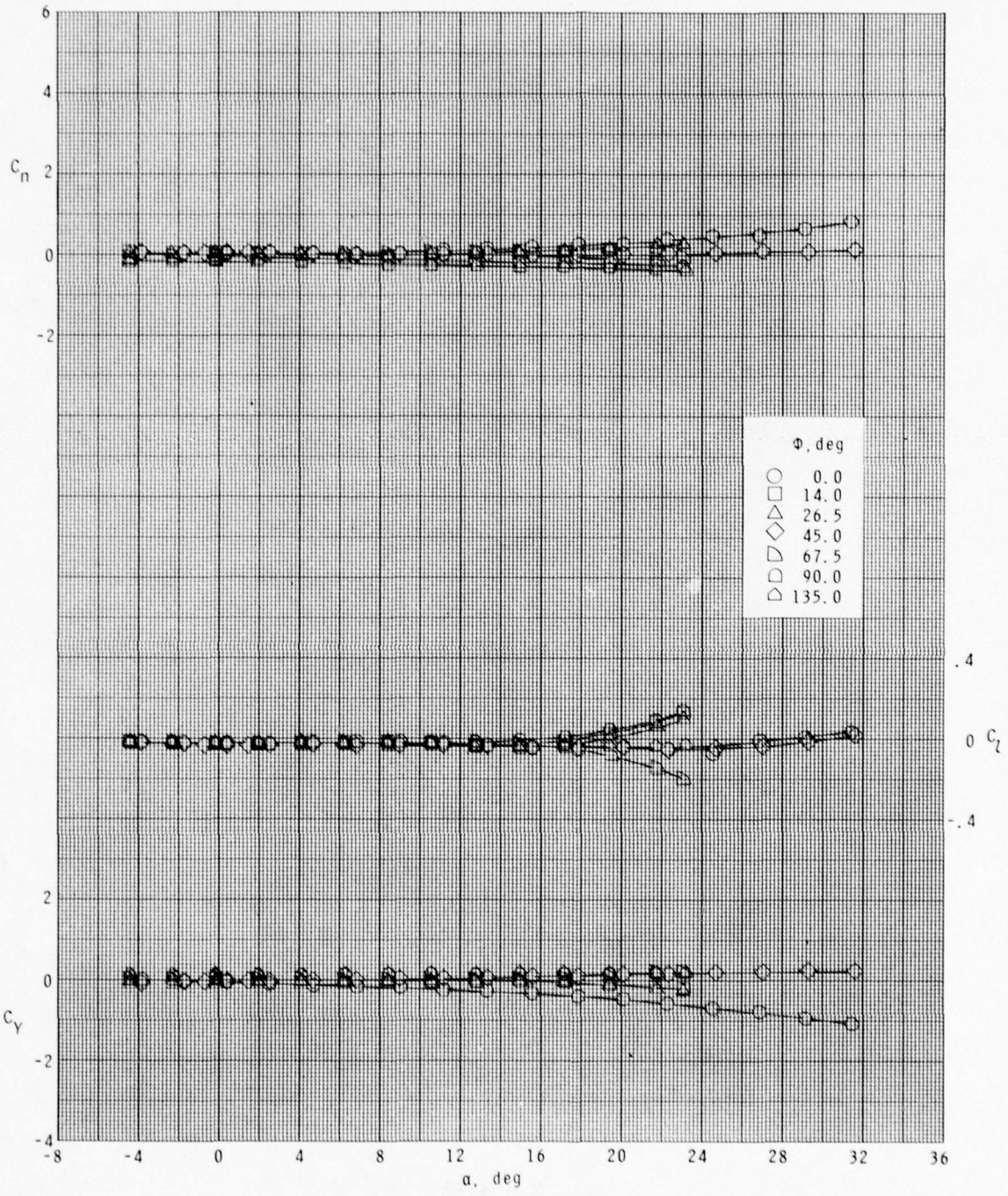

(e) Concluded.

Figure 10.- Continued.

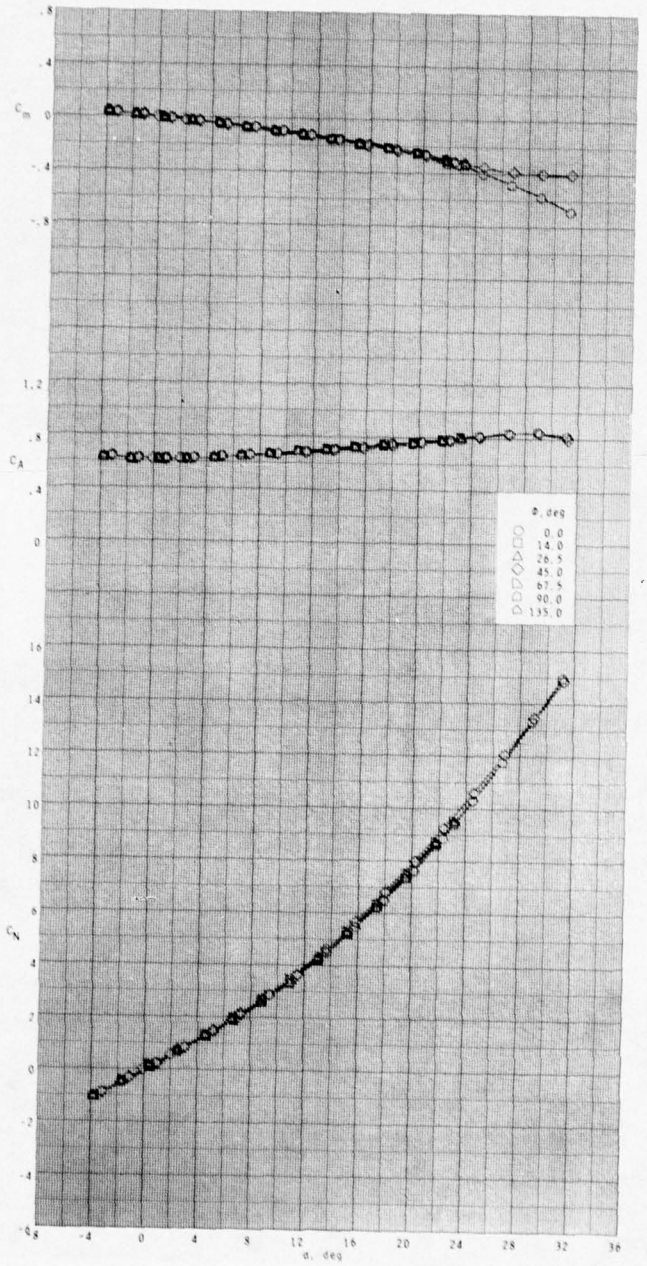

(f) M = 4.63.

Figure 10.- Continued.

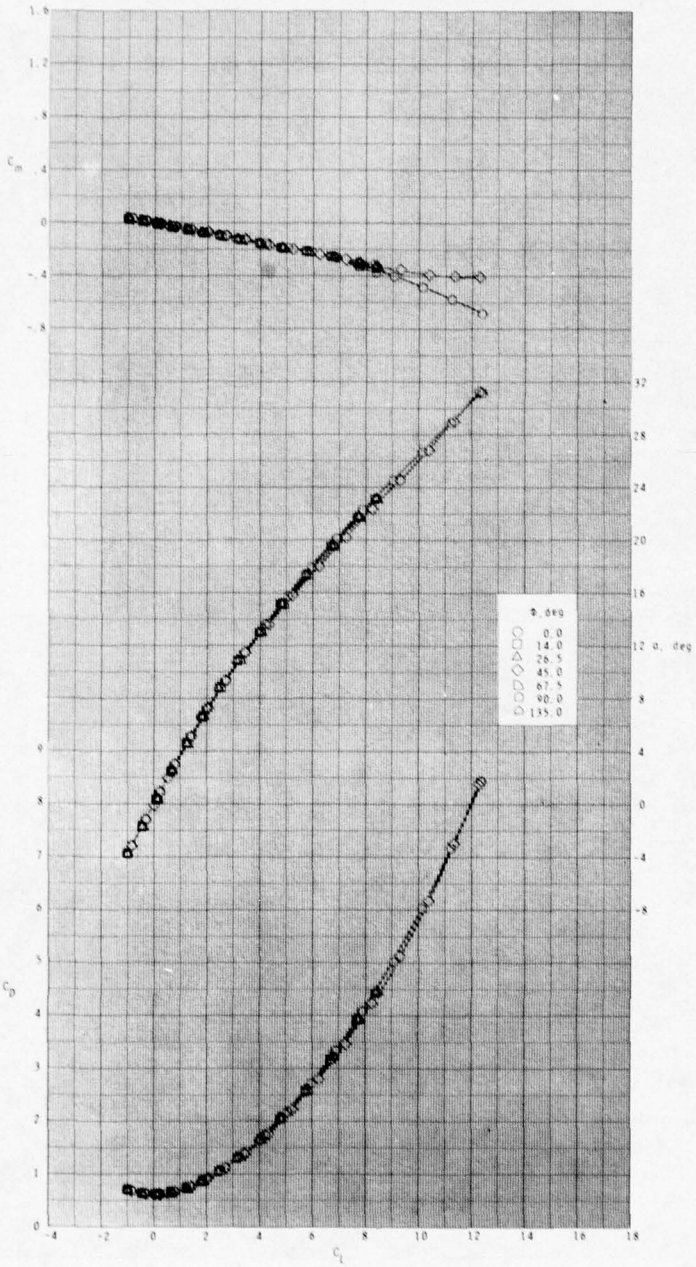

(f) Continued.

Figure 10.- Continued.

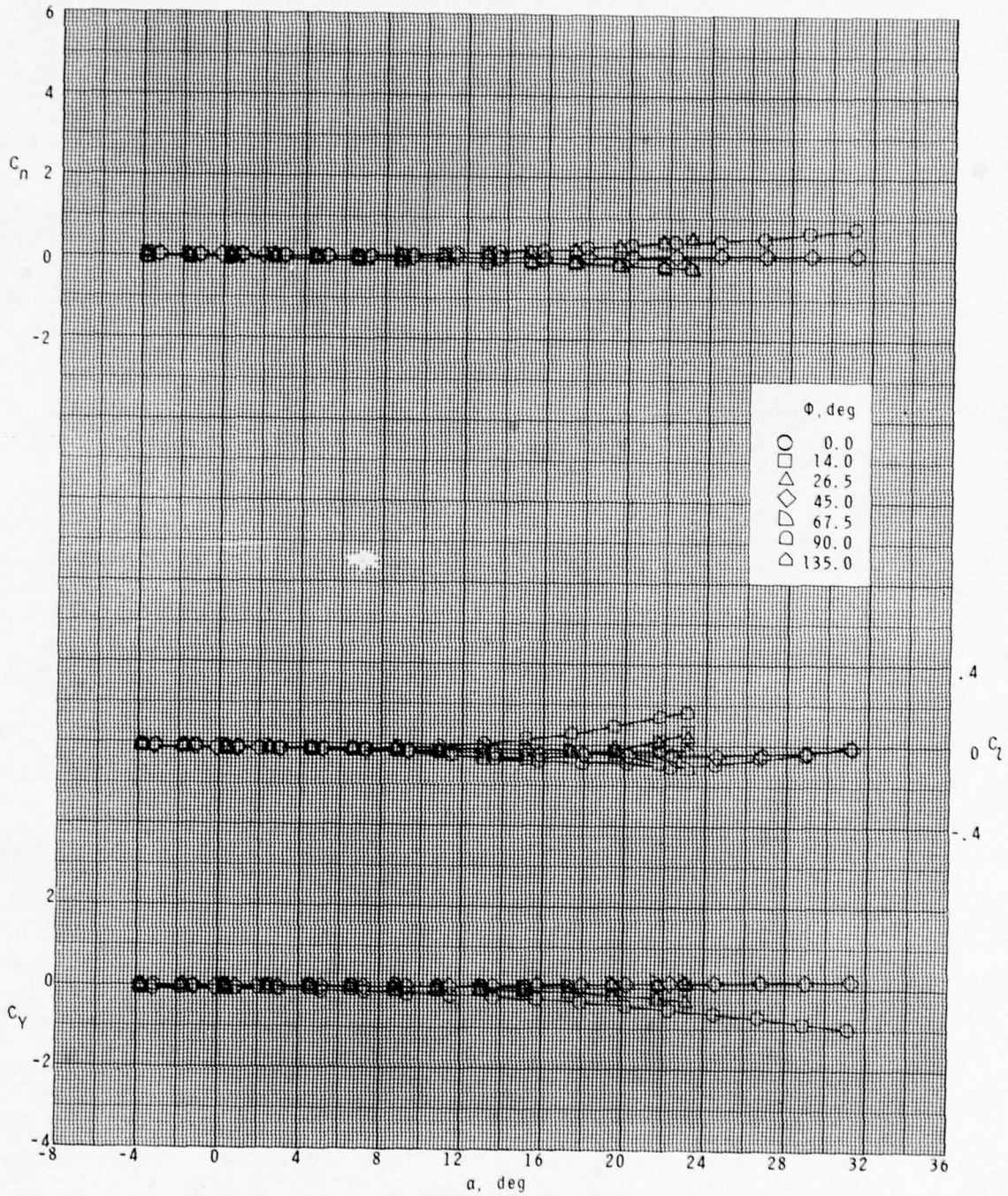

(f) Concluded.

Figure 10.- Concluded.

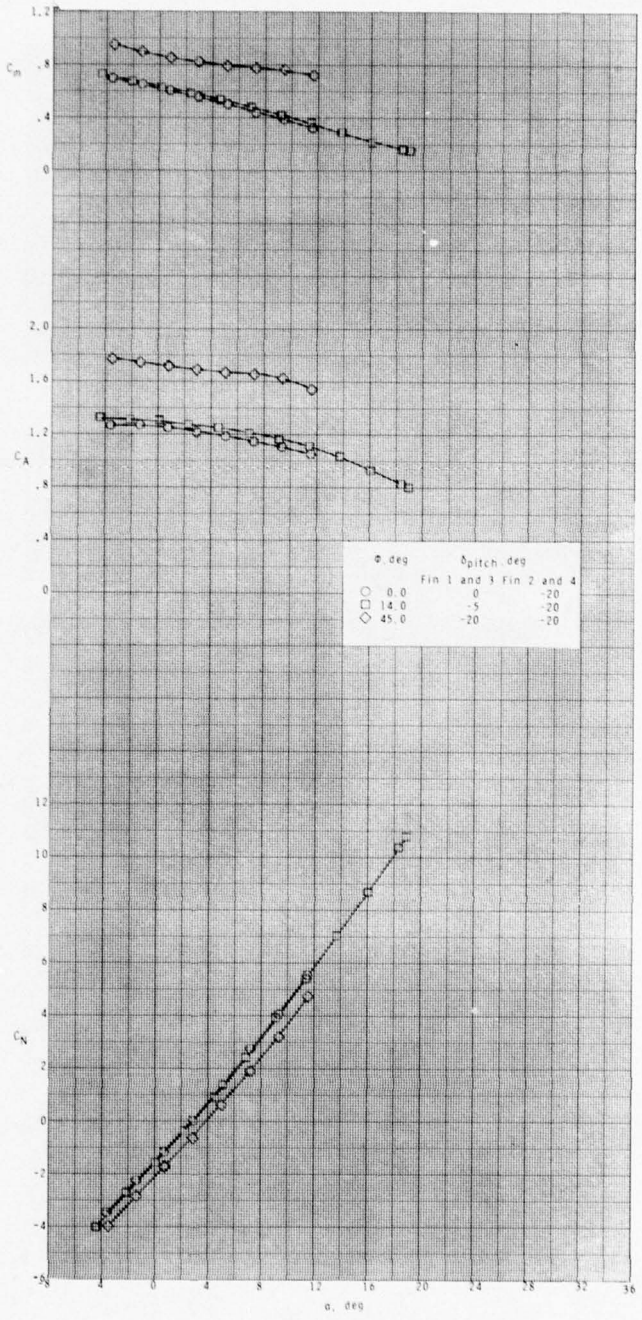

(a) M = 1.60.

Figure 11.- Effect of pitch-control deflections at various roll orientations; BTW configuration.

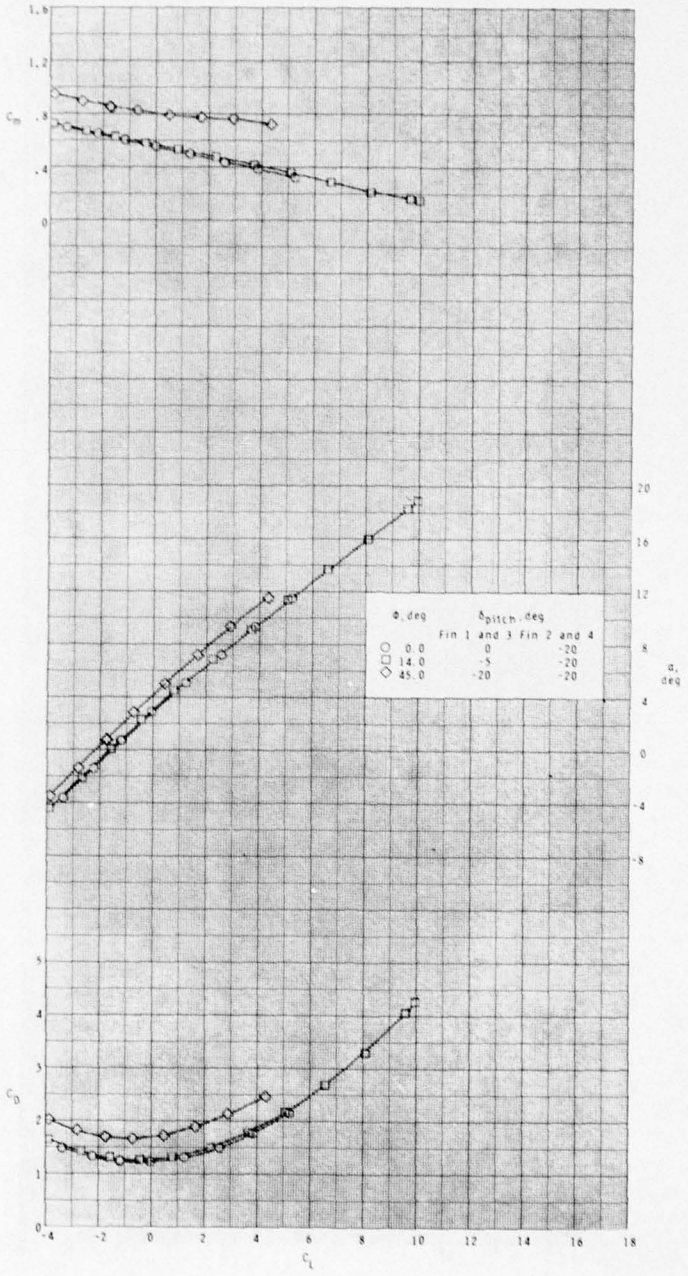

(a) Continued.

Figure 11.- Continued.

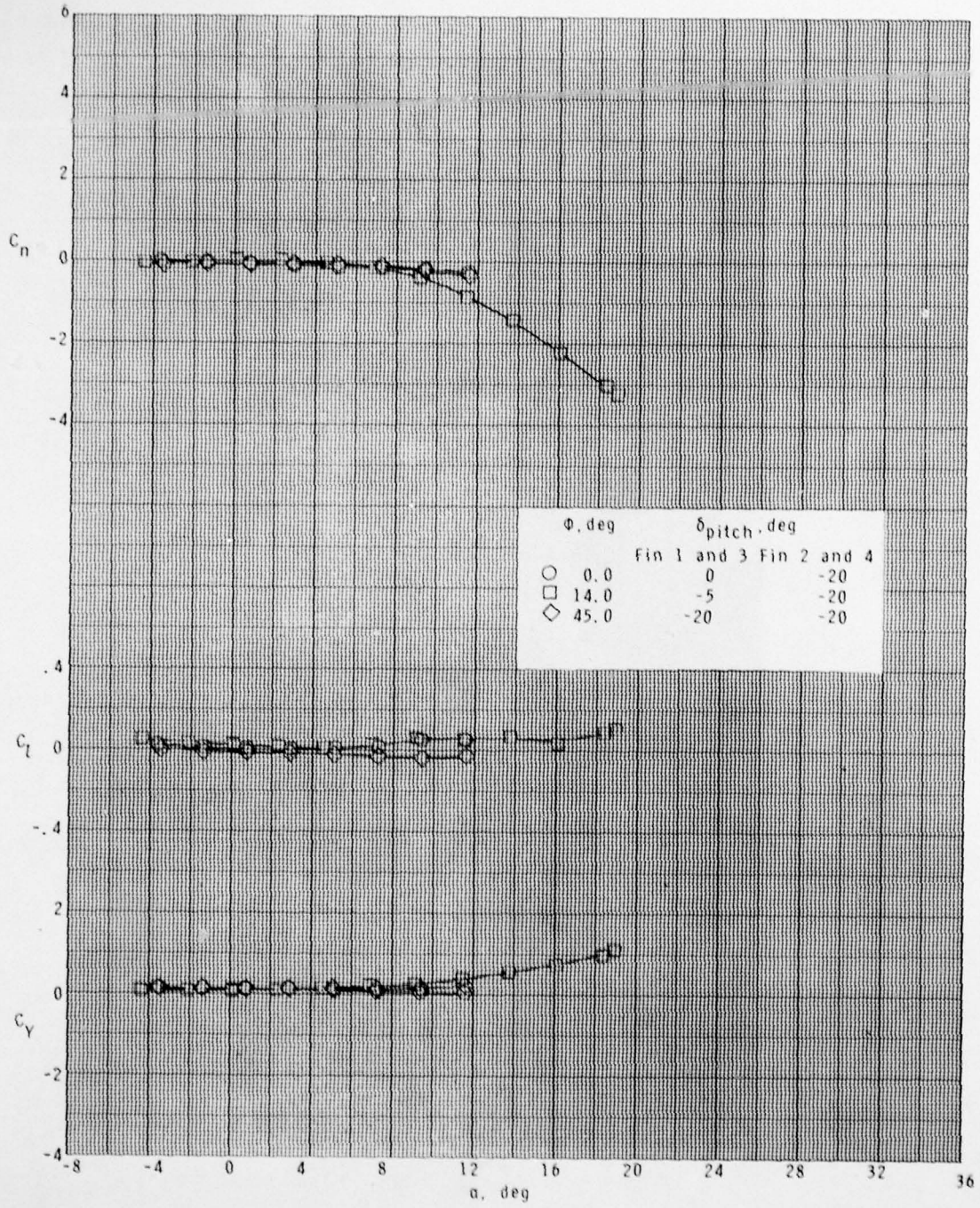

(a) Concluded.

Figure 11.- Continued.

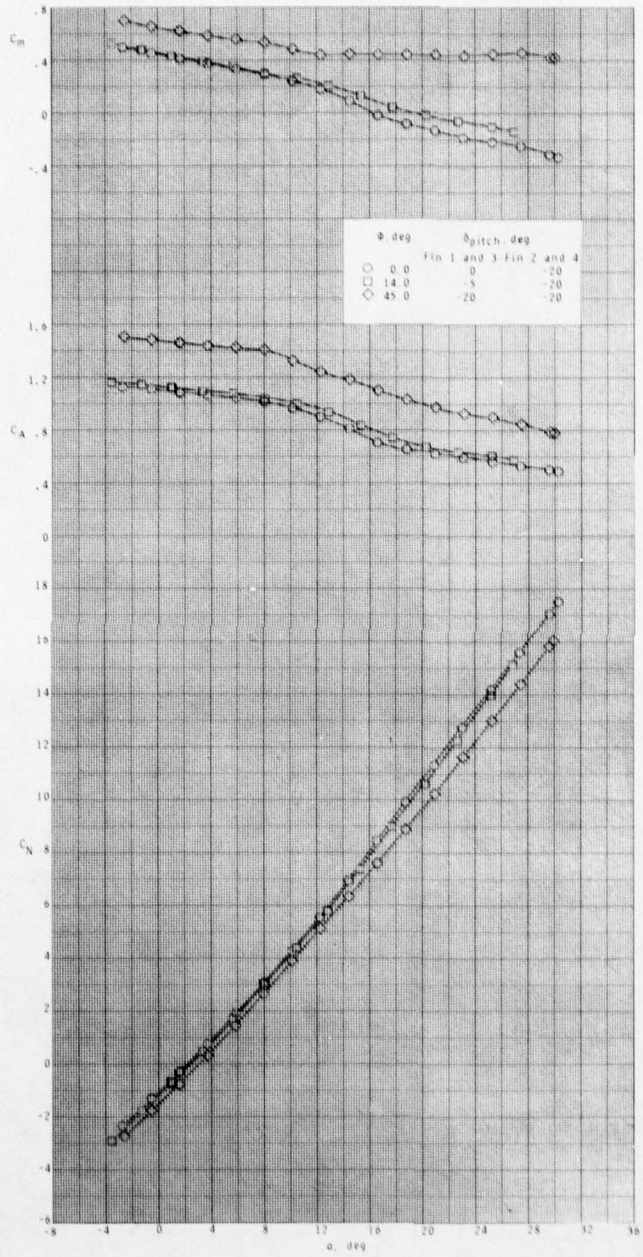

(b) M = 2.10.

Figure 11.- Continued.

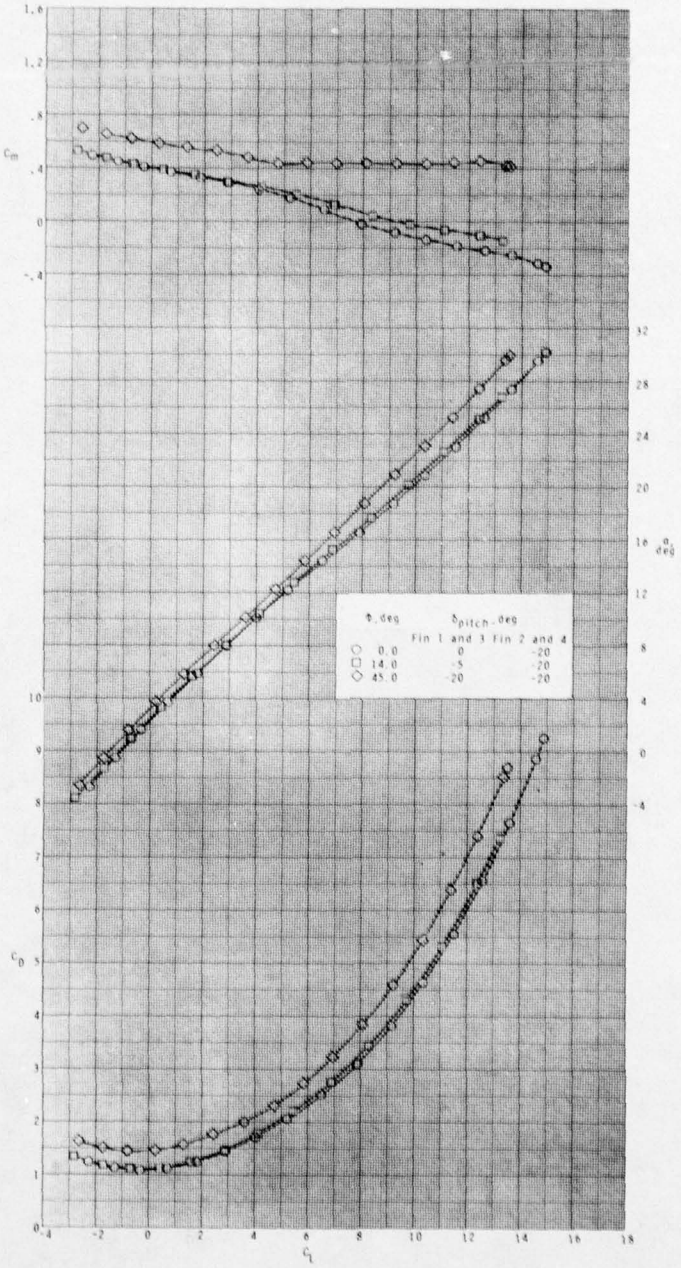

(b) Continued.

Figure 11.- Continued.

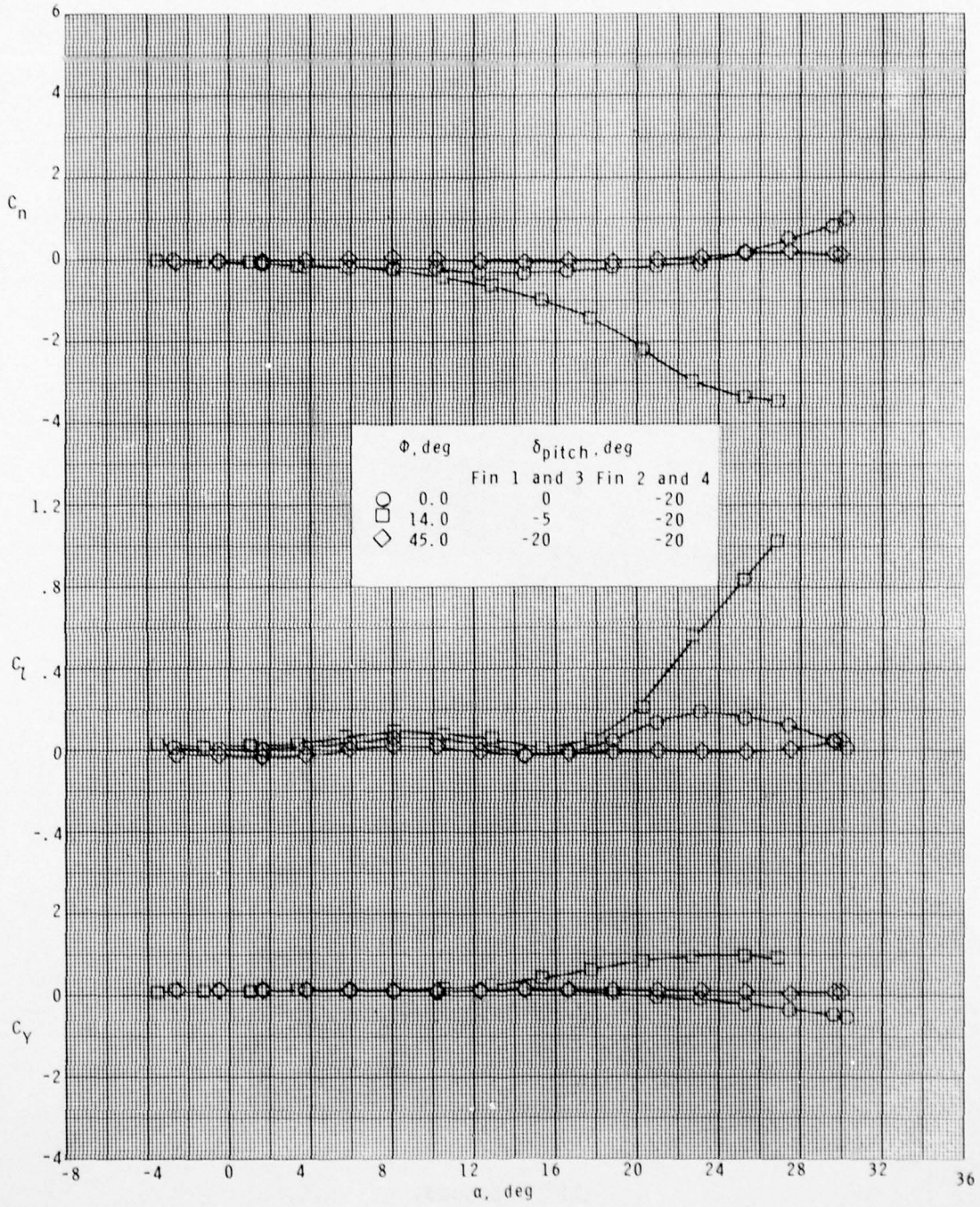

(b) Concluded.

Figure 11.- Continued.

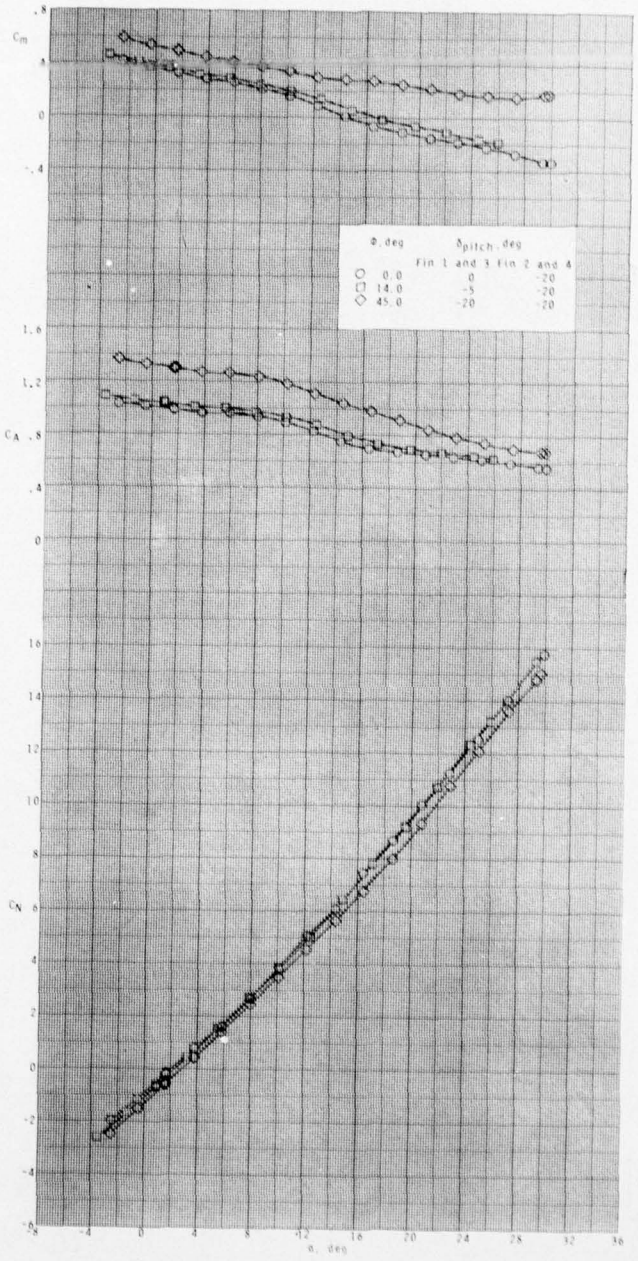

(c) M = 2.50.

Figure 11.- Continued.

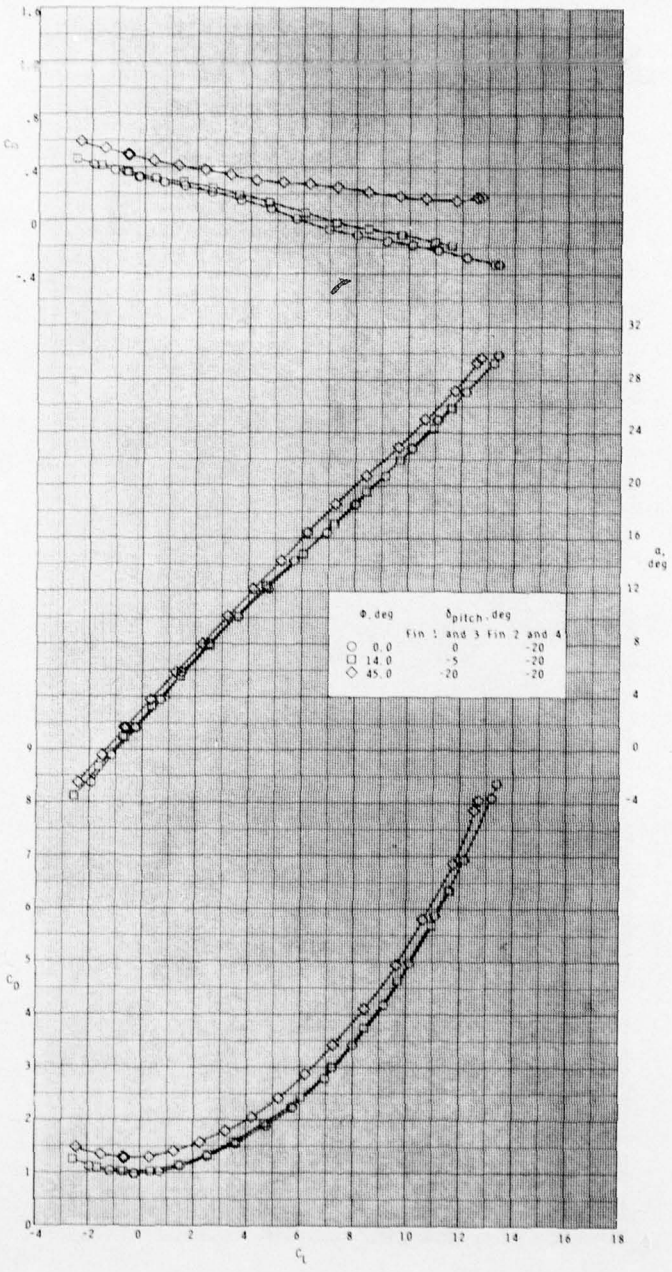

(c) Continued.

Figure 11.- Continued.

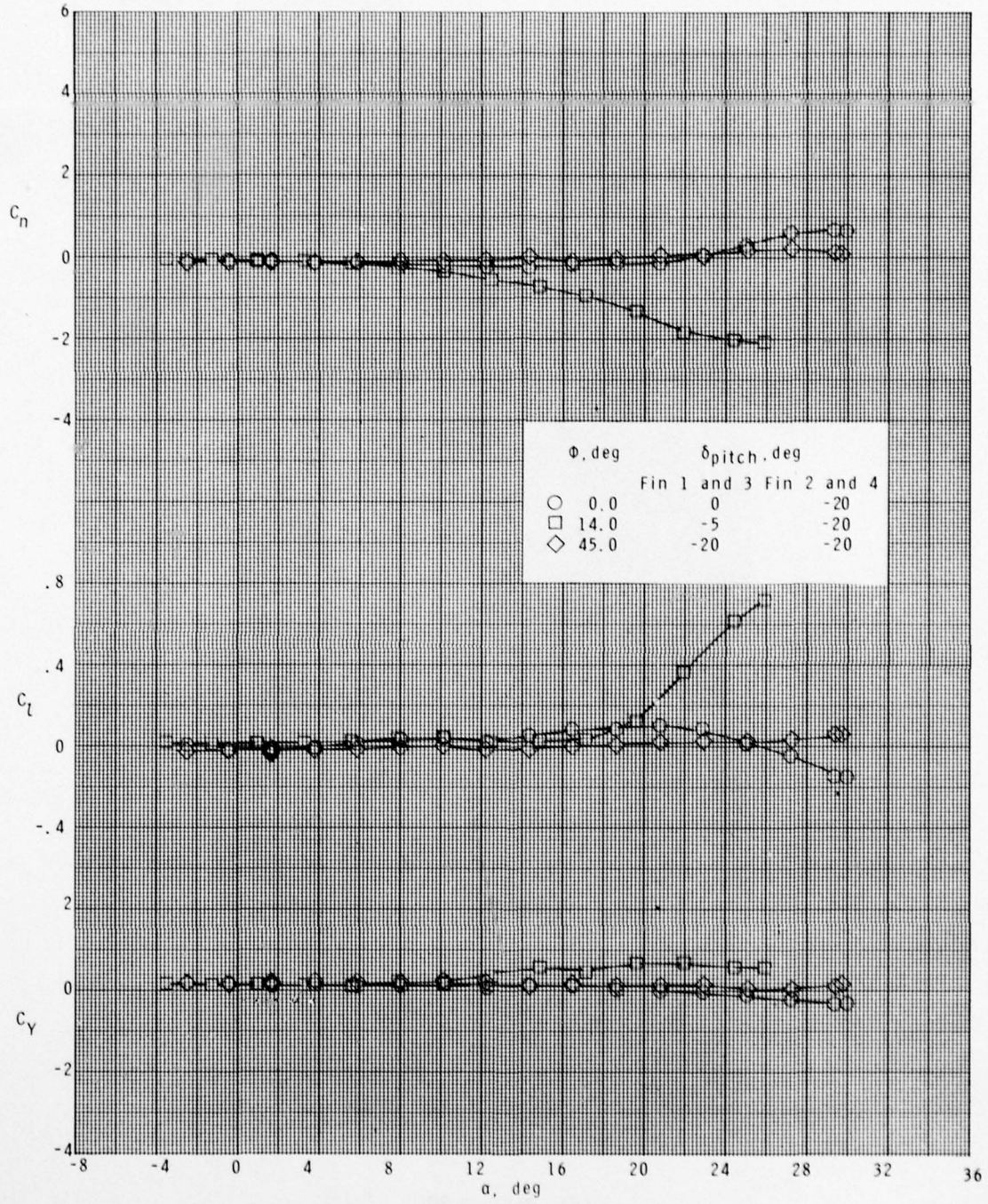

(c) Concluded.

Figure 11.- Continued.

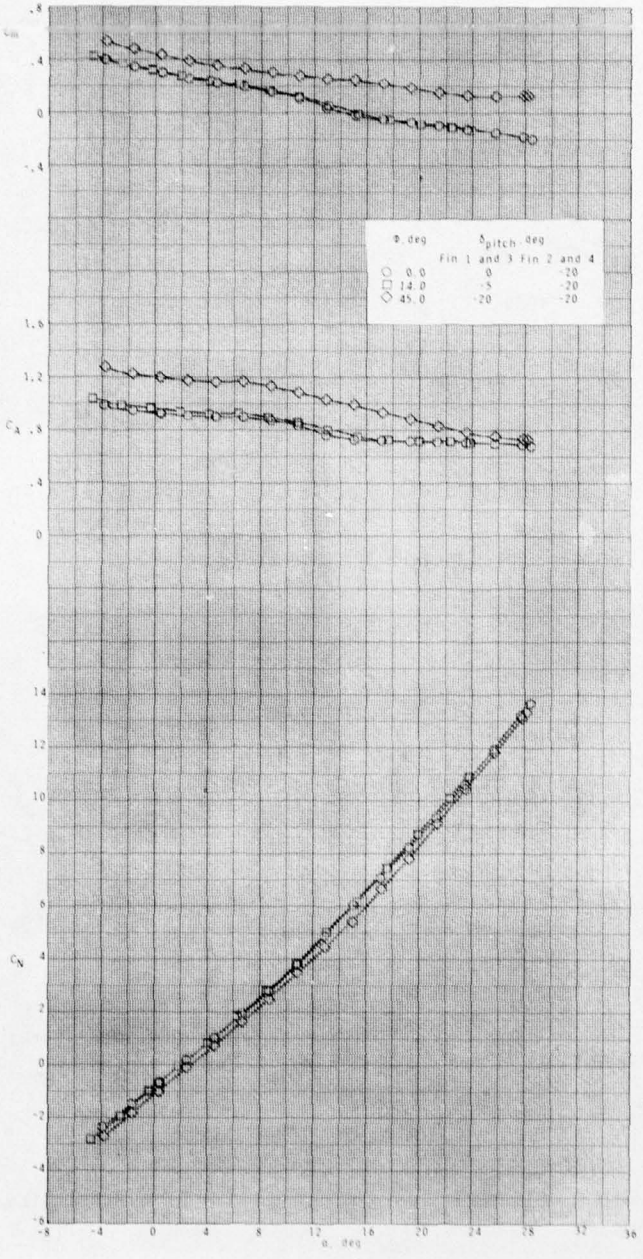

(d) M = 2.86.

Figure 11.- Continued.

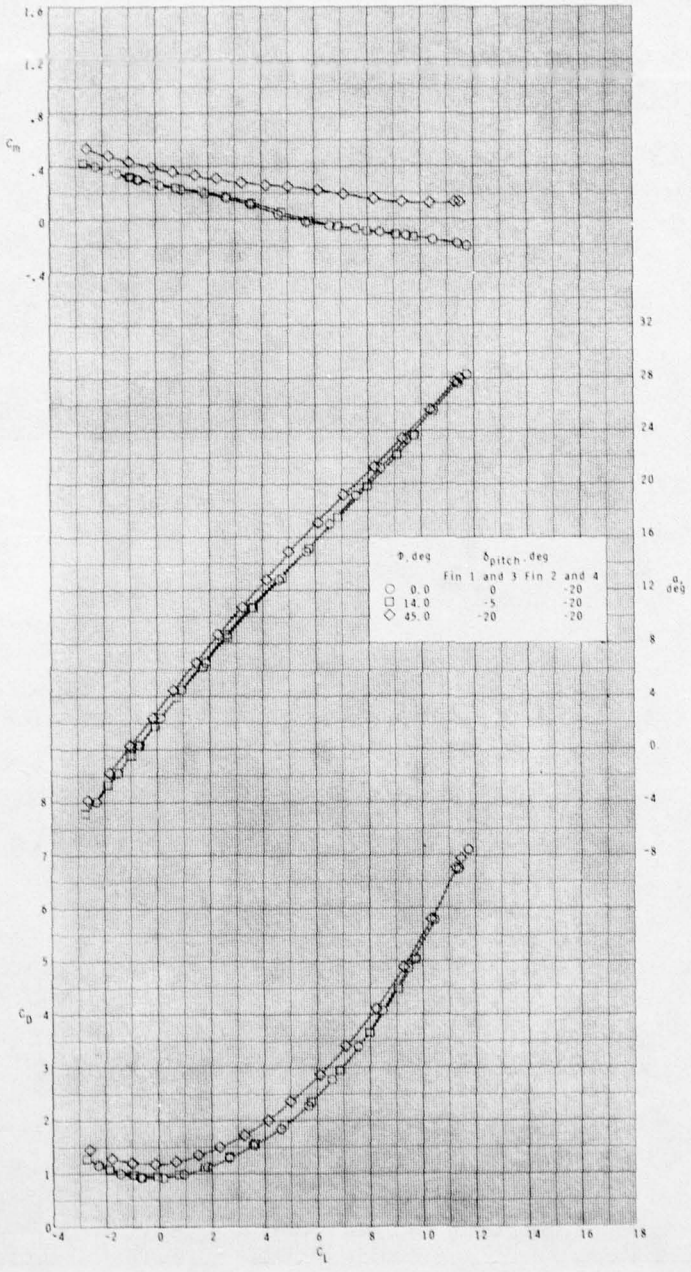

(d) Continued.

Figure 11.- Continued.

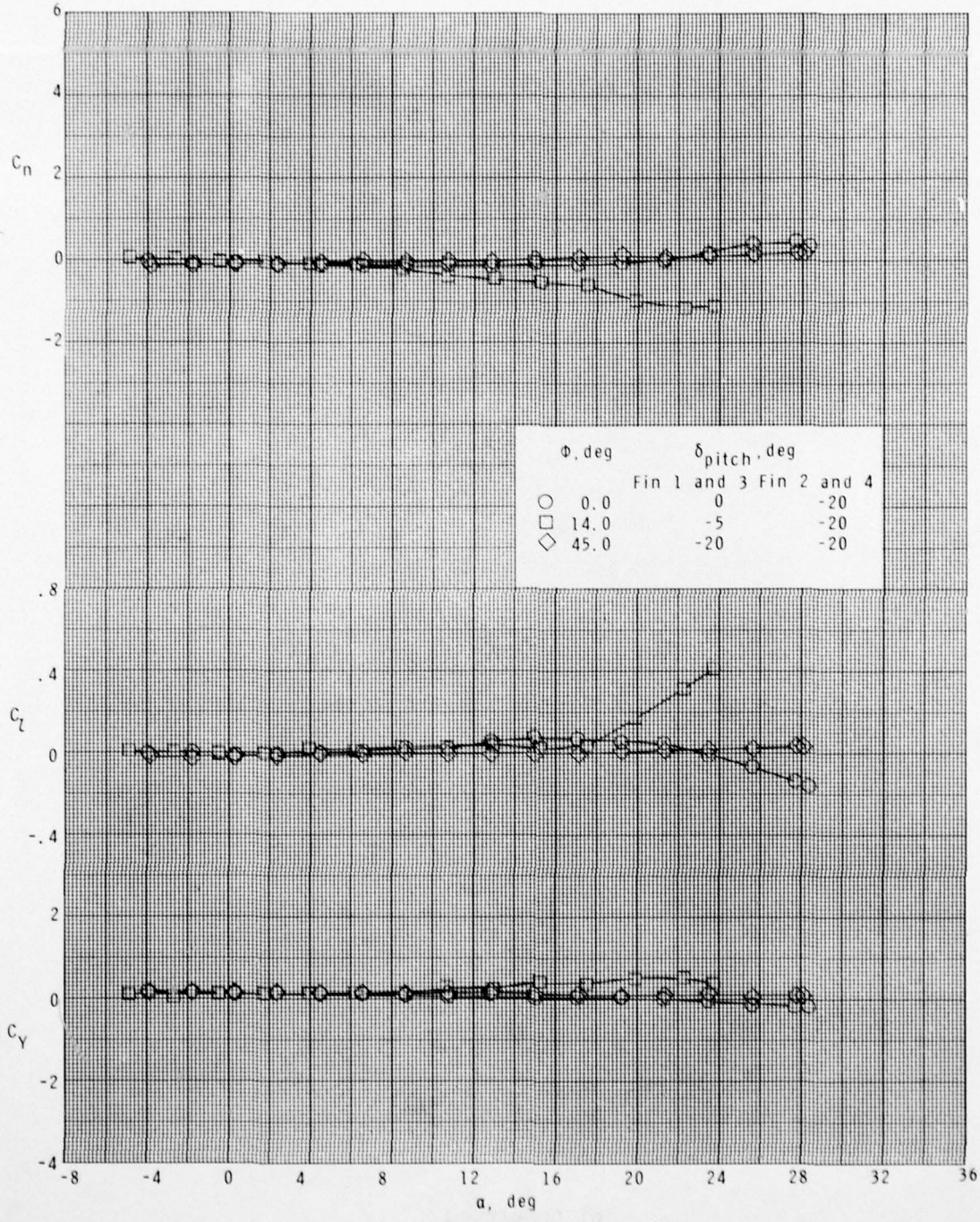

(d) Concluded.

Figure 11.- Continued.

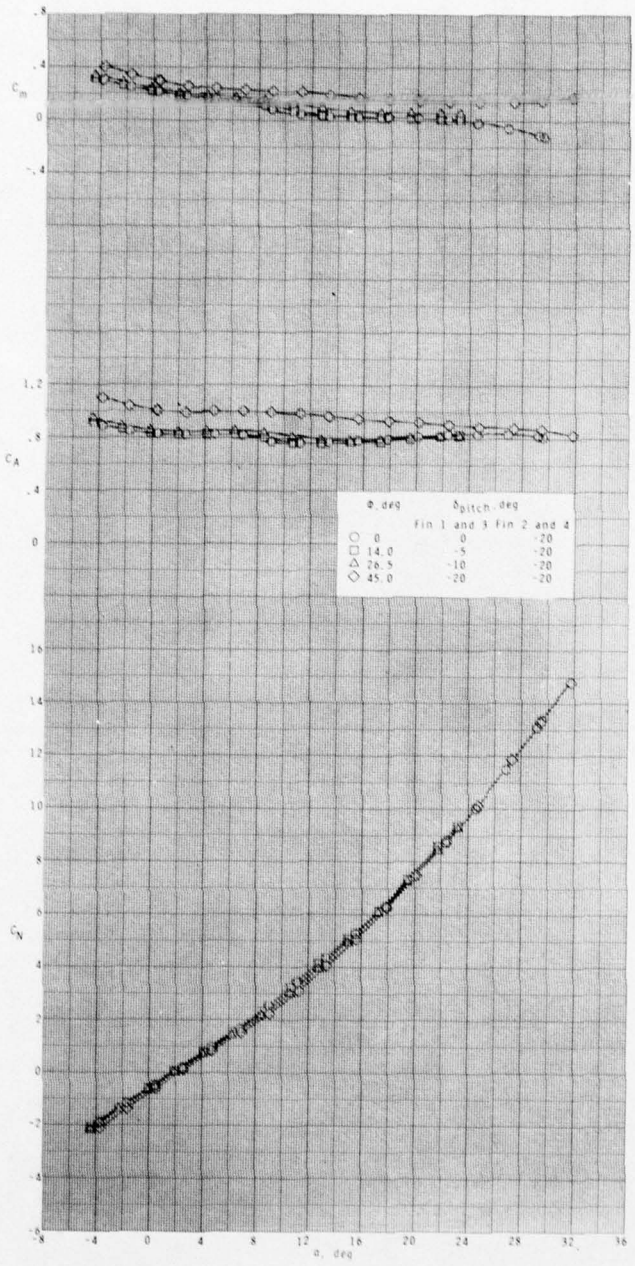

(e) M = 3.95.

Figure 11.- Continued.

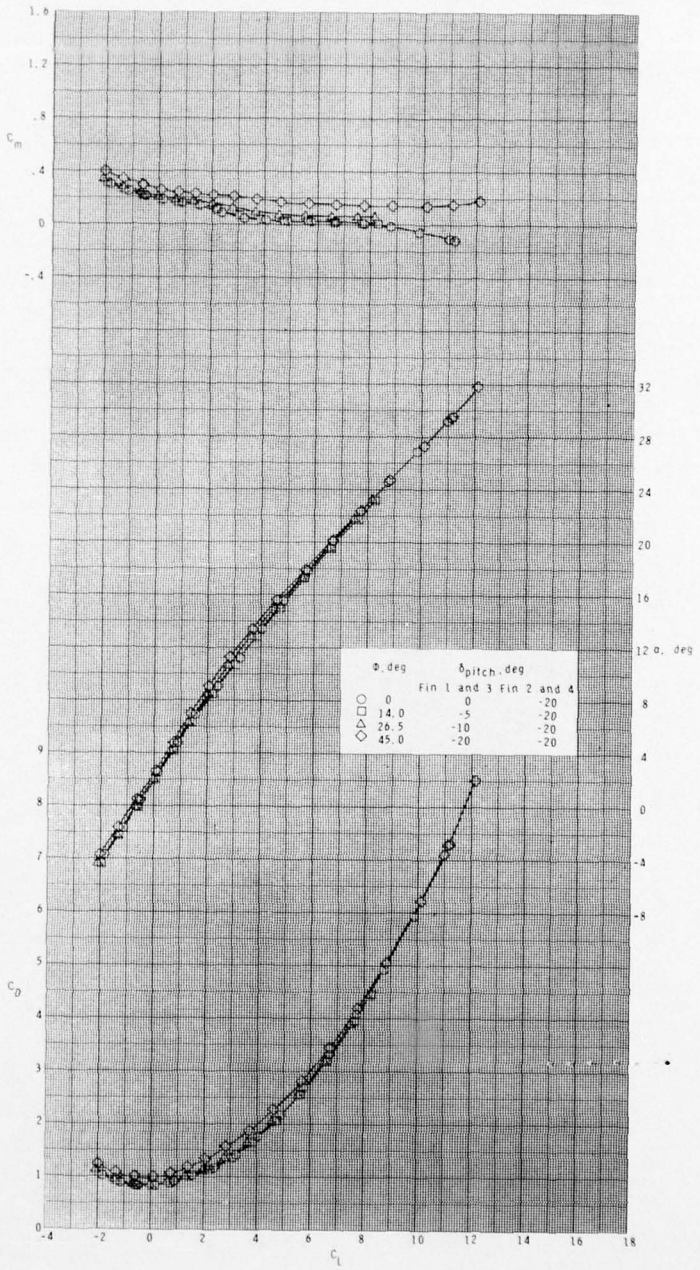

(e) Continued.

Figure 11.- Continued.

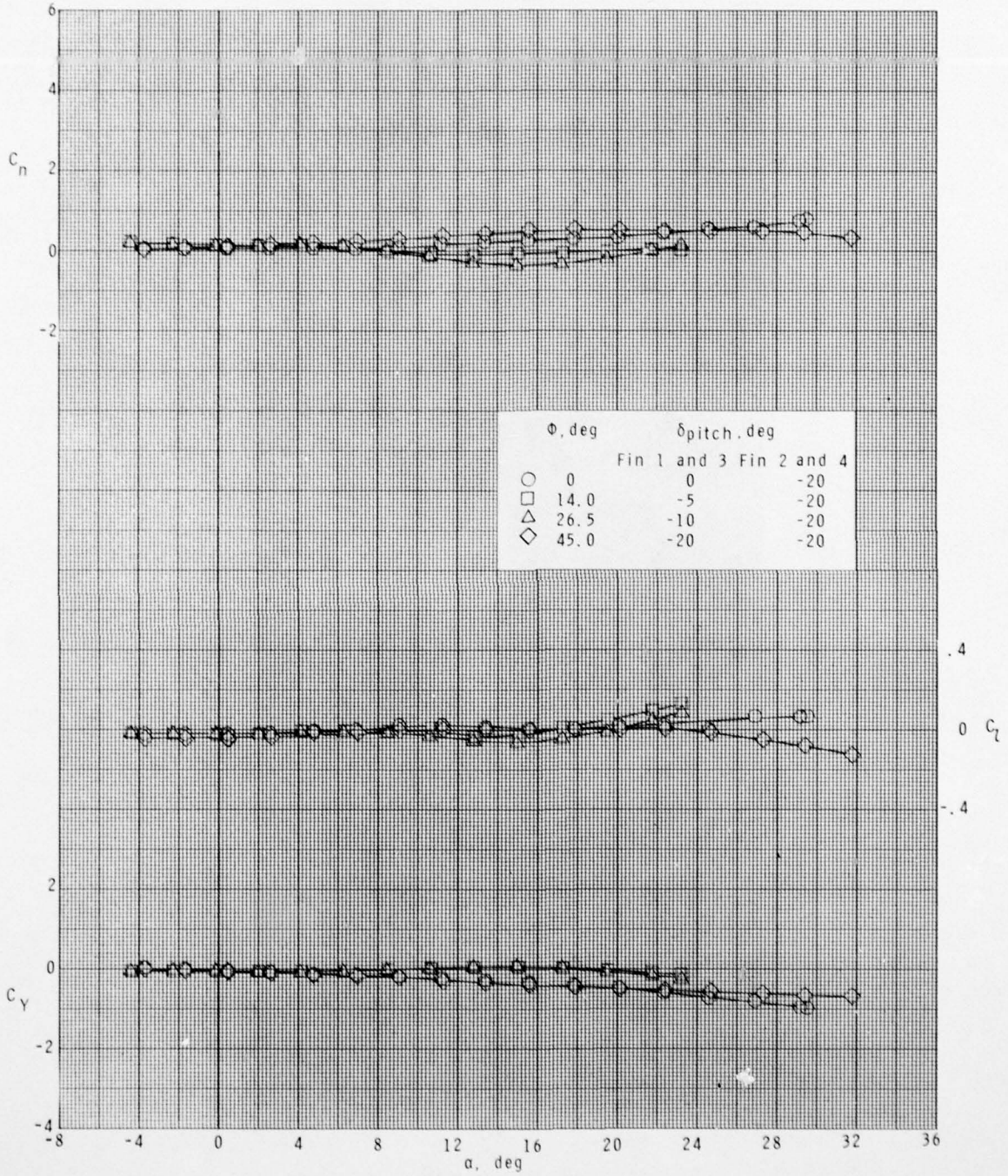

(e) Concluded.

Figure 11.- Continued.

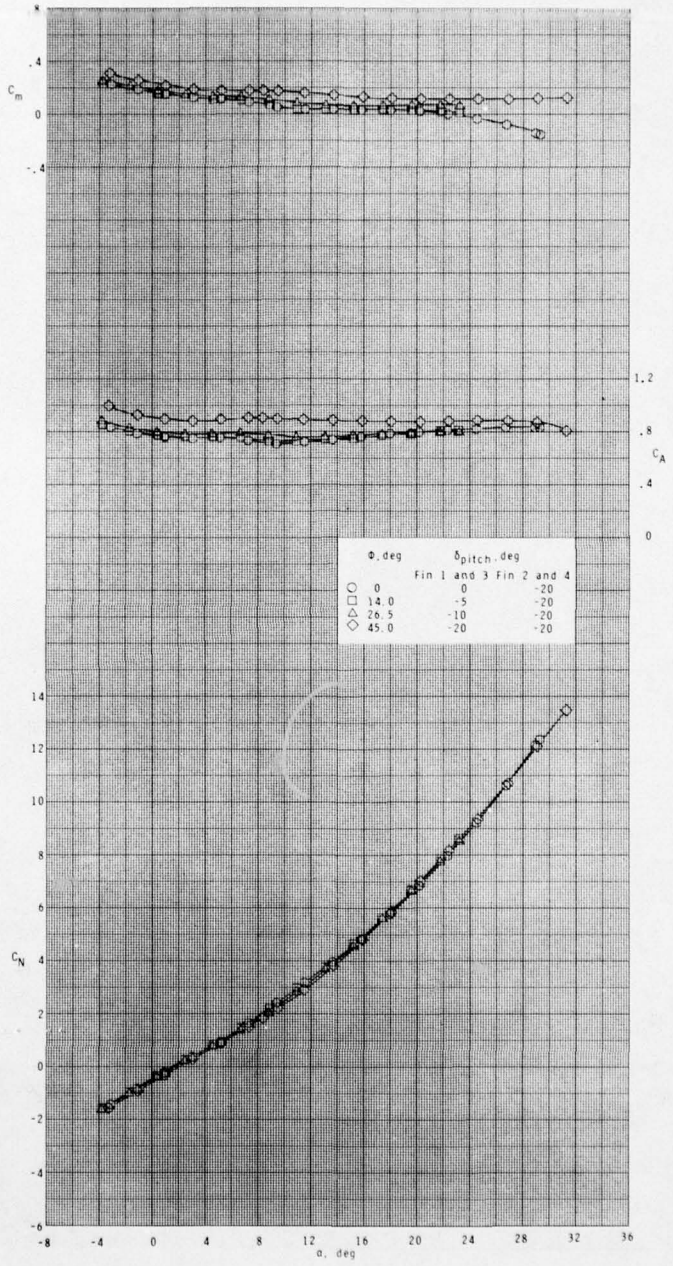

(f) M = 4.63.

Figure 11.- Continued.

AD-A078 611 NATIONAL AERONAUTICS AND SPACE ADMINISTRATION HAMPTO--ETC F/G 16/4
SUPERSONIC STABILITY AND CONTROL CHARACTERISTICS OF A CRUCIFORM--ETC(U)
DEC 79 W A CORLETT
UNCLASSIFIED NASA-L-13149 NASA-TM-80171 NL

2 OF 2
AD
A078611

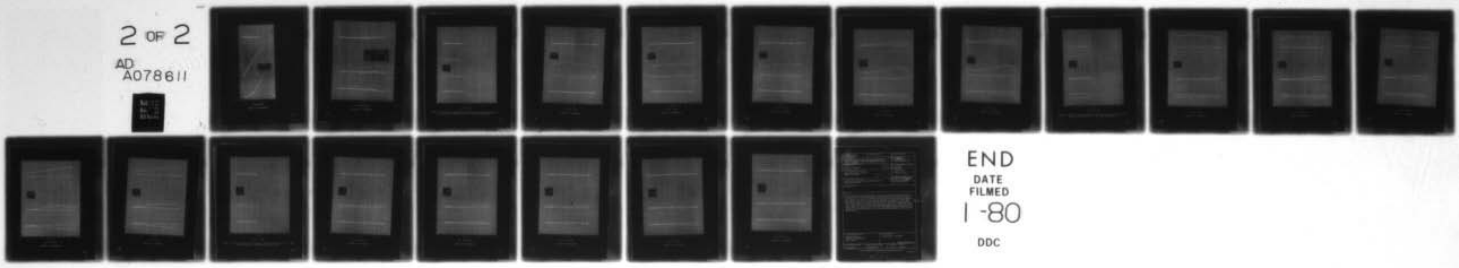

END
DATE
FILMED
1-80
DDC

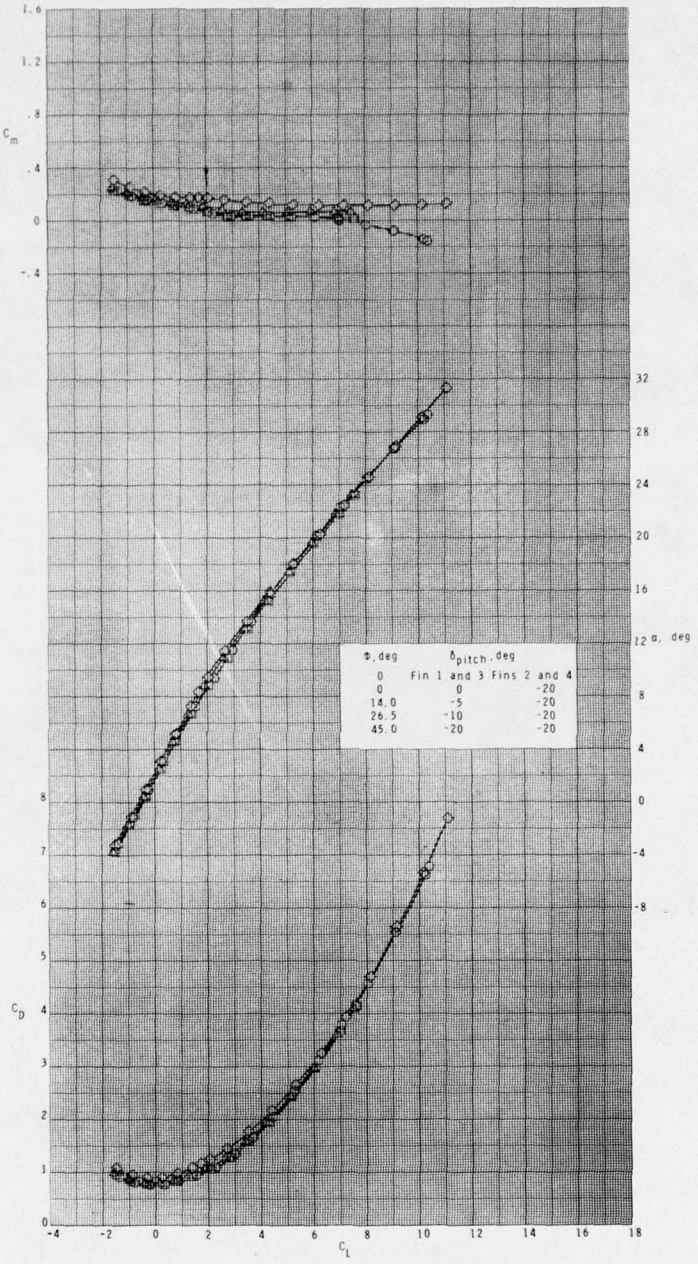

(f) Continued.

Figure 11.- Continued.

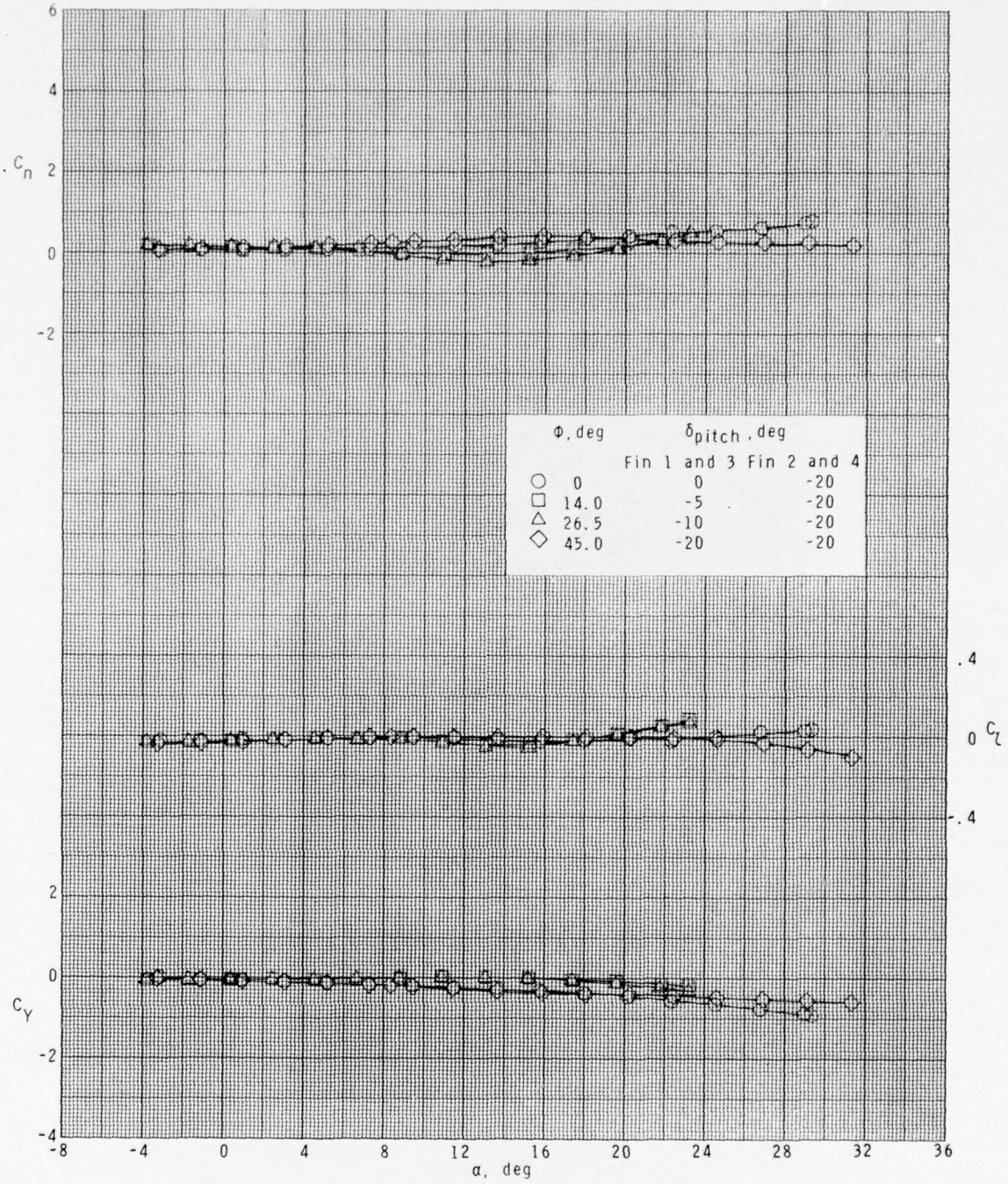

(f) Concluded.

Figure 11.- Concluded.

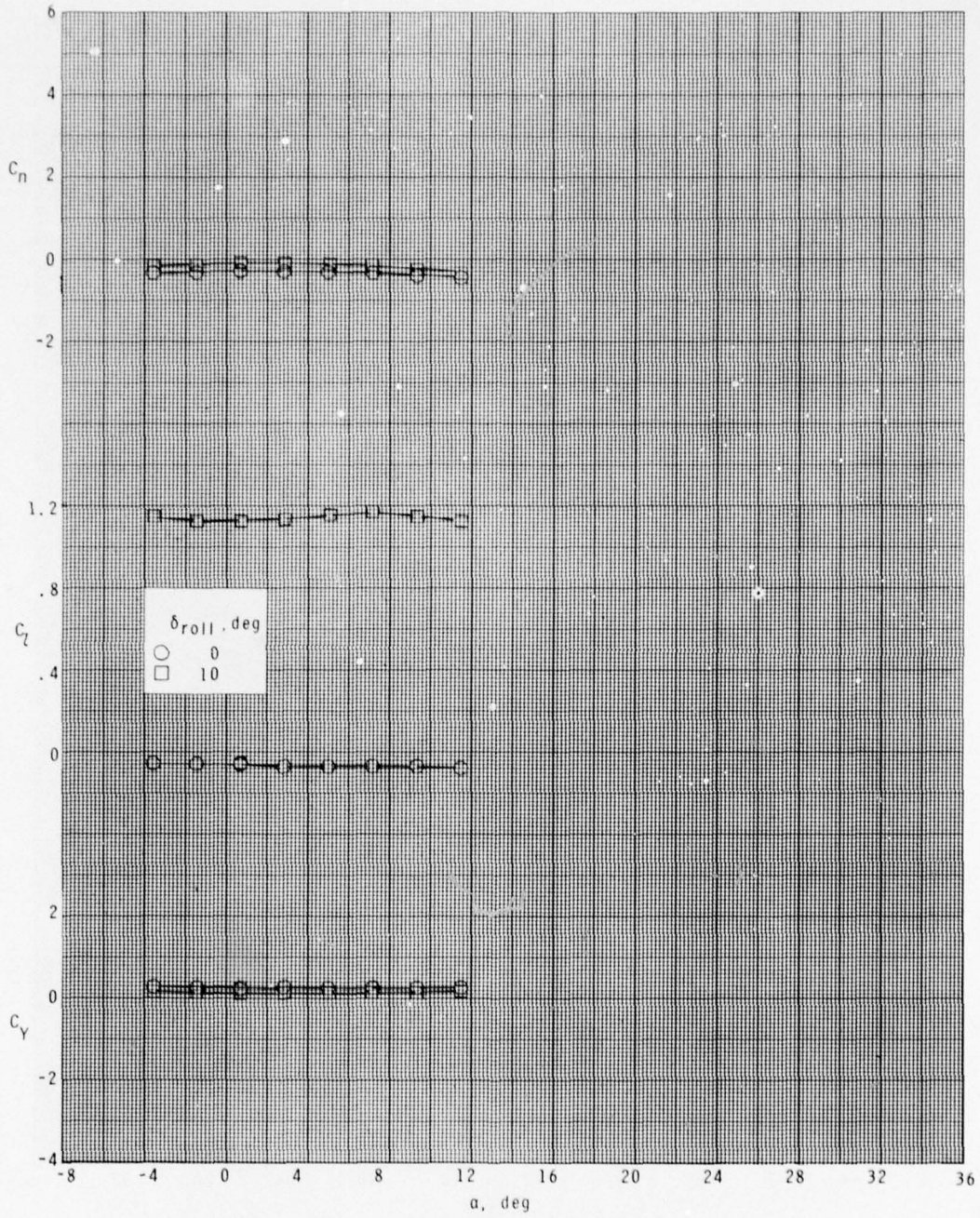

(a) M = 1.60.

Figure 12.- Effect of roll-control deflections on lateral characteristics with four fins deflected 10°; ϕ = 45°, BTW configuration.

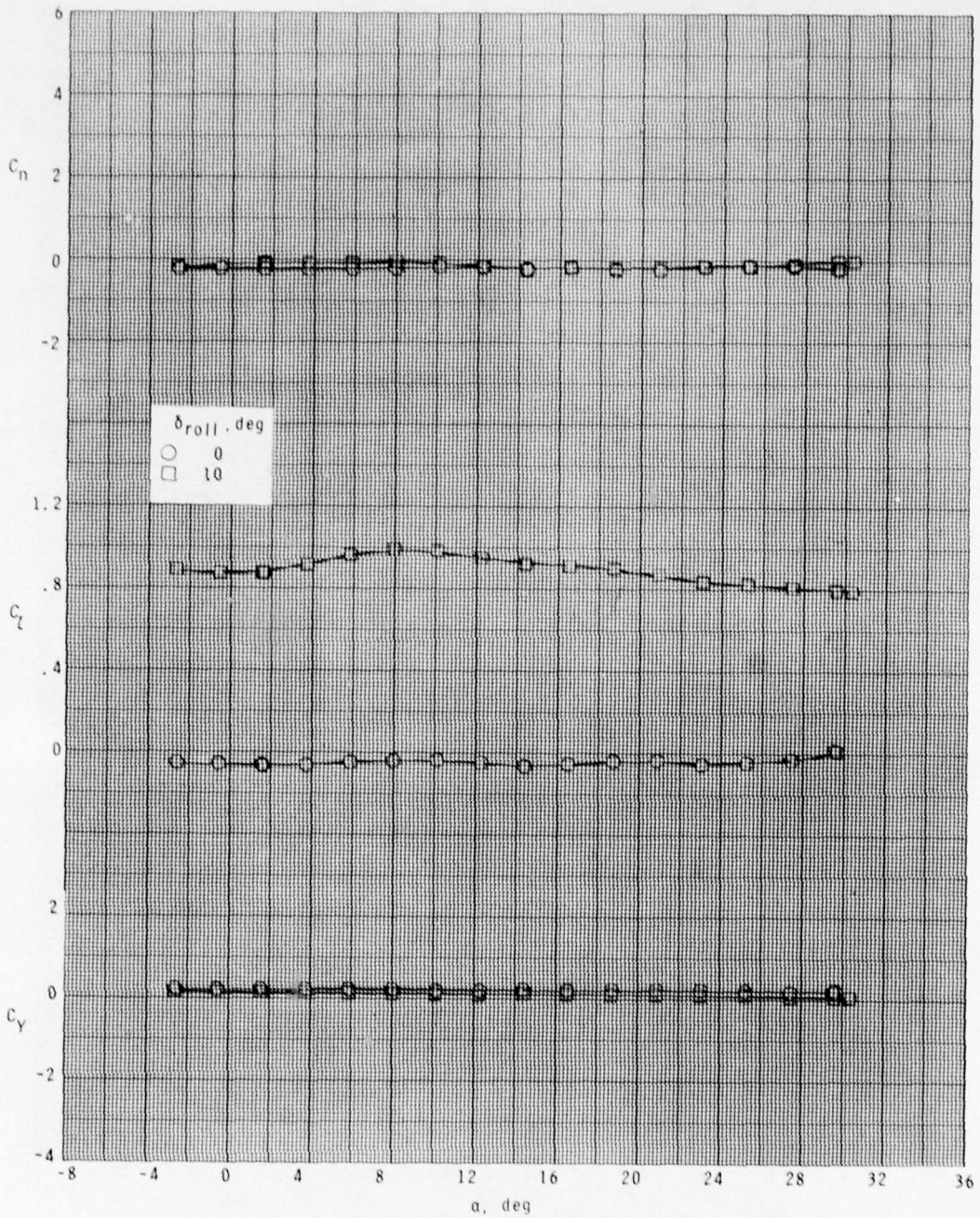

(b) M = 2.10.

Figure 12.- Continued.

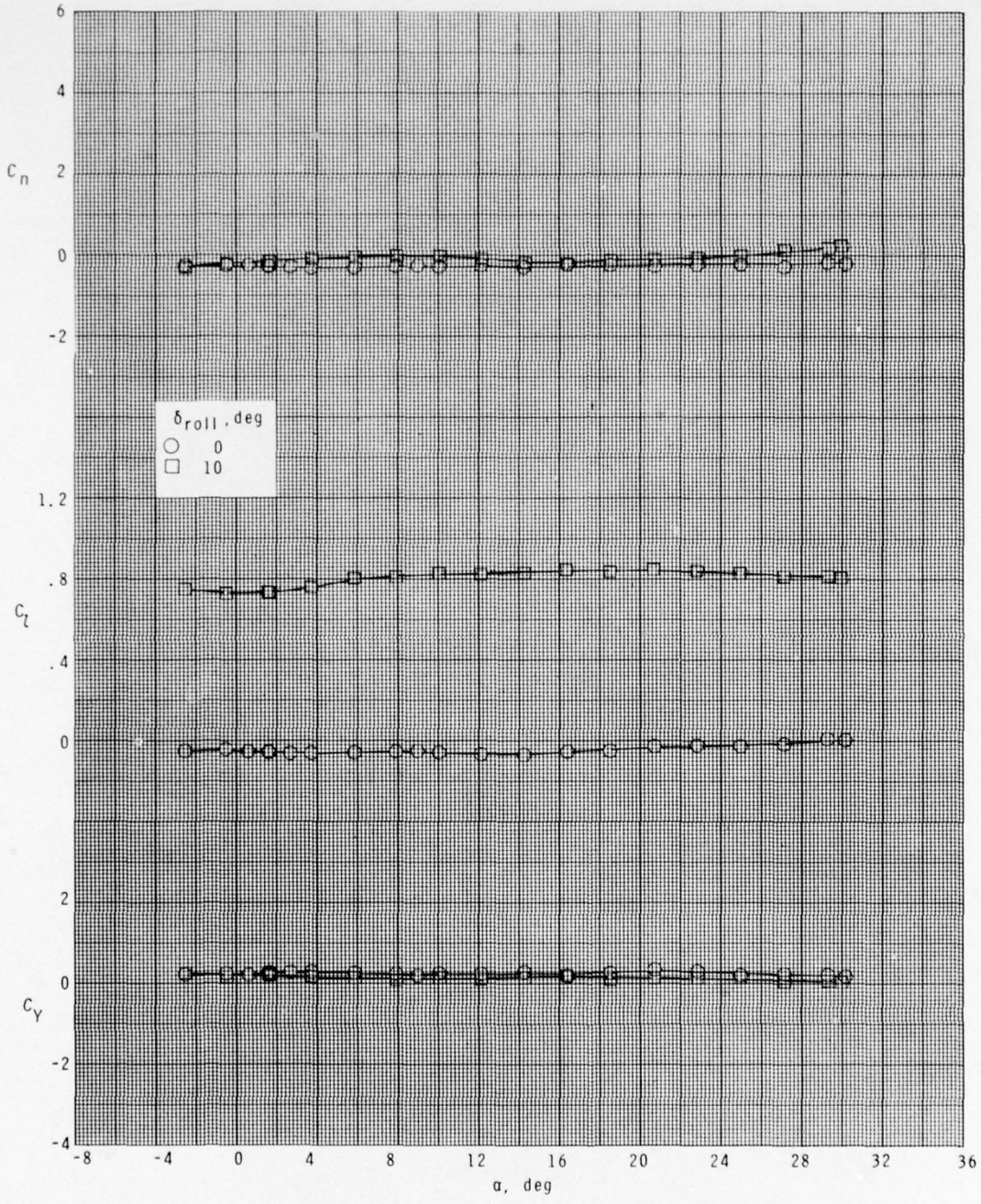

(c) M = 2.50.

Figure 12.- Continued.

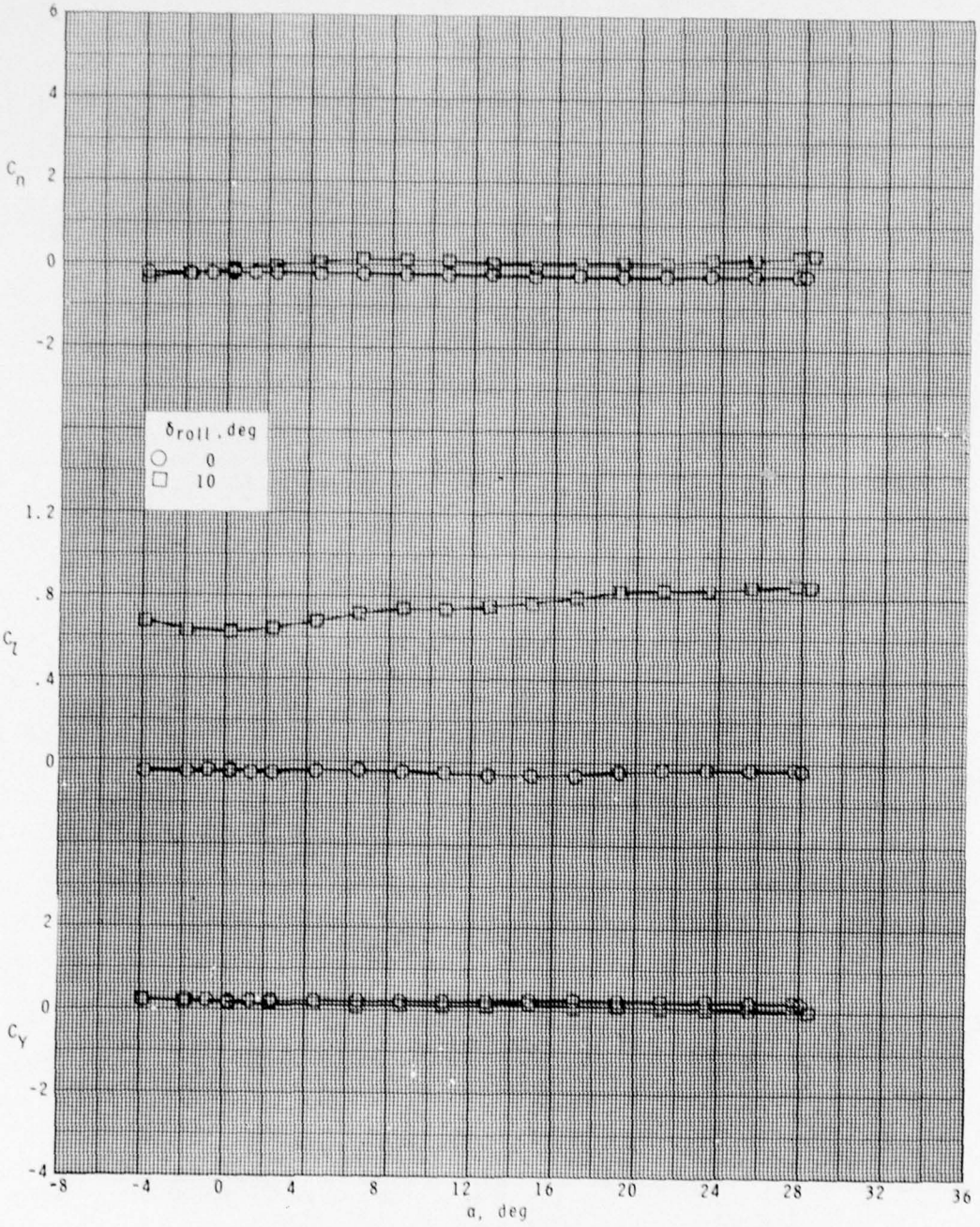

(d) M = 2.86.

Figure 12.- Continued.

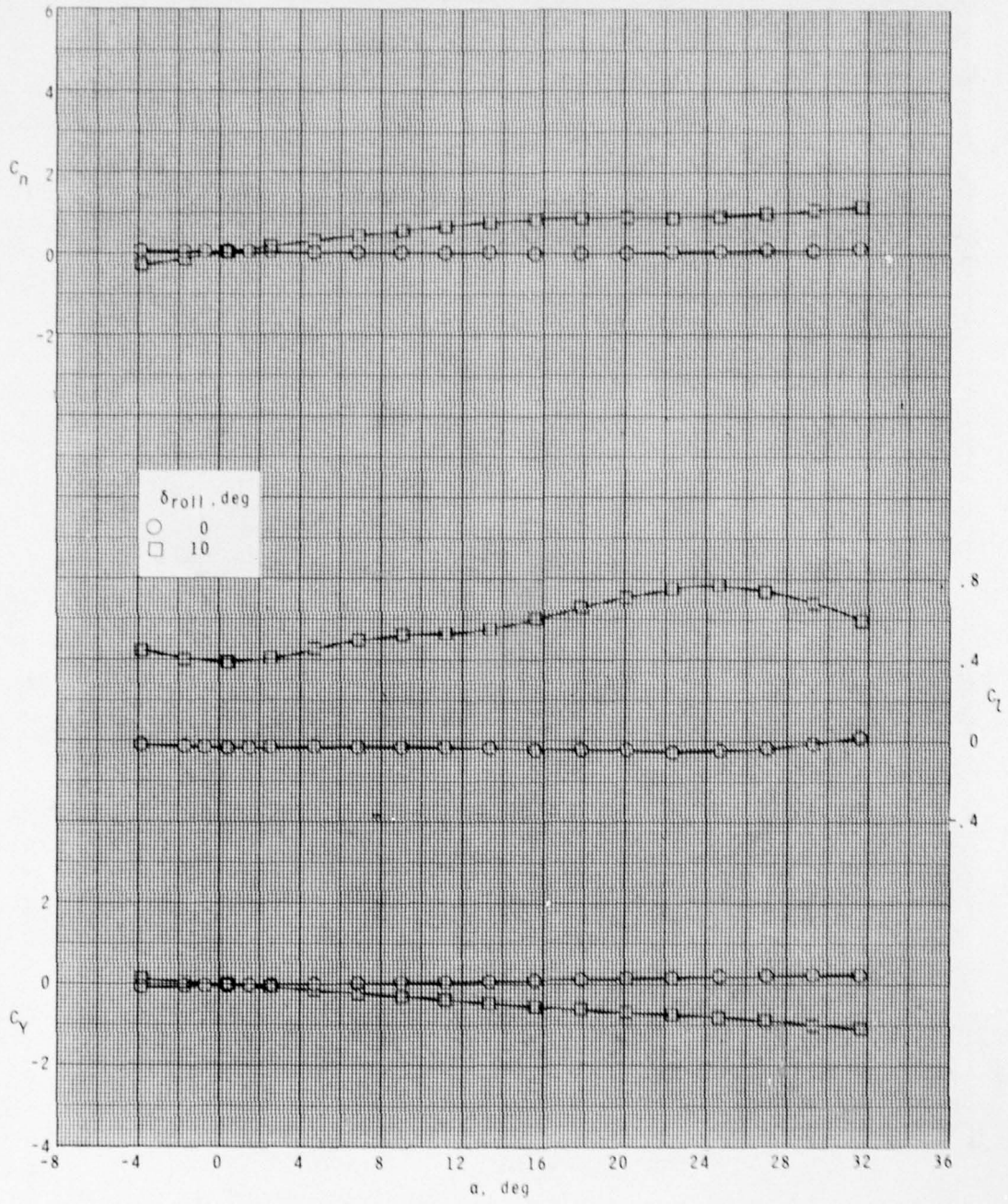

(e) M = 3.95.

Figure 12.- Continued.

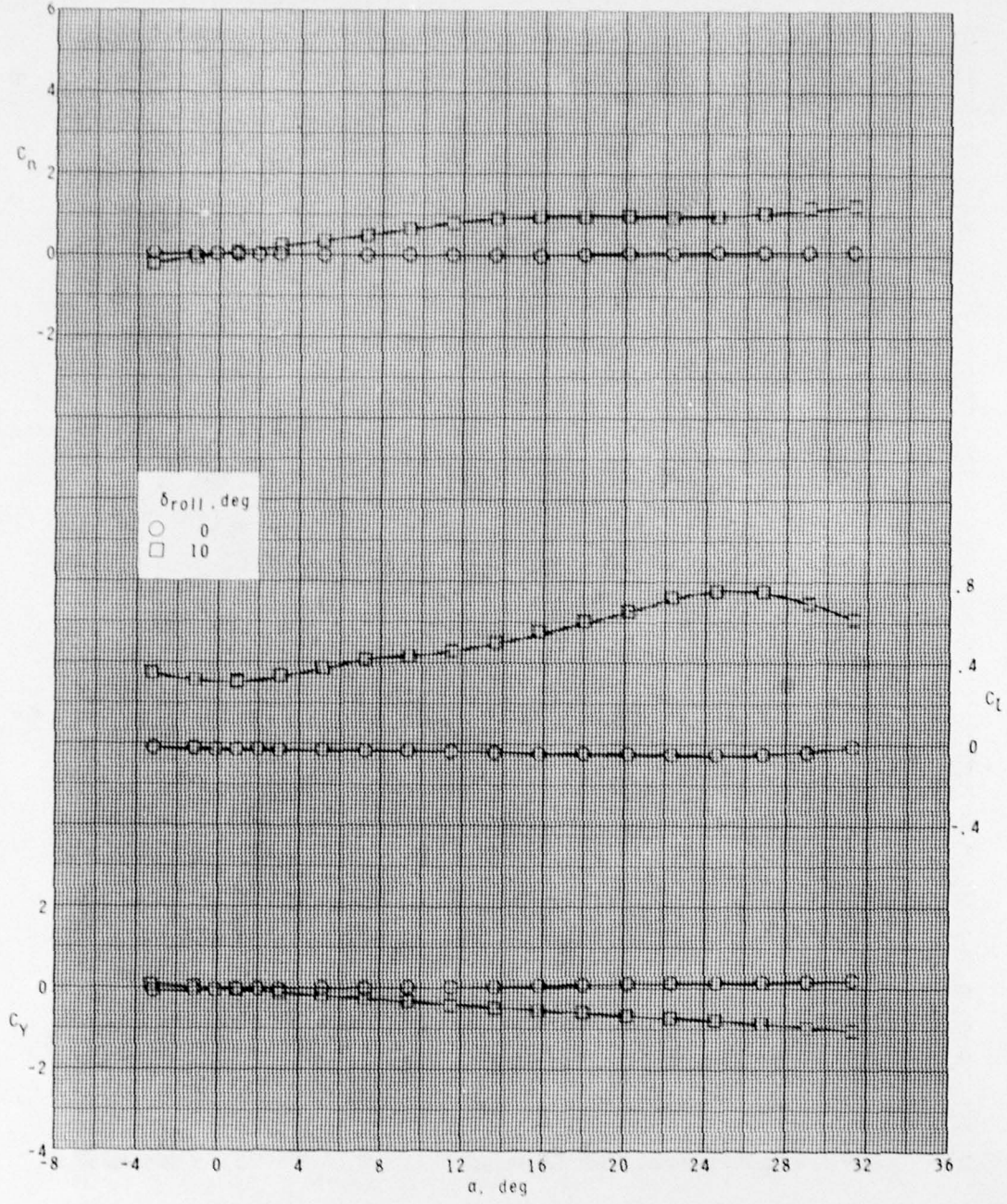

(f) M = 4.63.

Figure 12.- Concluded.

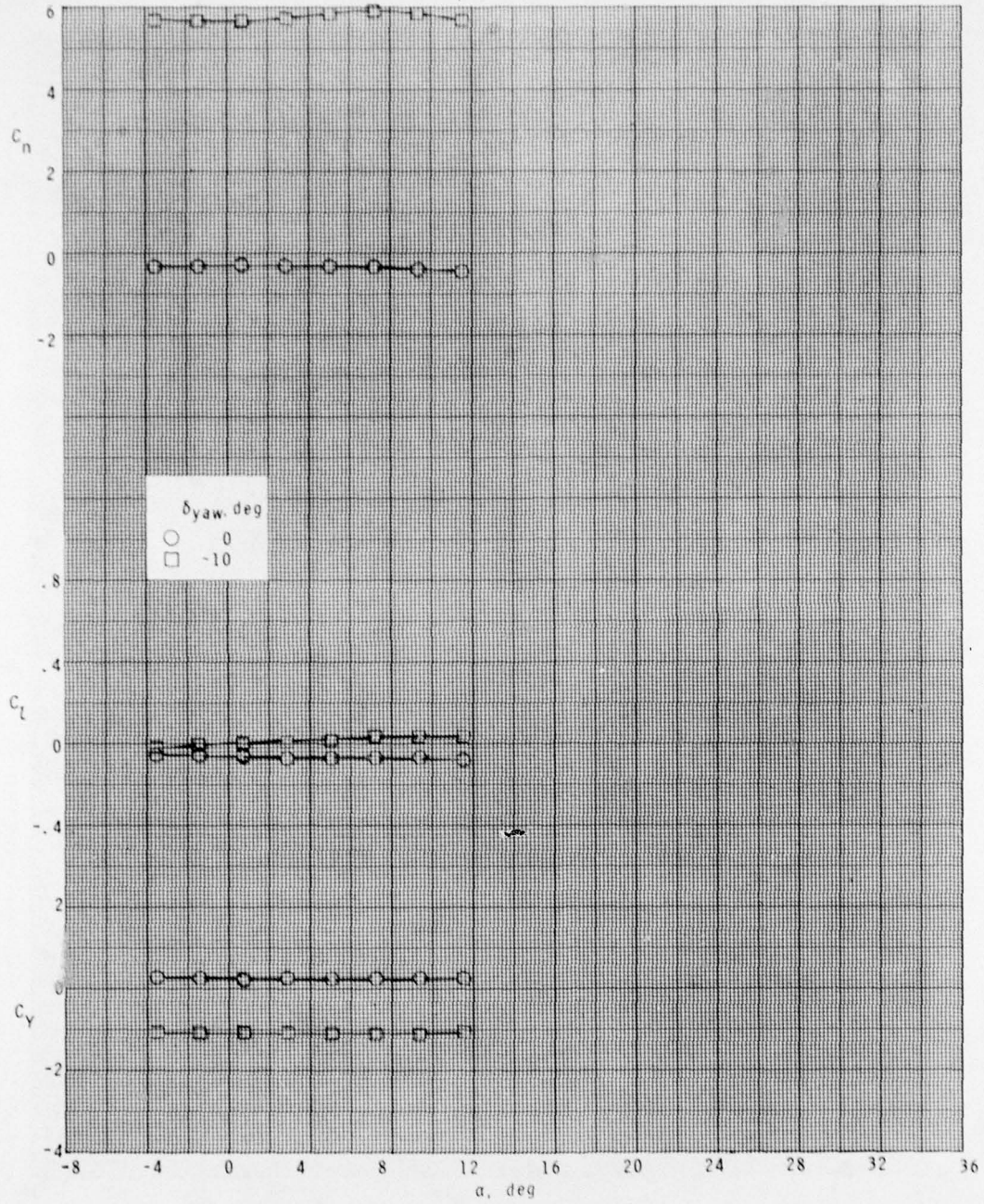

(a) M = 1.60.

Figure 13.- Effect of yaw-control deflections on lateral characteristics with four fins deflected 10°; ϕ = 45°, BTW configuration.

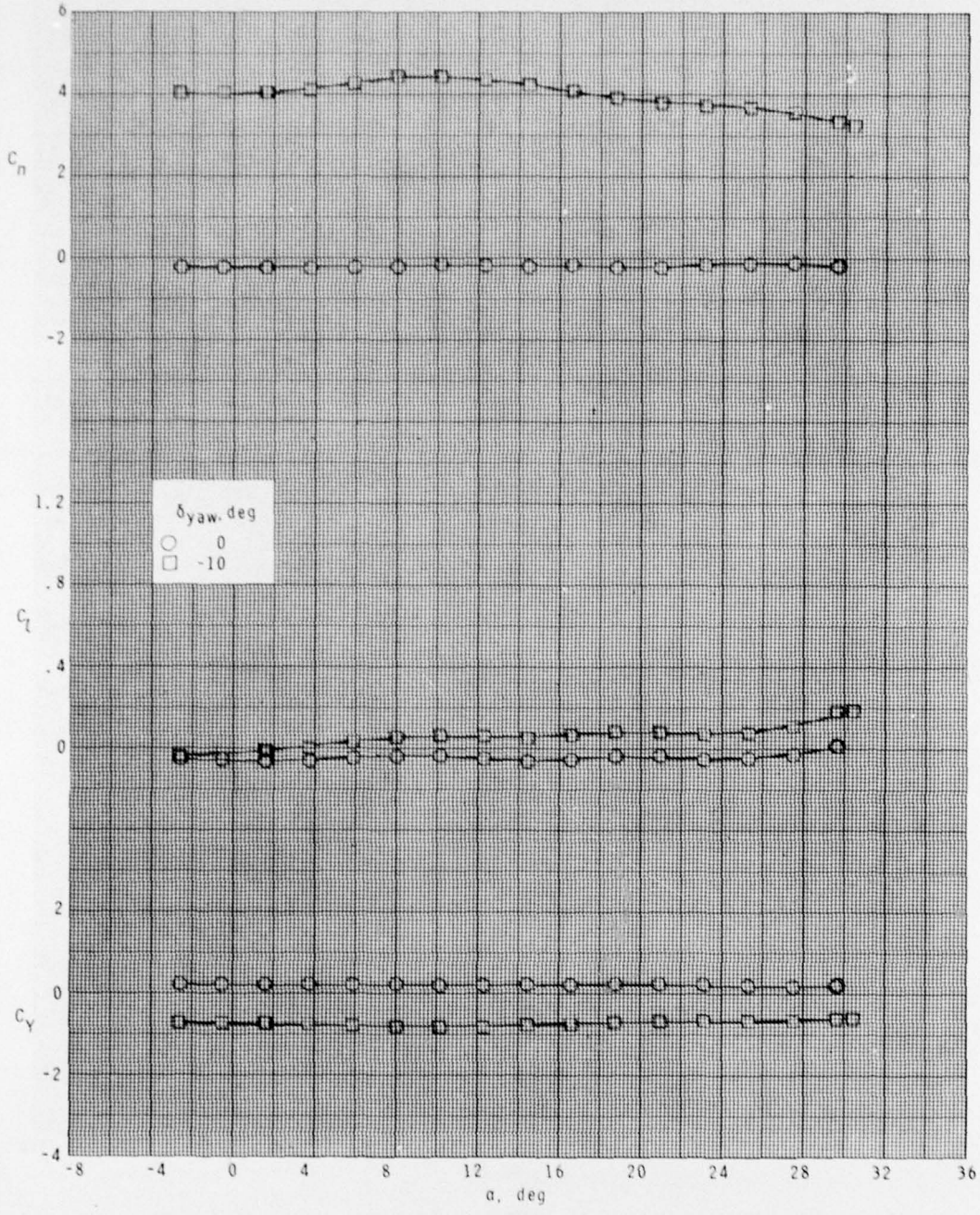

(b) M = 2.10.

Figure 13.- Continued.

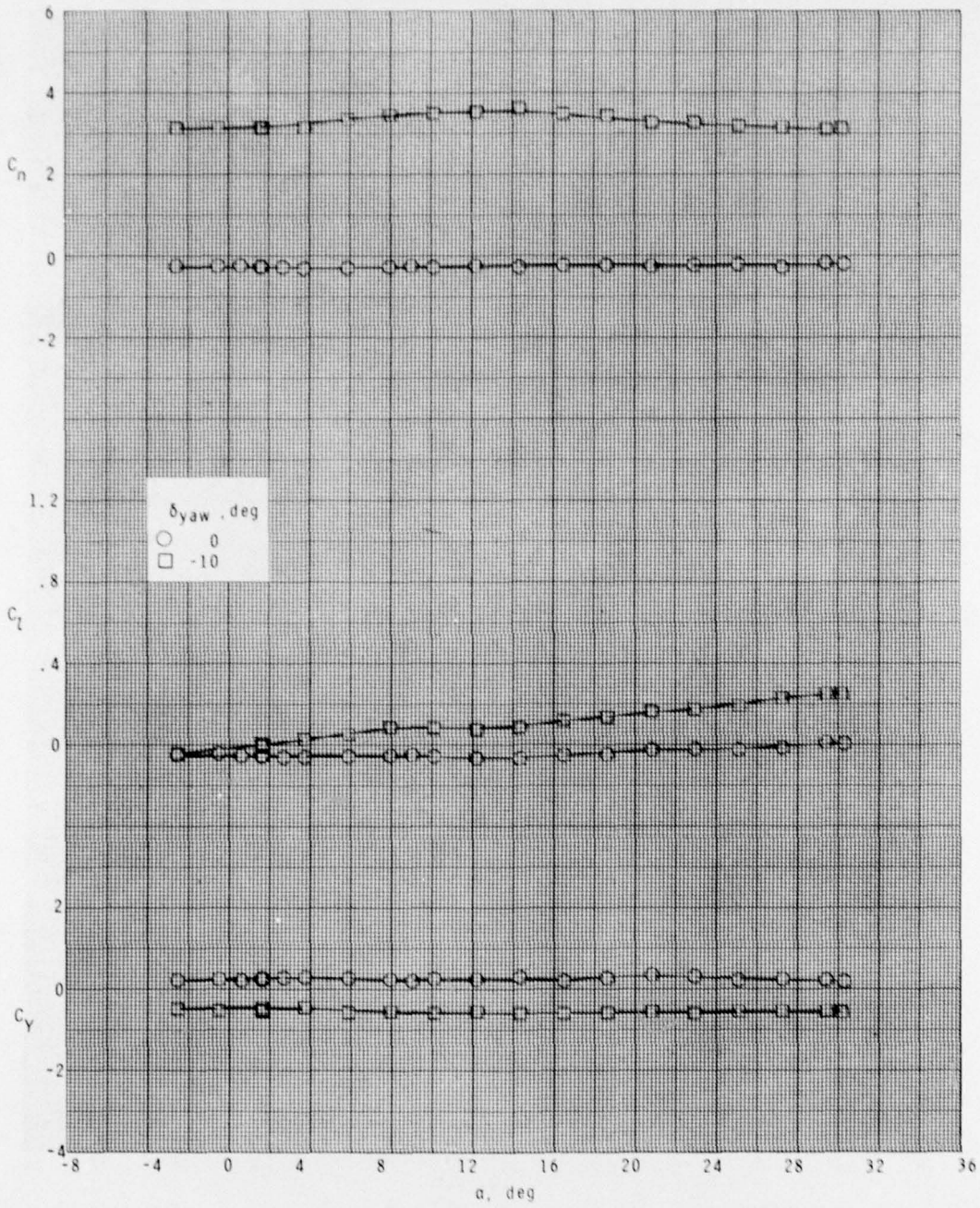

(c) M = 2.50.

Figure 13.- Continued.

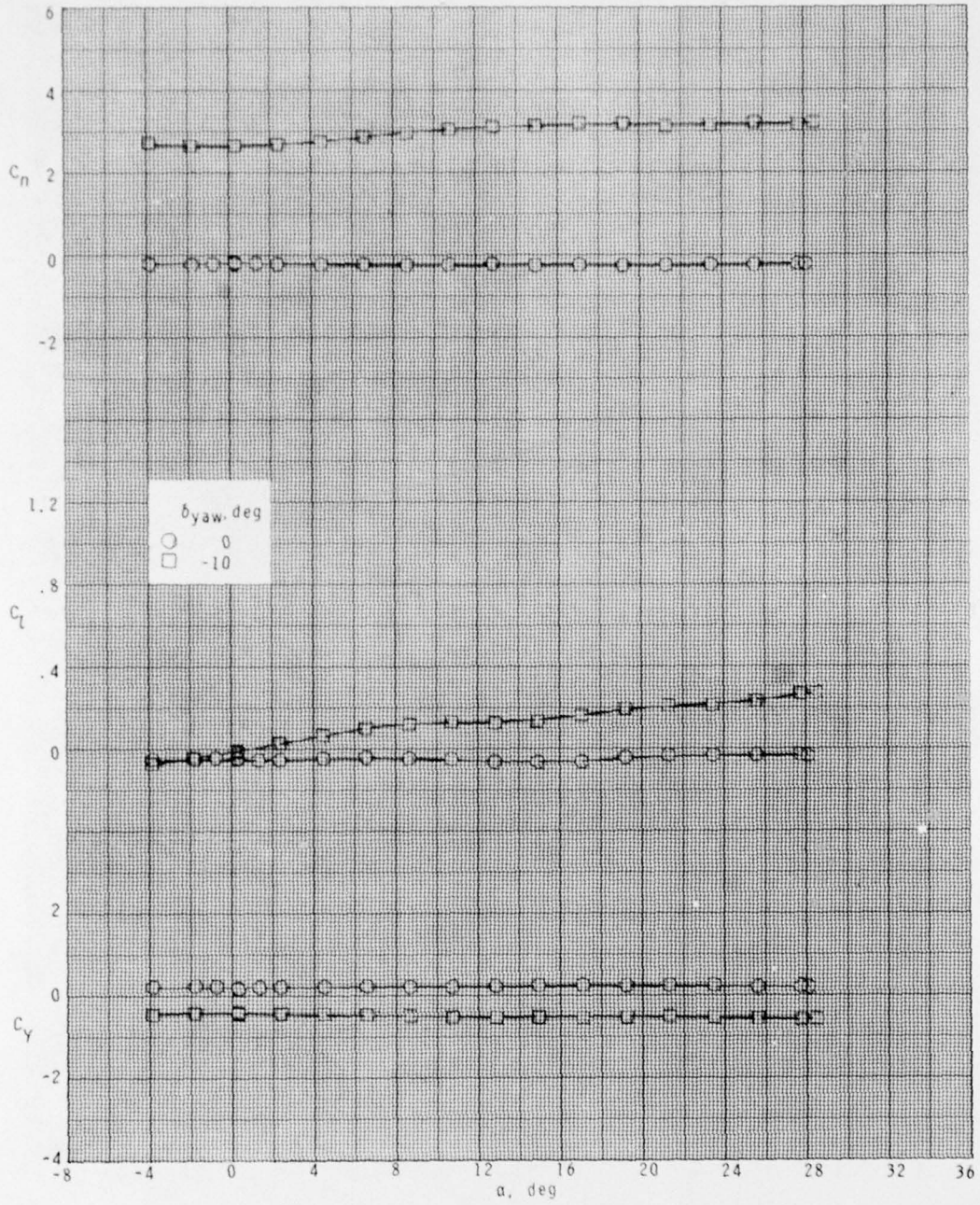

(d) M = 2.86.

Figure 13.- Continued.

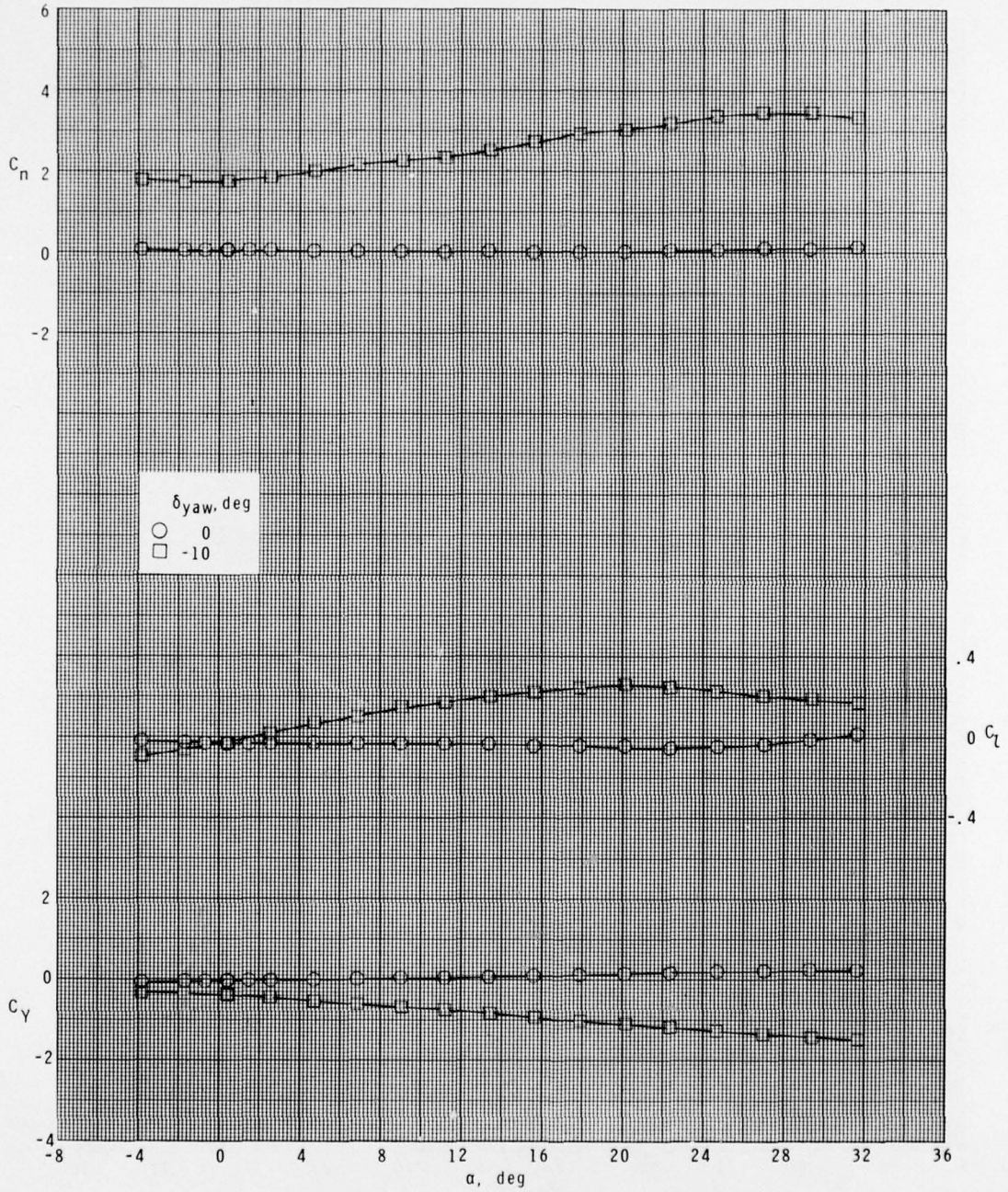

(e) M = 3.95.

Figure 13.- Continued.

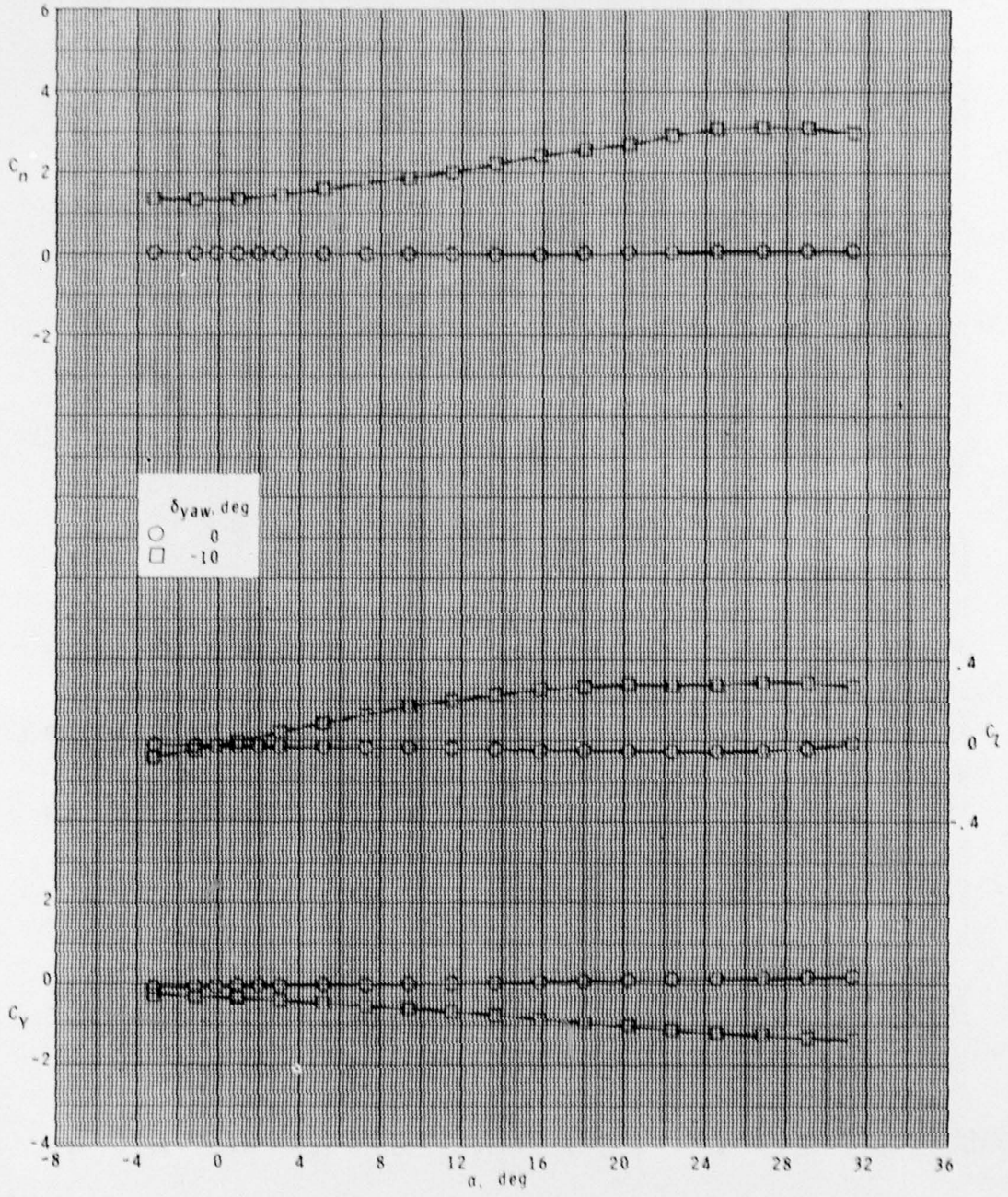

(f) M = 4.63.

Figure 13.- Concluded.

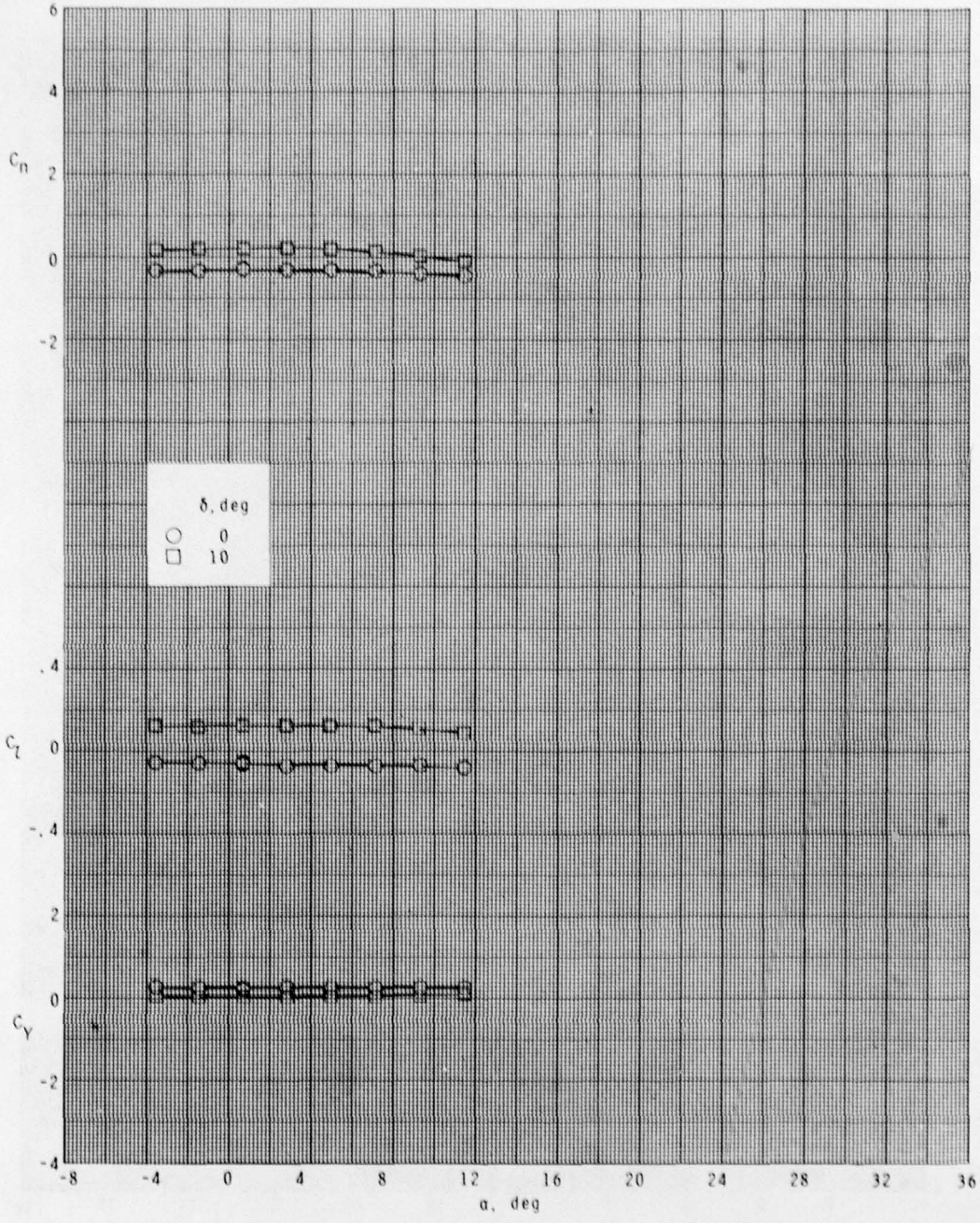

(a) M = 1.60.

Figure 14.- Effect of wing-tab deflections on lateral characteristics; $\phi = 45^{o}$, BTW configuration, control tab on wing 3 only.

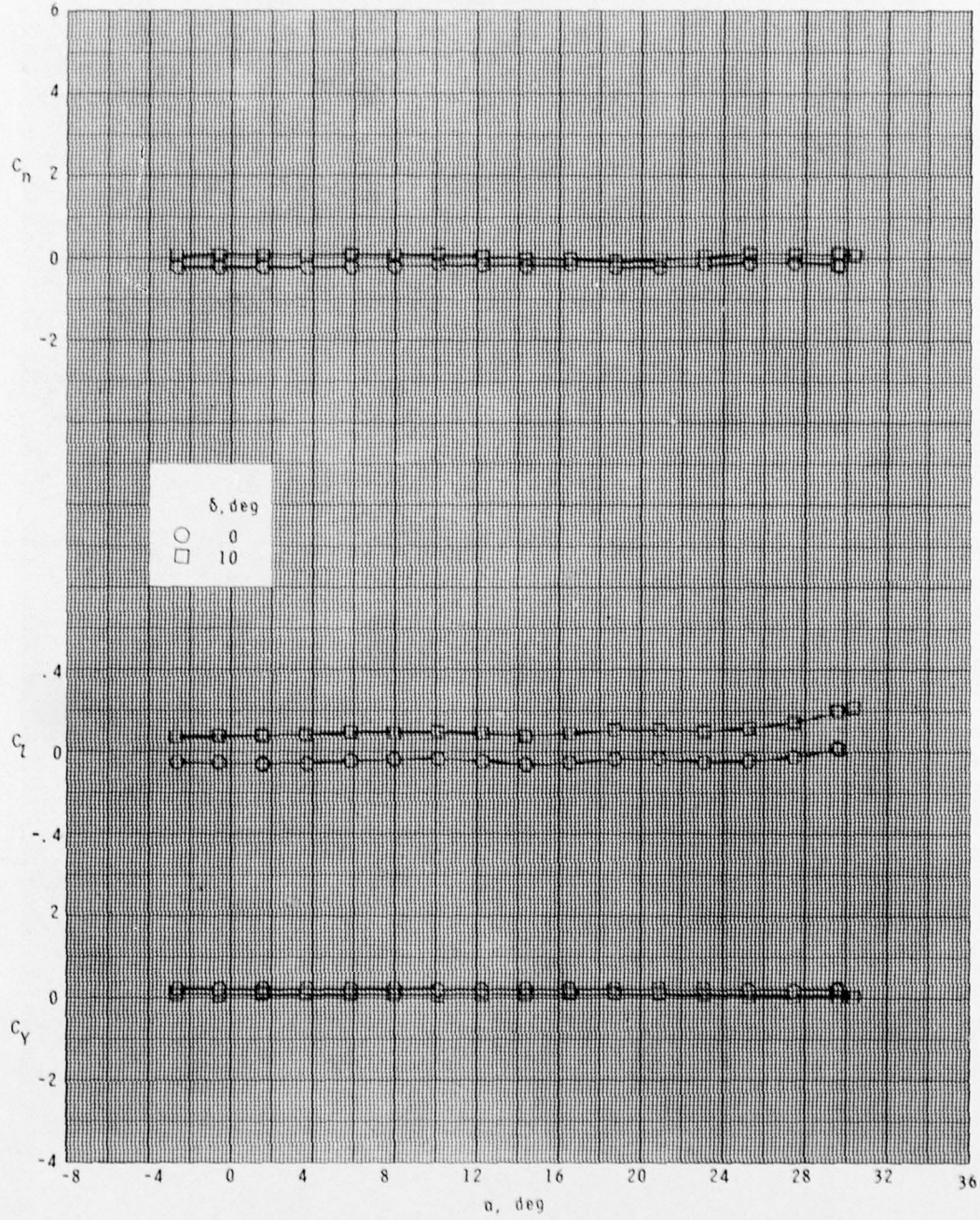

(b) M = 2.10.

Figure 14.- Continued.

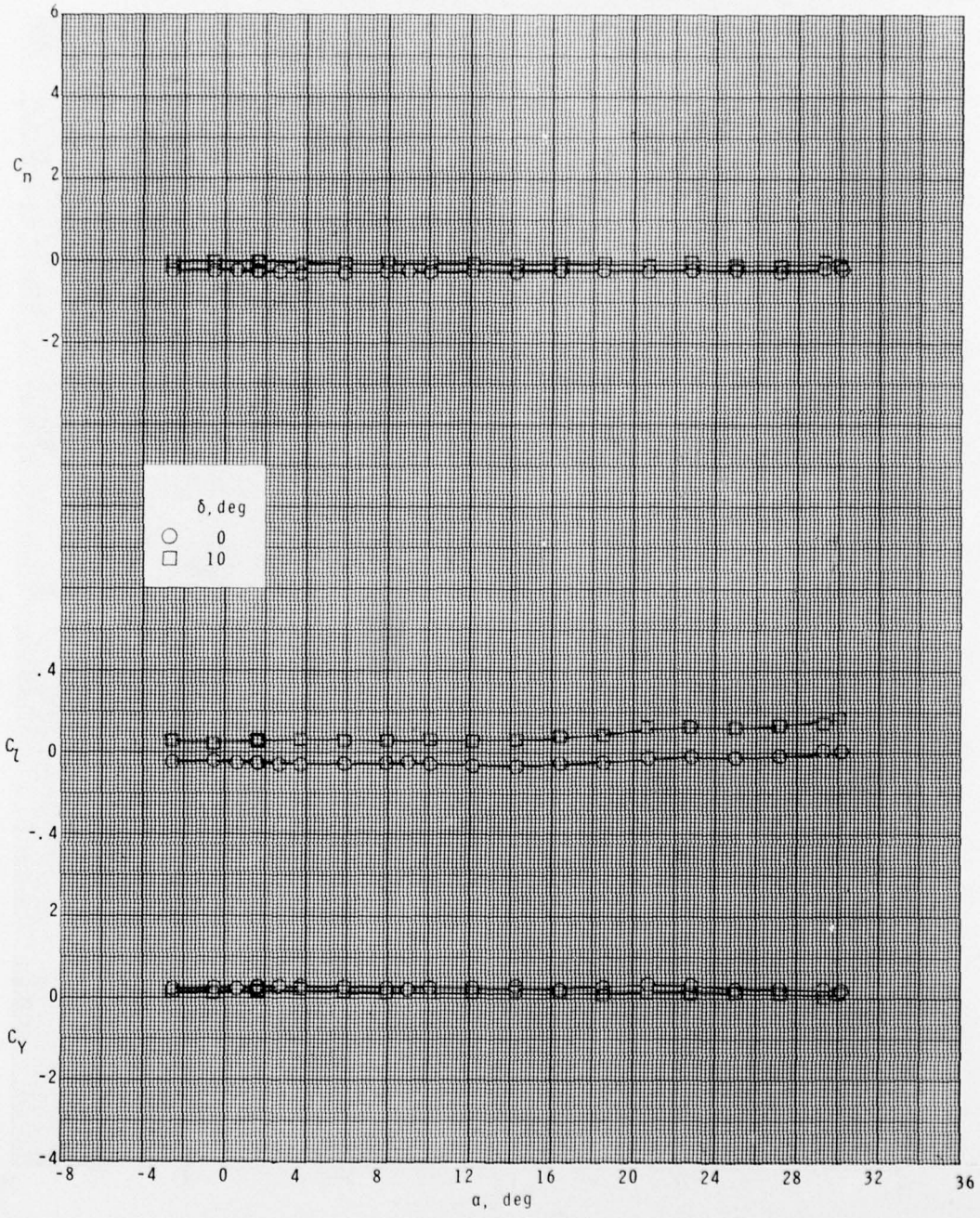

(c) M = 2.50.

Figure 14.- Continued.

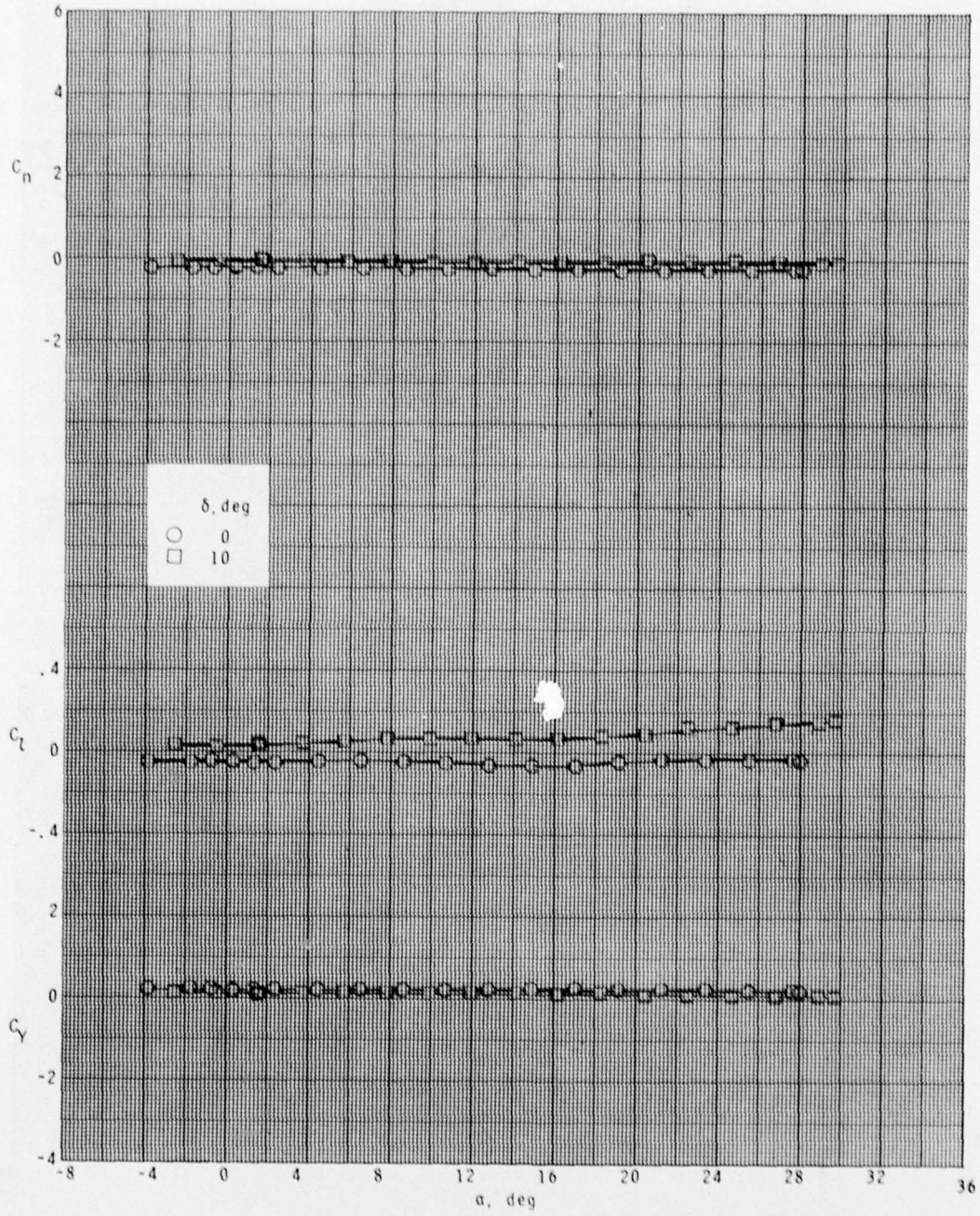

(d) M = 2.86.

Figure 14.- Continued.

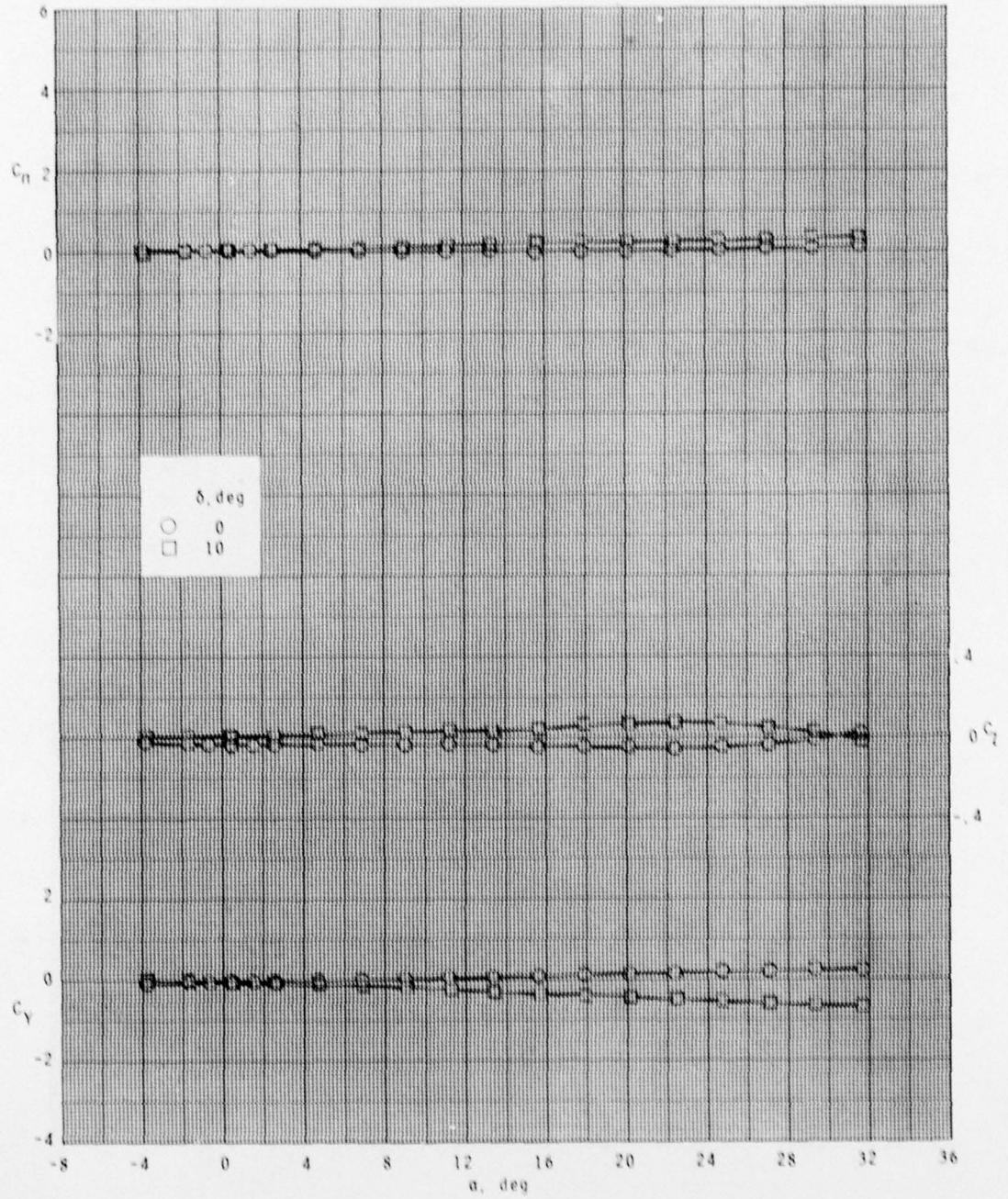

(e) M = 3.95.

Figure 14.- Continued.

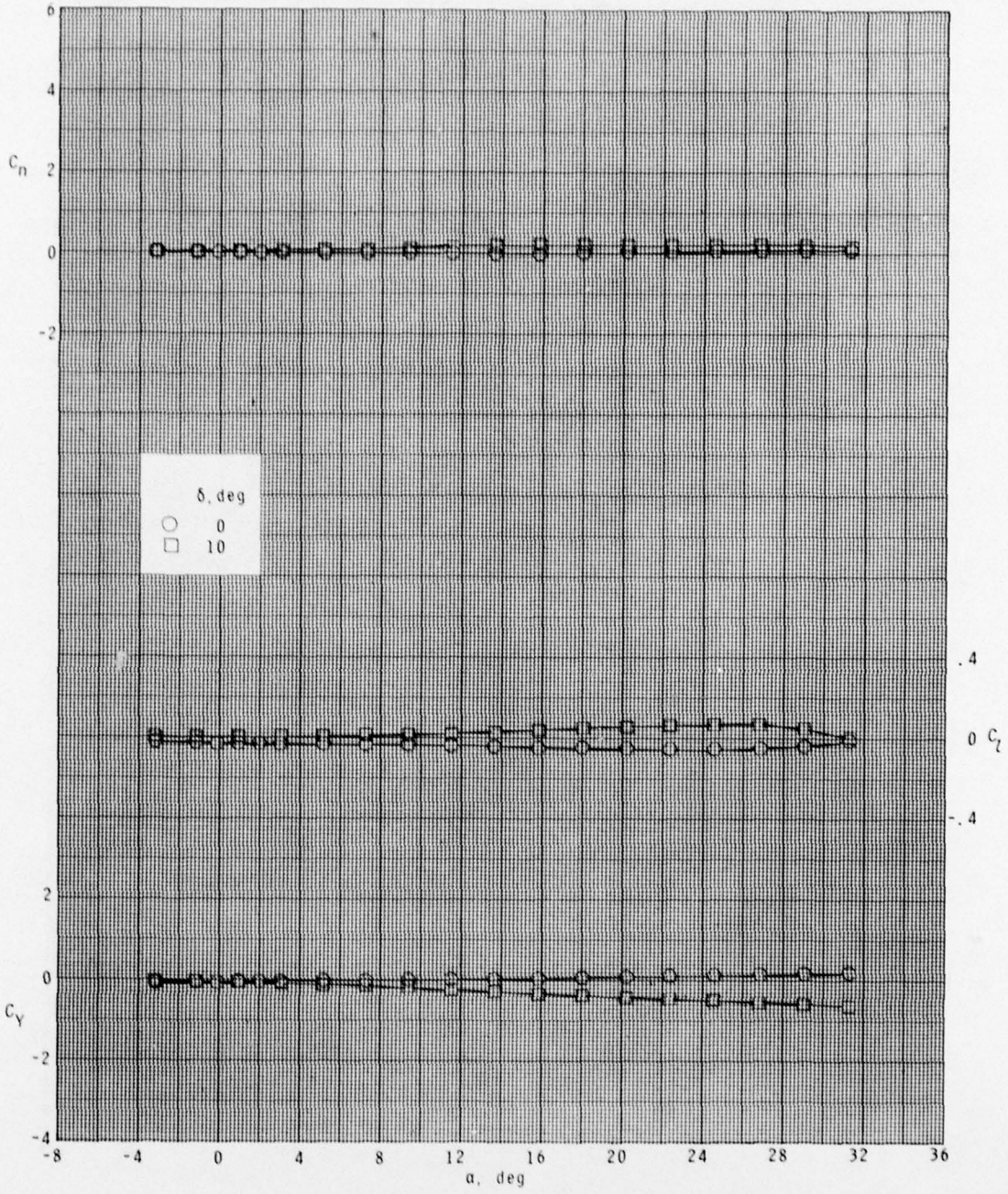

(f) M = 4.63.

Figure 14.- Concluded.

1. Report No. NASA TM-80171	2. Government Accession No.	3. Recipient's Catalog No.
4. Title and Subtitle SUPERSONIC STABILITY AND CONTROL CHARACTERISTICS OF A CRUCIFORM MISSILE MODEL WITH DELTA WINGS AND AFT TAIL FIN CONTROLS		5. Report Date December 1979 6. Performing Organization Code
7. Author(s) William A. Corlett		8. Performing Organization Report No. NASA-L-13149
9. Performing Organization Name and Address NASA Langley Research Center Hampton, VA 23665		10. Work Unit No. 505-43-33-04 11. Contract or Grant No.
12. Sponsoring Agency Name and Address National Aeronautics and Space Administration Washington, DC 20546		13. Type of Report and Period Covered Technical Memorandum 14. Sponsoring Agency Code
15. Supplementary Notes		

16. Abstract

An investigation has been conducted to determine the static stability and control characteristics of a cruciform missile configuration with delta wings and aft tail fin controls. The tests were conducted in the Langley Unitary Plan wind tunnel at Mach numbers from 1.60 to 4.63 through an angle-of-attack range of -4° to 30°. Model roll orientation was varied from 0° to 135°. The results indicated good longitudinal stability and control characteristics throughout the test Mach number range. Relatively high induced rolling and yawing moments were apparent at asymmetric model roll angles for the lower test Mach numbers; however, sufficient roll and yaw control was available to trim to relatively high angles of attack and lift coefficients.

17. Key Words (Suggested by Author(s))	18. Distribution Statement
Cruciform missile Supersonic aerodynamics Tail controls	Unclassified - Unlimited Subject Category 02

19. Security Classif. (of this report)	20. Security Classif. (of this page)	21. No. of Pages	22. Price*
Unclassified	Unclassified	114	$6.50

* For sale by the National Technical Information Service, Springfield, Virginia 22161

NASA-Langley, 1979